ISSN:2309845 7

2022 年 12 月
第 37 期

半年刊

中國地熱能

CHINA GEOTHERMAL ENERGY

承印人：中国地热能出版社有限公司　　地址：香港中环干诺道中 62-63 号中兴商业大厦 8 楼　　售价：人民币 20 元

中节能咨询有限公司
CECEP Consulting Co.,Ltd.

绿色产业智库 | Green Industry Think Tank

中节能咨询有限公司是中国节能环保集团公司所属专业从事节能环保综合性咨询服务的全资子公司，同时也受集团公司委托，承担“中国节能环保集团公司产业研究中心”这一产业智库的建设任务。公司自 2002 年底成立伊始，就肩负着在节能环保领域为包括中央和各级地方政府提供咨询服务的使命，同时也面向国内外各类企事业单位、国际机构提供优质专业化咨询服务。

近年来，公司完成数百项各级政府及国际机构委托的政策、课题及规划研究项目，同时在火电热电、市政热力燃气、城市固废处理、污水处理、生态建设和环境工程、工业节能、建筑节能和新能源等领域开展了大量项目咨询。

公司累计开展咨询服务 6500 余项，项目涉及投资额超过 9000 亿元，在中国节能环保领域具有很高知名度和良好声誉，被誉为节能环保领域的“智库”。由于成绩显著，公司被发改委、财政部和环保部评为“十一五”节能减排先进单位。

自 2009 年起，公司受集团公司委托，具体承担国资委“中央企业节能减排监测中心”的建设、运维任务，对于我们的出色服务，国资委综合局每年都给集团致信表示感谢。

地址：北京市海淀区西直门北大街42号节能大厦A座16层
信箱：consulting@cecep.cn 邮编：100082
电话：(010)83052158 传真：(010)83052159
网址：www.consulting.cecep.cn

我们获得的荣誉 | Awards & Recognitions

- 《黑龙江紫金铜业有限公司铜冶炼项目节能评估报告》荣获“2017年度黑龙江省优秀工程咨询成果一等奖”
- 《蕉岭县生活污水处理设施全县捆绑PPP项目》荣获“2016-2017年度广东省优秀工程咨询成果一等奖”
- 《大观净水厂可行性研究报告技术审查报告》荣获“2016-2017年度广东省优秀工程咨询成果三等奖”
- 《湖北华电江陵发电厂一期工程项目申请报告评估报告》荣获“2016 年湖北省优秀工程咨询成果二等奖”
- 《大别山电厂二期2x660MW扩建工程项目申请报告评估报告》荣获“2016年湖北省优秀工程咨询成果优秀奖”
- 荣获国家开发银行信息科技局颁发的“2015年度优秀合作伙伴”
- 《基于环境管理战略转型的产业支撑能力案例评估》荣获“2015 年度北京市优秀工程咨询成果一等奖”
- 《绿色信贷节能环保效益评价系统》荣获“2015 年度北京市优秀工程咨询成果三等奖”

Scopes Of Business | 我们专注的业务

01	Policy and Research Analysis 政策与专题研究	受政府部门、国际机构及企事业单位委托,开展节能、环保、低碳、新能源等领域的政策法规、技术标准、行业规范的研究制定,以及行业现状、发展动态与趋势、投资机会、综合解决方案等方面的专题研究。
02	Planning Consulting 规划咨询	行业发展、区域节能环保、循环经济、低碳发展、新能源开发利用、热电联产、绿色发展、空间、环境、节水等专项规划的编制。
03	Green Financial Services 绿色金融服务	绿色金融政策研究、区域绿色金融体系规划、绿色信用评级体系和相关评估服务、绿色信用调查、绿色项目建设可行性研究、绿色项目管理咨询、绿色项目后评价、ESG 报告编制、金融机构绿色信贷统计管理整体解决方绿色项目后评价、金融机构绿色信贷统计管理整体解决方案构建、绿色项目第三方评估认证、绿色债券存续期跟踪评估。
04	Engineering Consulting 工程咨询	投资机会研究、项目建议书及可研的编制与评估、固定资产投资项目节能评估与审查、项目核准(资金)申请报告编制与评估、初步设计概算审查、融资方案咨询、项目后评价。
05	Third-party Services 第三方业务	作为政府和企业之间的独立第三方,提供包括能源审计、清洁生产审核、节能量审核、碳核查等在内的专业服务。
06	Technology Dissemination 技术推广	主要承担节能、低碳、环保技术推广政策咨询,行业共性技术市场研究,审核、碳核查等在内的专业服务。
07	Information System Services 信息系统开发	为各级政府部门、企业设计开发节能环保综合信息化管理系统,为金融机构开发绿色金融项目环境效益评估系统。

恒有源科技发展集团有限公司
EVER SOURCE SCIENCE &TECHNOLOGY DEVELOPMENT GROUP CO.,LTD.

恒有源科技发展集团有限公司（简称恒有源集团），是中国节能环保集团公司旗下的中国地热能产业发展集团有限公司（香港上市号 8128.HK，简称中国地热能）在北京的科技实业发展总部。

Ever Source Science and Technology Development Group Co. Ltd. (HYY Group) is the Beijing Head Office for science and technology development owned by China Geothermal Industry Development Group Ltd. (HKEx: 08128, China Geothermal) which is subordinate to the China Energy Conservation and Environment Protection Group.

在京港两地一体化管理框架下，恒有源集团专注于开发利用浅层地能（热）作为建筑物供暖替代能源的科研与推广；致力于原创技术的产业化发展；实现传统燃烧供热行业全面升级换代成利用浅层地能为建筑物无燃烧供暖（冷）的地能热冷一体化的新兴产业；利用生态文明建设成果，促进传统产业升级换代；走出中国治理雾霾的新路子。

With integrated administrative framework of Beijing and Hong Kong offices, the HYY Group is fully engaged in the R&D and market promotion of using shallow ground source (heat) energy as the substitute energy source of heating for buildings; in industrialized development of its original technology; to the upgrading of traditional heating industry into a new industry of integrated combustion-free heating and cooling with ground source energy; and in pioneering ways to improve ecological construction and curb haze in China.

- **员工行为准则：**
  Code of Conduct :

  安全第一，标准当家
  With safety first, standard speaks

  扎扎实实打基础，反反复复抓落实
  To form a solid foundation, to make all strategies practicable

  负责任做每件事，愉快工作每一天
  All develop sense of responsibility,and achieve pleasure at work

---

- **我们的宗旨：** 求实、创新
  Our Mission: Pragmatism and Innovation
- **我们的追求：** 人与自然的和谐共生
  Our Pursue: Harmonious Coexistence of Human and Nature
- **我们的奉献：** 让百姓享受高品质的生活
  Our Dedication: Improve comfort level of the people's livelihood
- **我们的愿景：** 原创地能采集技术实现产业化发展——让浅层地能作为建筑物供暖的替代能源；进一步完善能源按品位分级科学利用；在新时期，致力推广利用浅层地能无燃烧为建筑物智慧供暖（冷）；大力发展地能热冷一体化的新兴产业。
  Our Vision: Work for greater industrialized development of the original technology for ground source energy collection, while promoting the use of shallow ground energy as the substitute energy of heating for buildings; furthering scientific utilization of energies by grades; propelling combustion-free intelligent heating (cooling) for buildings with ground source energy; and forcefully boosting the new industry of integrated heating and cooling with ground source energy.

中国地热能

CHINA GEOTHERMAL ENERGY

主 办 **Sponsor**
承 印 **Printed by**
中国地热能出版社有限公司 China Geothermal Energy Press Limited
地 址 **Address**
香港中环干诺道中 62-63 号中兴商业大厦 8 楼 8/F., Chung Hing Commercial Building, 62-63 Connaught Road Central, Central, Hong Kong

协 办 **Co-Sponsor**
北矿大（南京）新能源环保技术研究院 Nanjing Institute For New Energy & Environmental Science And Technology
首都科技发展战略研究院 Capital Institute of Science and Technology Development Strategy
北京节能环保促进会浅层地（热）能开发利用专业委员会 Special Committee on Shallow Ground Source (Thermal) Energy Development and Utilization under Beijing Association to Promote Energy Conservation and Environmental
北京工业对外经贸促进会 Beijing Industrial Association for the Promotion of Foreign Trade & Economic
中国地热与温泉产业技术创新战略联盟 China's Geothermal and Hot-Spring Industry Union
中国热冷一体化清洁能源研究院 China Integrated Heating and Cooling Clean Energy Research Institute

国际标准刊号 :23098457 ISSN:23098457

发行部 **Publishing Department**
纪少樱　彭　芳 Kei Siu Ying, Peng Fang
广告部 **Advertising Department**
彭　芳 Peng Fang
地址、联系电话 **Address,Telephone**
北京市海淀区杏石口路 102 号　+8610-62592988 Address: No.102,Xingshikou Road, Haidian District, Beijing +8610-62592988

目录

CONTENTS

本期焦点

CURRENT FOCUS

氢能是清洁高效的二次能源。具有资源丰富、来源广泛、燃烧热值高、清洁无污染、利用形式多样、可作为储能介质等诸多优点。浅层地热能是清洁的可再生能源。具有储量巨大、再生迅速、分布广泛、温度适中、稳定性好等优点，是取之不尽、用之不竭的巨大绿色能源宝库。

封面 / 目录图片 供图：王赫

中国地熱能
CHINA GEOTHERMAL ENERGY

2022 年 12 月
第 37 期
半年刊

CONTENTS

中國地熱能
CHINA GEOTHERMAL ENERGY

Dec 2022
Issue 37
Biannual Publication

氢能 + 浅层地热能耦合供暖（冷）系统初探

A PRELIMINARY STUDY ON THE COUPLING HEATING（COOLING）SYSTEM OF HYDROGEN ENERGY AND SHALLOW GEOTHERMAL ENERGY

作者：刘宝红（恒有源科技发展集团副总裁）

1. 提要

氢能是清洁高效的二次能源，具有资源丰富、来源广泛、燃烧热值高、清洁无污染、利用形式多样、可作为储能介质等诸多优点。浅层地热能是清洁的可再生能源，是指地表以下 200 米深度范围内，在当前技术经济条件下具备开发利用价值的蕴藏在地壳浅部岩土体和地下水中温度低于25°C的低温地热资源。具有储量巨大、再生迅速、分布广泛、温度适中、稳定性好等优点。本文提出氢能 + 浅层地热能耦合供暖（冷）系统技术方案，利用氢能燃料电池发电驱动浅层地热能热泵系统工作，构建可以独立运行的清洁供电、供暖、制冷、供生活热水系统，形成低成本、高效、清洁的分布式综合能源利用系统。探讨不同耦合方式对初投资、运行费用和用户负担的影响，确定并优化耦合方式和比例。

氢能 + 浅层地热能的耦合供暖（冷）系统适合不具备电力条件的地区，特别适合广大缺少电的农村地区，能降低供暖成本、提高供暖可靠性，实现采暖领域的节能、环保、节约、居民可承受。

2. 研究的目的

中国在 2020 年将氢能纳入“十四五”规划及 2035 愿景，助力我国“碳达峰、碳中和”战略目标的实现。尤其是，我国幅员辽阔，具有丰富的清洁能源资源，在清洁低碳的氢能供给上具有很大的潜力。

当前，我国已开启氢能产业顶层设计，地方政府与企业积极参与氢能布局，氢能技术链逐步齐全完善，氢能产业链也正在逐渐形成。

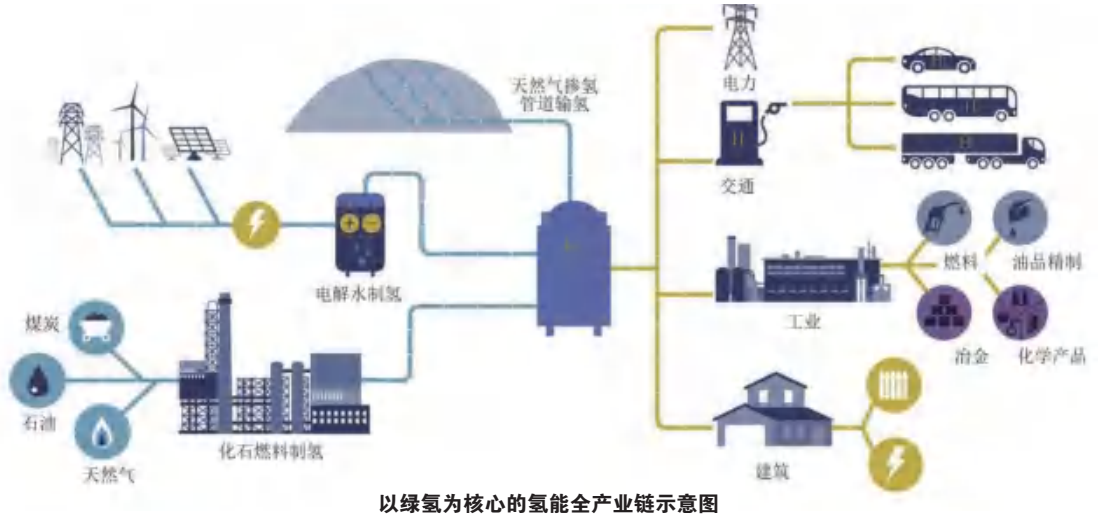

以绿氢为核心的氢能全产业链示意图

氢能 + 浅层地热能耦合供暖（冷）系统可实现分布式冷热电联供，可为电力系统调峰、提高供电可靠性，可作为清洁可再生综合能源为建筑供暖（冷）及提供生活热水，在未来建筑供暖领域可发挥不可替代的重要作用。显然，氢能 + 浅层地热能耦合供暖系统能解决我国新能源大规模接入带来的间歇性问题、清洁供暖电网、环境污染和碳减排问题，无疑将极大推动新能源在我国的快速发展，促进能源转型，满足我国国民经济和社会发展的需要。

3. 氢能 + 浅层地热能耦合供暖（冷）系统

3.1 氢能 + 浅层地热能耦合供暖系统

氢能 + 浅层地热能耦合供暖系统可以形成完全独立、连续稳定的离网供电、供暖、制冷、提供热水系统。根据产品的适应性和系统特点，分为分布式发电分户供暖（冷）系统和分布式发电集中供暖系统。

3.1.1 分布式发电分户供暖系统

3.1.1.1 氢能家用热电联供燃料电池 + 分户自采暖系统耦合

类似天然气 + 地能热泵三联供系统，氢能与燃料电池也可耦合应于建筑物供能。燃料电池系统的燃料为城市燃气，具体为天然气、煤气、LPG 等。

氢能家用热电联供燃料电池 + 分户自采暖系统耦合的三联供系统由六部分组成：燃料处理子

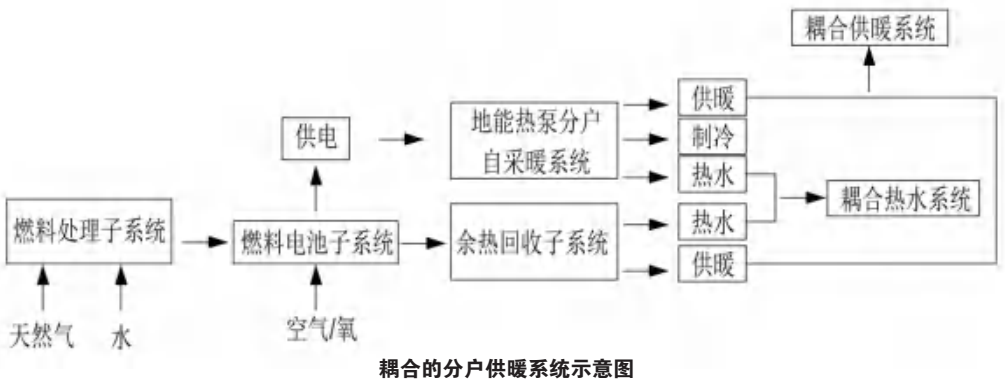

耦合的分户供暖系统示意图

系统、燃料电池系统、电力电子子系统（供电）、余热回收子系统、耦合热水系统、耦合供暖（冷）系统。首先，燃料处理子系统将燃气重整为氢气，输送至燃料电池系统进行发电；其次，电力电子子系统将燃料电池产生的直流电转化为交流电，供地能热泵分户自采暖系统使用或并入电网；然后，余热回收子系统将燃料电池发电产生的余热回收、储存，用于供暖、供热水；最后，根据冬季、夏季建筑物的冷热需求组成耦合的热水系统、耦合供暖（冷）系统。

3.1.1.2 国内外可选配的设备

① 燃料电池设备

在欧美、日本等国家，燃料电池建筑供能系统已进入商业化应用阶段。德国的 SOLIDPOWER 公司是小型 SOFC 燃料电池行业先驱，具有强大技术创新能力。其核心产品 BlueGEN 号称世界上最高效的 m-CHP 设备，全球安装数量已经超过 1000 台。BlueGEN 利用天然气发电作为燃料源供能，输入 2.5kW 燃料，输出 1.5kW 电和 0.6kW 热，综合效率达 85%。

日本已有超过 20 万套家用燃料电池供能系统在运行，是世界上燃料电池应用最广泛的国家。日本家用燃料电池供能系统以城市燃气为燃料，主要由燃料电池和储热水箱组成，燃料电池用于发电，水箱用于回收余热。市面上主流产品包括松下、爱信精机和东芝等，具体参数如下所示。

ENE-FARM系列

制造商		爱信精机	松下	东芝
燃料电池类型		固体氧化物	聚合物电解质	聚合物电解质
输出功率		700W	700W	700W
热水存储量		90升，约70°	140升，约60°	200升，约60°
效率	发电效率	46.5%（净热效率）	39.0%（净热效率）	39.0%（净热效率）
	总效率	90.0%（净热效率）	95.0%（净热效率）	95.0%（净热效率）
耐久性		10年	10年	10年

耦合的分户供暖系统示意图

② 地能热泵分户供暖设备

地能热泵分户供暖设备在我国已大面积推广应用，根据末端系统形式可分为地能热冷一体机末端为冷热风型、地能热冷一体机户式热水型设备。

1) 热能热冷一体机变频产品

序号	工质	产品系列	规格型号		严寒地区【注 1】	寒冷地区【注 2】		冬冷夏热地区【注 3】		参考供暖面积（㎡）
					制热量（kW）	制热量（kW）	制冷量（kW）	制热量（kW）	制冷量（kW）	
1	R410A	地能热冷一体机（变频）	变频 2P 一拖二卧机	卧 DNV-I-56AN2	5.0	5.6	5.6	6.2	5.6	≤ 60（单间房≤ 30）
2			变频 2P 一拖二挂机	挂 DNV-I-56AN2	5.0	5.6	5.6	6.2	5.6	≤ 60（单间房≤ 30）
3			变频 3P 一拖三卧机	DNV-I-75AN3	6.8	7.6	7.6	8.3	7.6	≤ 90（单间房≤ 30）
4			变频 3P 一拖三挂机	DNV-I-75AN3	6.8	7.6	7.6	8.3	7.6	≤ 90（单间房≤ 30）

一拖二变频（内卧机和内挂机可以随意搭配）

一拖三变频（内卧机和内挂机可以随意搭配）

设备均为 220V 小功率配电，末端为热（冷）风型，供暖速度快，分间配置和使用，人在哪屋开哪屋设备，可最大限度的实现行为节能。

2) 热能热冷户式热水机产品

地热能户式热水机设备为 220V 小功率配电，末端为热（冷）水型，可与地板辐射采暖、散热器、风机盘管末端系统结合。

序号	工质	产品系列	规格型号		严寒地区【注 1】	寒冷地区【注 2】		冬冷夏热地区【注 3】		参考供暖面积（㎡）
					制热量（kW）	制热量（kW）	制冷量（kW）	制热量（kW）	制冷量（kW）	
1	R410A	地能热泵锅炉	3P 地能热泵锅炉	DNS-II-75A	7.2	8	6.4	9.4	6.4	≤ 130
2			6P 地能热泵锅炉	DNS-II-150A	14.4	16	12.8	18.8	12.8	≤ 260
3			9P 地能热泵锅炉	DNS-II-225A	21.6	24	19.2	28.2	19.2	≤ 390

注 1：严寒地区制热量是指在哈尔滨、长春、沈阳、呼和浩特等地区，当室外极端温度 -48.5℃时，浅层地热能温度 9℃左右，热泵的稳定供热量。

注 2：寒冷地区制热量是指在延安、北京、天津、石家庄、济南、太原、郑州、西安等地区，当室外极端温度 -25℃时，浅层地热能温度 15℃左右，热泵的稳定供热量。

注 3：冬冷夏热地区制热量是指在上海、南京、杭州、合肥、武汉、南昌、福州、长沙等地区，室外极端温度 -12℃时，浅层地热能温度 19℃左右，热泵的稳定供热量。

3.1.1.3 耦合供暖系统特点

特点：每户是独立的能源利用系统，不依赖电网运行，减少了能源输送投资和运行成本；运行灵活，环保无有害物质排放。

发展前景：可以分布式实现单户自发自用、发用结合，清洁无污染，是最理想的用户端用能方式。

3.1.2 分布式发电集中供暖系统

3.1.2.1 氢能燃料电池发电站与地能热泵集中供暖系统耦合

氢能能量密度高，较传统储能方式，能够实现储能容量数量级的提升。通过废弃的风力发电、光伏发电等可再生能源可低成本制取氢气，完成电 - 氢 - 电循环的转化，可实现可再生电力更加可控、稳定、安全的供应。国内氢能燃料电池发电站应用技术较为成熟，已成功的应用交通、应急电源等场景。利用氢能燃料电池发电站与地能热泵集中供暖系统的耦合系统能为大面积建筑或建筑群供暖、制冷、提供热水。

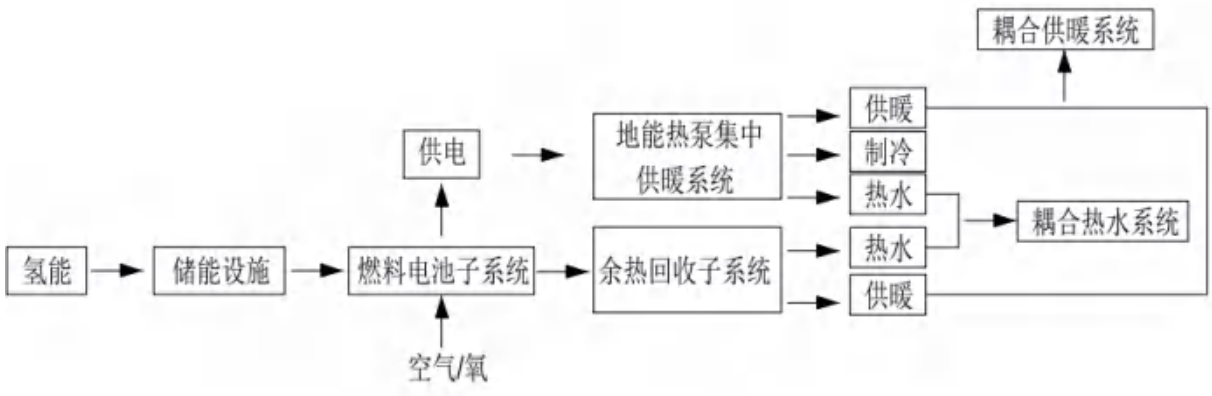

耦合的集中供暖系统示意图

3.1.2.2 国内外可选配的设备

① 氢能燃料电池发电站设备

2013 年，德国建成了第一个商业化的风电制氢多能互补项目— —h2-herten。该项目每年能够提供 250MW · h 的电力和将近 6500kg 的氢气，其中一部分氢气通过燃料电池为附近的一个办公建筑提供足够的电力。同样，法国在科西嘉岛启动完成 MYRTE 发电项目，该项目装设了 560kW 的光伏发电设备，50kW 的电解水装置以及 100kW 的 PEMFC 燃料电池。

国内氢能燃料电池发电站技术很成熟，多应用与汽车、应急电源等场景。上海恒劲动力 100kW 的氢能燃料电池发电站设备相关参数如下：

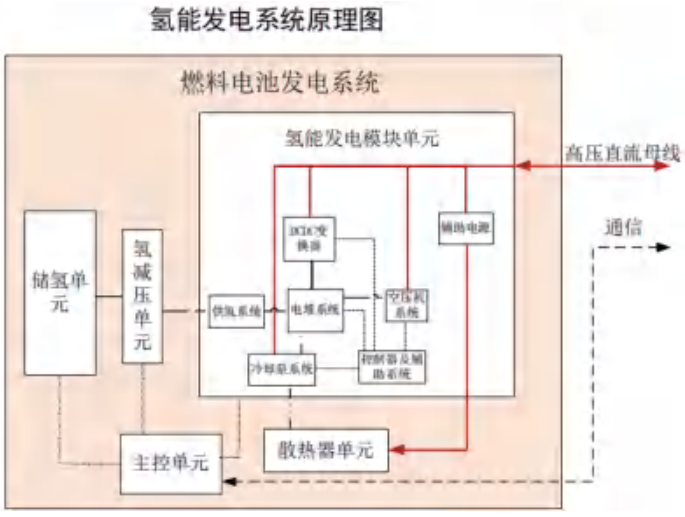

氢能发电模块单元（电堆模块）1150*660*476mm

氢能发电模块单元（综合模块） 1135*660*591mm

00kW 独立氢能燃料电池发电站参数如下表：

范畴	项目	参数
氢能电源发电系统	型号	HAWS30K/60K/130K-A01
	类型	PEM
	额定输出功率（kW）	37/68/131
	最大输出功率（kW）	41/74/143
	额定电压(V)	87/174/348
	启动温度范围(℃)	-15
	电堆最高工作温度(℃)	85
	累计连续寿命(hrs)	3000
	工作年限(years)	10年
	电堆比功率(kW/kg)	2.20
	电堆功率密度(kW/l)	2.65
	启动电池(kWh)	3
	效率	53%
	电堆启动时间（无启动电池）	15s
	单位面积功率密度(W/cm2)	0.58
	额定单片电压(V)	0.65

② 浅层地热能集中供暖设备

地能热泵集中供暖产品规格型号较多，从涡旋压缩机到螺杆压缩机、离心机等都有对应规格，单台热泵主机可满足几千甚至上万平米规模建筑的供暖需求，常见地能热泵主机单台制热量从 10kW-2000kW 不等。

涡旋压缩机热泵（民用）：
供冷热功率：10～100kW

供冷热功率：150～2000kW

供冷热功率：500～2000kW

海水源热泵机组：
供冷热功率：500～2000kW

污水源热泵机组：
供冷热功率：500～2000kW

高温热泵机组：
供冷热功率：200～1500kW

3.1.2.3 耦合供暖系统特点

耦合供暖系统功能：为一栋建筑或是多个建筑群集中供暖、制冷、提供热水。

特点：一栋建筑或是多个建筑群是独立的能源利用系统，不依赖电网运行，无有害物质排放；氢能装置设备置于建筑公共地带，具体实施安全性能更易满足。

发展前景：可以分布式实现区域建筑自发自用、发用结合，清洁无污染，是新型分布式综合能源利用方式。

3.2 氢能 + 浅层地热能耦合供暖系统的成本及经济环境效益

3.2.1 初始投资

① 氢能家用热电联供燃料电池 + 分户自采暖系统耦合

日本东京 2020 年奥运选手村 5000 多住户全部采用氢能家用热电联供燃料电池系统供能，每户设备总成本约 140 万日元，折合人民币 8.84 万元；对应 100 ㎡建筑地能自采暖系统投资约 2.5 万元；耦合系统总投资约 11.34 万元 / 户。参考 BlueGEN 设备参数，每户配置发电功率为 1.5kW 的氢能家用热电联供燃料电池，耦合浅层地热能分户热泵系统能供热 6kW，加上发电供热水负荷 0.6kW，户小时最大供热 6.6kW。氢能家用热电联供燃料电池系统投资按发电功率核计 5.89 万 /kW，按耦合供暖功率核计 1.34 万 /kW；另浅层地热能分户热泵系统投资按耦合供暖功率核计 0.38 万元 /kW；耦合系统整体投资合计 1.72 万元 /kW。

② 氢能燃料电池发电站与地能热泵集中供暖系统耦合

氢能燃料电池系统成本价约 1 万元 /kW，成套 100kW 氢能燃料电池发电站市场售价约 180 万元。参考上海恒劲动力 100kW 的氢能燃料电池发电站设备相关参数，对应地能热泵系统供暖功率 400kW，加上发电供热水负荷 60kW，合计供暖功率 460kW，可以担负 9000 平米建筑供暖。地能热泵系统投资约 200 万元（不含采暖末端系统），耦合系统总投资约 380 万元，耦合系统整体投资合计 0.826 万元 /kW。

3.2.2 运行成本

运行费用的影响因素有制氢成本、系统发电效率等，主要因素是制氢成本。首先是制氢成本高，目前制氢成本和运输加注成本几乎是 1:1 的，煤质氢成本约 2 元 / 立方米，到了加氢站就变成了 4 元 / 立方米，按照 11 立方米约一千克计算，氢气成本约 44 元 / 千克。目前市场氢气售价 70 元 / 千克，能源价格较高，运行成本按产业化发展后的氢能成本 10 元 / 千克核算比较。

供暖系统	设备供热量	一个采暖季能耗	能源单价	运行成本（元）
电采暖系统	6kW	耗电 10500kWh	电价 0.52 元 / 度	5460
地热能热泵系统	6kW	耗电 2625kWh	电价 0.52 元 / 度	1365
氢能锅炉系统	6kW	折合氢气 3233m³，293.8 千克	氢气 44 元 / 千克	12927.2
			氢气 10 元 / 千克	2938
氢能家用热电联供燃料电池 + 分户自采暖系统耦合	6.9kW	折合氢气 4565m³，计 415 千克	氢气 44 元 / 千克	18260
			氢气 10 元 / 千克	4150

当氢能成本 10 元 / 千克时，氢能家用热电联供燃料电池 + 分户自采暖系统耦合供暖系统运行成本为 4150 元（6.9kW,1 个采暖季），较电采暖系统便宜 23.9%，但较氢能锅炉系统高 29%，较地热能热泵系统高 67%。

3.2.3 综合能源效率

综合能源效率受制氢技术、燃料电池发电效率以及综合热转化效率影响。电能与浅层地热能的耦合供暖（冷）系统效率如下图所示。

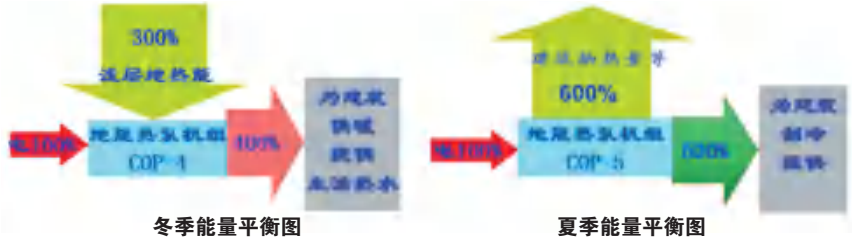

冬季能量平衡图　　夏季能量平衡图

① 氢能家用热电联供燃料电池 + 分户自采暖系统耦合采用基于天然气、煤气等的氢能燃料电池发电技术路线，具体为“天然气 / 煤→天然气 / 煤气化制氢（取天然气重整效率 65%）→储氢（效率 90%）→氢燃料电池发电（效率 60%）+ 发电产热（效率 24%）→地能热泵系统供暖”。

供暖总效率 65%×90%×（60%+24%）×400%=196%；

制冷总效率 65%×90%×60%×500%=175%。

② 氢能燃料电池发电站与地能热泵集中供暖系统耦合采用基于可再生清洁风能发电、光伏发电→电解水制氢（取电解水效率 60%）储氢（效率 90%）→氢燃料电池发电（效率 50%）+ 发电产热（效率 30%）→地能热泵系统供暖”。

供暖总效率 60%×90%×（50%+30%）×400%=172%；

制冷总效率 60%×90%×50%×500%=135%。

3.2.4 运行节能量分析

参考北京地区 100 ㎡建筑冬季供暖热负荷 10500kWh 分析，其中发电按全国 6000 千瓦及以上火电厂供电标准煤耗 312 克 / 千瓦时考虑、氢燃料热值 32352 大卡 / 千克、2.4m^3 氢气的热值相当于 1 千克标煤的热值、1m^3 氢气（11m^3 氢气重量 1kg）发电 1.5 度、参考 BlueGEN 设备参数发电效率 60%、热水效率 24%。氢气压缩（损失 3% ~ 6%）、运输（损失 2% ~ 3%）、零售（损失 10%），整体取能源运输损失 15%。不同方式的供暖能耗和节能量分析如下表：

供暖系统	能源转换方式	设备供热量	供暖系统效率	能源输送损耗后效率	一个采暖季能耗	折合标煤（kg）	节能量（%）
电采暖系统	集中电网输送至每户，电能转换为热能	6kW	1	0.6	耗电 10500kWh	5460	0
地热能热泵系统	集中电网输送电能驱动热泵工作	6kW	4	2.4	耗电 2625kWh	1365	75.0
氢能锅炉系统	氢能燃烧转换为热能	6kW	0.95	0.8	折合氢气 3233m^3，293.8 千克	1683.9	69.2
氢能家用热电联供燃料电池 + 分户自采暖系统耦合	利用氢能发电驱动热泵工作	6.9kW	2.3	2.3	折合氢气 4565m^3，415 千克	827.0	84.9

以上分析得出，在电采暖系统、地热能热泵系统、氢能锅炉系统、氢能家用热电联供燃料电池 + 分户自采暖系统耦合供暖系统中，节能效率从大到小依次为氢能家用热电联供燃料电池 + 分户自采暖系统耦合供暖系统 > 地热能热泵系统 > 氢能锅炉系统 > 电采暖系统，氢能家用热电联供燃料电池 + 分户自采暖系统耦合供暖系统较氢能锅炉节能高出 15.7%。

3.2.5 环境效益

1. 氢能家用热电联供燃料电池 + 分户自采暖系统耦合采用基于天然气、煤气等的氢能燃料电池发电技术路线，整个过程只有氢能制取过程会产生 CO2 的排放，热电联供燃料电池和地能热泵系统均为零污染零排放过程。其中制取每 Kg 氢气，采用天然气重整技术 CO2 的排放量为 9Kg，采用煤气化技术 CO2

的排放量为 12Kg。

2. 氢能燃料电池发电站与地能热泵集中供暖系统耦合采用基于可再生清洁风能发电、光伏发电电解水制取氢路线，由于采用风能发电、光伏发电清洁电力来源，整个过程没有 CO2 的排放。

3.3 不同方式耦合的供暖系统投资、运行成本分析

氢能家用热电联供燃料电池 + 分户自采暖系统的耦合系统投资主要是受热电联供燃料电池价格影响，系统供热负荷小，敏感性波动较大。

选用氢能燃料电池发电站与地能热泵集中供暖系统的耦合系统与地热能热泵系统进行不同比例复合系统的分析。其中燃料电池系统效率取 0.8，发电效率 0.5、供热水热效率 0.3；燃料发电系统投资按成本 1 万元 /kW 和产业化后 0.5 万元 /kW、0.1 万元 /kW 分别核算。

不同耦合方式的初投资、运行成本分析表

供暖系统	能源转换方式	电功率（kW）	分项供暖负荷（kW）	供暖总负荷（kW）	供暖系统效率	能源输送损耗后效率	供暖面积（㎡）	一个采暖季能耗	能源单价	运行成本（元/kW）	运行成本（元/平米）	投资（元/kW）燃料发电系统1万元/kW	投资（元/kW）燃料发电系统0.5万元/kW	投资（元/kW）燃料发电系统0.1万元/kW	氢能+浅层地热能耦合系统承担供暖负荷比例（%）
电采暖系统	集中电网输送至每户，电能转换为热能	100	100	100	1	0.6	2000	耗电21万kWh	电价0.52元/度	1092	54.6	2200	2200	2200	/
地热能热泵系统	集中电网输送电能驱动热泵工作	100	400	400	4	2.4	8000	耗电21万kWh	电价0.52元/度	273	13.65	4000	4000	4000	0
氢能燃料电池发电站与地能热泵集中供暖系统的耦合	氢能就地发电利用驱动热泵工作	100	400	460	2.3	2.3	9200	折合氢气42万m3，计38.18吨	氢气44元/千克	3652	182.6	5652.2	4565.2	3695.7	100
			60						氢气10元/千克	830	41.5				100
50%（氢能+浅层地热能耦合）+50%地热能复合系统	氢能就地发电利用驱动热泵工作	50	200	470	3.15	1.89	9400	折合氢气21.5万m3，计19.5吨	氢气44元/千克	1961.6	98.1	4808.5	4276.6	3851.1	50
			30						氢气10元/千克	551.0	27.5				50
	地热能热泵系统	60	240					耗电12.3万kWh	电价0.52元/度	/	/				50
30%（氢能+浅层地热能耦合）+70%地热能复合系统	氢能就地发电利用驱动热泵工作	30	120	458	3.49	1.726	9200	折合氢气12.6万m3，计11.45吨	氢气44元/千克	1290.7	64.3	4497.8	4170.3	3908.3	30
			18						氢气10元/千克	440.7	21.9				30
	地热能热泵系统	80	320					耗电16.8万kWh	电价0.52元/度	/	/				70

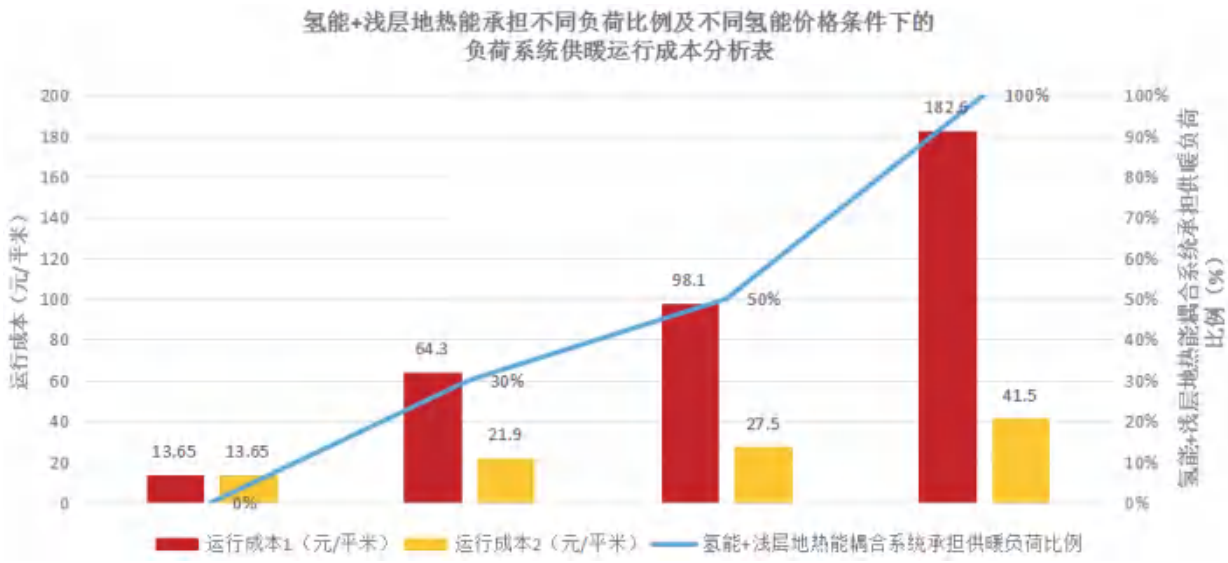

运行成本 1——氢能售价 44 元 / 千克

运行成本 2——氢能售价 10 元 / 千克

综上对应不同方式的系统分析，当氢能售价 44 元 / 千克时，30%(氢能 + 浅层地热能耦合）+70% 的地热能复合系统供暖费用为 64.3 元 / 平米，高于电采暖系统 15%，供暖费用偏高；当氢能售价 10 元 / 千克时，50%(氢能 + 浅层地热能耦合）+50% 地热能复合系统和 30%(氢能 + 浅层地热能耦合）+70% 地热能复合系统供暖费用分别为 27.5 元 / 平米、21.9 元 / 平米，与城市热力取费标准接近，用户能承受。

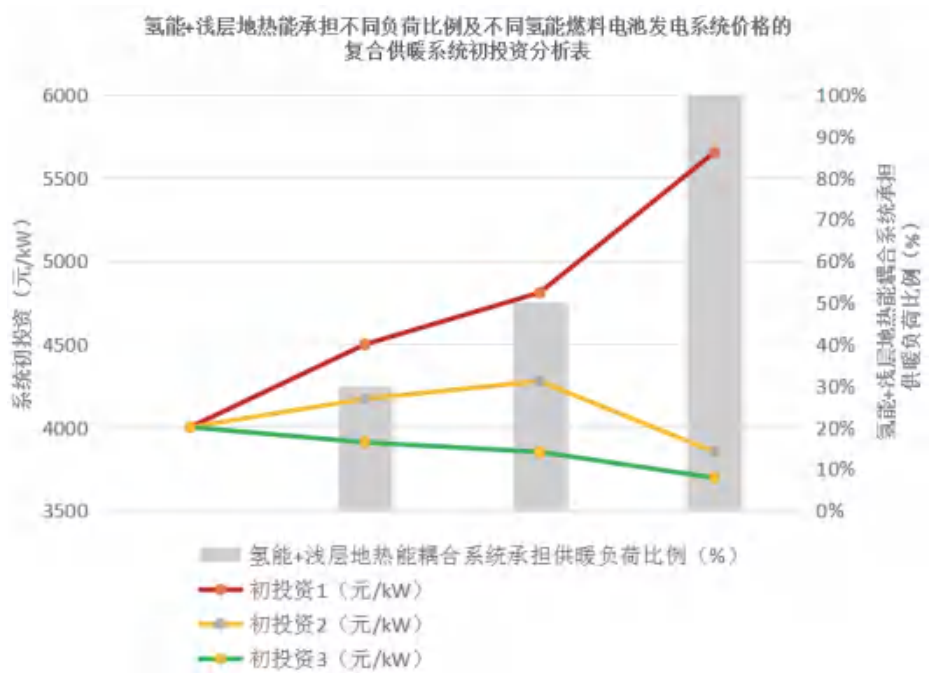

初投资 1——氢能燃料电池发电系统投资按成本 1 万元 /kW

初投资 2——氢能燃料电池发电系统投资按成本 0.5 万元 /kW

初投资 3——氢能燃料电池发电系统投资按成本 0.1 万元 /kW

按现有氢能燃料电池发电系统投资按成本 1 万元 /kW 核算，氢能燃料电池发电系统与地能热泵集中供暖系统的复合投资为 5652.2 元 /kW 最高，50%(氢能 + 浅层地热能耦合）+50% 地热能复合系统和 30%(氢能 + 浅层地热能耦合）+70% 地热能复合系统投资分别高于地热能热泵系统 16.8%、11%，投资略高。按现有燃料发电系统产业化后投资按成本 0.1 万元 /kW 核算，地热能热泵系统投资为 4000 元 /kW 最高，依次为 30%(氢能 + 浅层地热能耦合）+70% 地热能复合系统投资 3908.3 元 /kW > 50%(氢能 + 浅层地热能耦合）+50% 地热能复合系统 3851.1 元 /kW > 氢能燃料电池发电站与地能热泵集中供暖系统的耦合投资 3695.7 元 /kW 。

3.4 耦合系统的创新点

为保证燃料电池在适宜的温度下工作，须采用冷却方法消除热量，冷却带走的热量可以作为热水供暖、提供热水，水 / 水换热器因换热系数高、换热器面积小、传热高效稳定，适合燃料电池系统使用。

对于氢能 + 浅层地热能耦合供暖系统，冬季和过渡季燃料电池发电产热量可以作为供暖、生活热水热源。而对于同一个系统来说，夏季建筑自身需要排走大量热量来降低室内环境温度，燃料电池发电产热量会变成多余热量，浅层地热能系统可以作为很好的低温冷却源为电池堆系统降温，包括冬季和夏季工况，浅层地热能冷却系统也可作为燃料电池系统的低温冷却源。通过耦合系统的合理设计配置及控制，利用浅层地热能冷却系统可以提高浅层地热能供给温度，冬季提高地能热泵系统效率，作为提高耦合系统综合能源效率的一个重要措施。

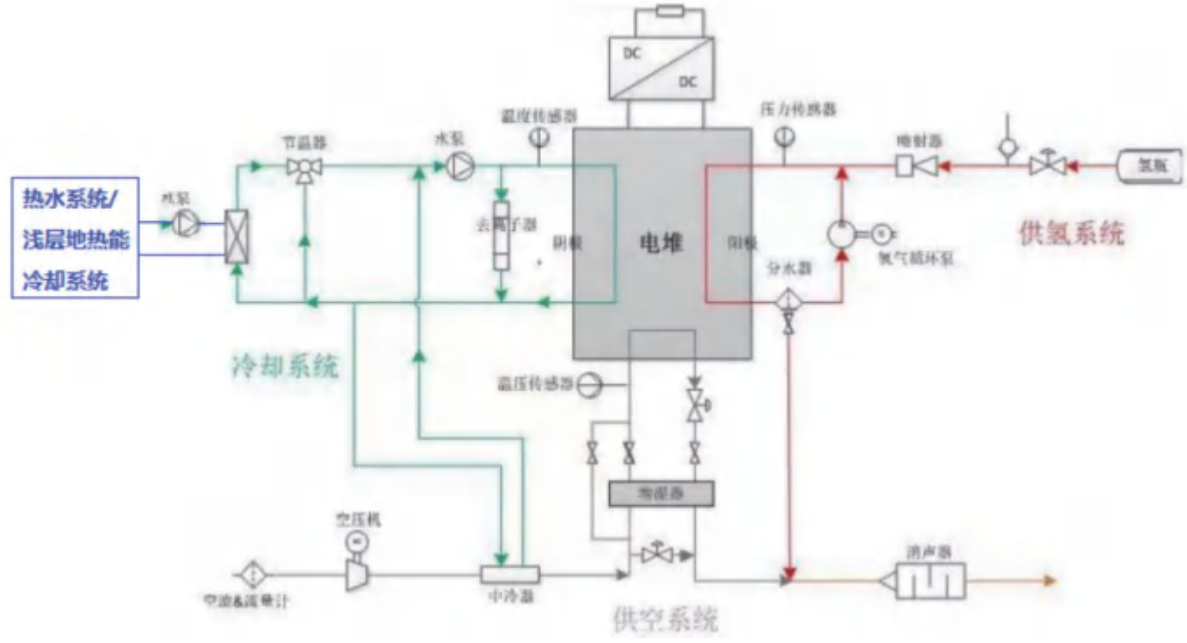

燃料电池堆的热水系统 / 浅层地热能冷却系统示意图

4. 结论

氢能是氢（H）在物理与化学变化过程中释放的能量，具有清洁高效、可储能、可运输、应用场景丰富等特点。可以通过多种方式制取，资源制约小，利用燃料电池，氢能通过电化学反应直接转化成电能和水，不排放污染物，发电效率超过 50%，是零污染的高效能源。

浅层地热能作为绿色环保的可再生资源，由于它具有储量巨大、再生迅速、分布广泛、稳定性好等优点，已成为替代传统供暖能源的首选能源，因此浅层地热能的开发与利用对中国构建资源节约型和环境友好型社会发挥着重要作用，在中国能源结构改革中也占重要地位。

氢能和浅层地热能科学耦合，得到初投资低、运行成本低、安全可靠的清洁供暖方案是可以期待的。

全球温室气体浓度再创新高

GLOBAL CONCENTRATIONS OF GREENHOUSE GASES HAVE HIT NEW HIGH

作者：许小峰（现任中国气象服务协会会长，中国气象局原副局长）

10 月 26 日，世界气象组织（WMO）公布了一份令人不安的最新温室气体公报（Greenhouse Gas Bulletin）。根据报告提供的信息，在世界各国为应对气候变化不断做出努力的进程中，影响气候增暖的三种主要温室气体——二氧化碳（Carbon Dioxide，CO2）、甲烷（Methane，CH4）和一氧化二氮（Nitrous Oxide，N2O）在大气中的水平，在 2021 年均创下了历史新高，2015 年至 2021 年是有记录以来最热的七年

2021 年的二氧化碳浓度为 415.7 ppm，甲烷为 1908 ppb，一氧化二氮为 334.5 ppb。相对于人类开始工业化之前，即人类活动开始改变大气中这些气体存在的自然平衡之前，这些含量分别为原均值的 149%、262% 和 124%，都有了较大幅度的提升。

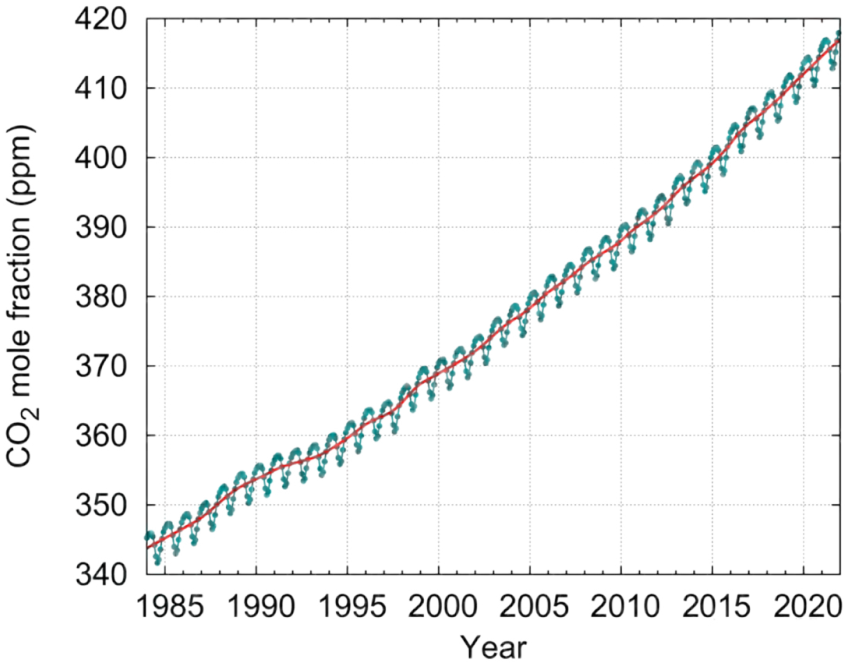

二氧化碳历年增长变化（WMO 网站）

受到广泛关注的二氧化碳含量，2020 至 2021 年的增幅超过了过去十年的平均年增长率。且根据 WMO 全球大气观测网站的测量结果显示，2022 年的含量水平仍在继续上升。1990 年至 2021 年，通过辐射强迫引发气候变暖的温室气体已增加了近 50%，其中二氧化碳增长占比约为 80%。

从 40 年前开始有了系统测量以来，2021 年甲烷浓度出现了最大同比增幅。对这种异常增长的原因尚有待分析，但初步认为是由生物过程和人类活动共同引发的结果。

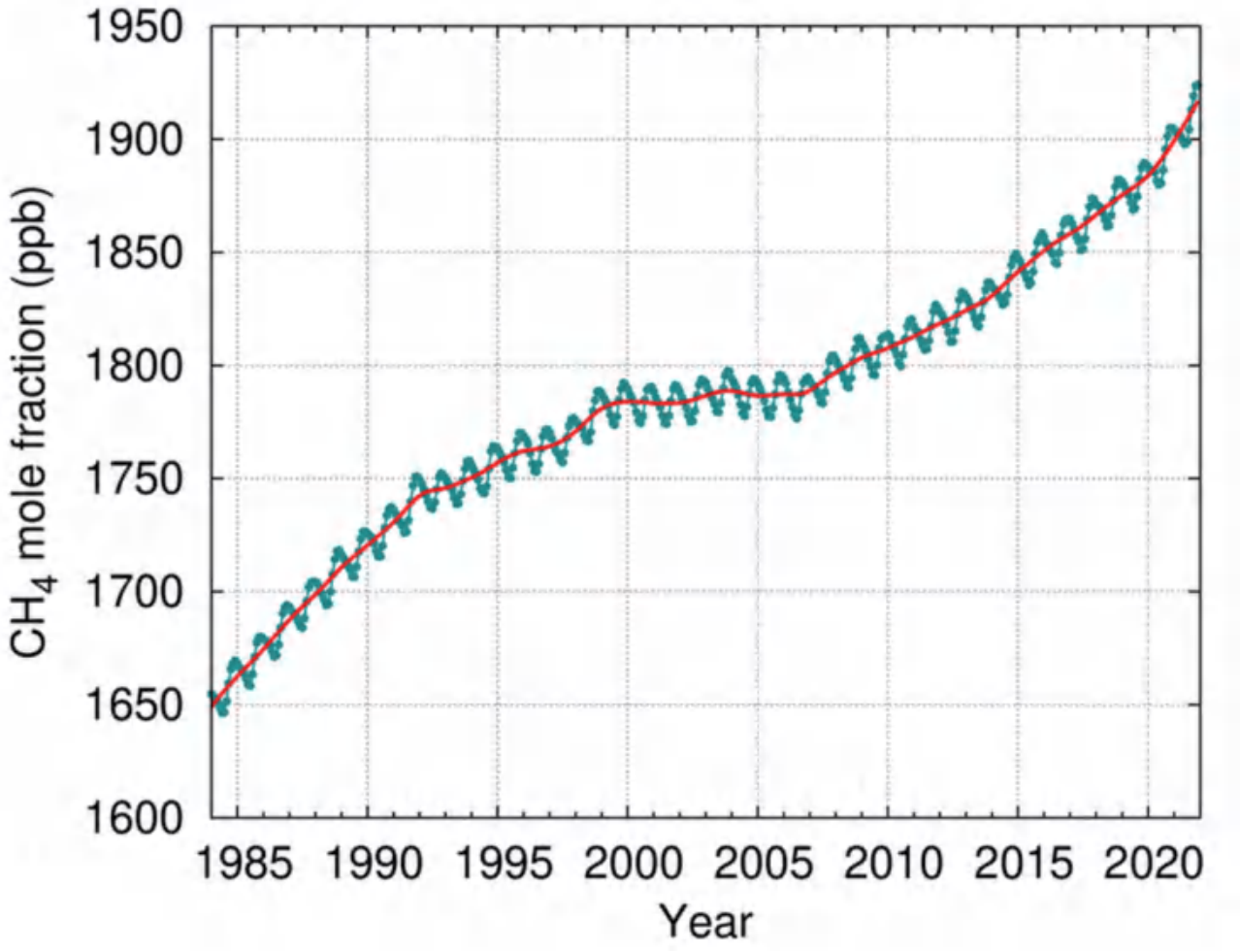

甲烷历年增长变化（WMO 网站）

WMO 秘书长塔拉斯（Petteri Taalas）教授说：“WMO 的《温室气体公报》再次强调了采取紧急行动减少温室气体排放，以防止全球气温进一步上升的巨大挑战和至关重要性。主要温室气体浓度的持续上升，包括甲烷水平的创纪录加速，表明我们仍在朝着错误的方向行进。”

一氧化二氮历年变化（WMO 网站）

塔拉斯特别强调，“我们需要改变我们的工业、能源和运输系统，及整个生活消耗能源方式，特别是要降低化石燃料产生排放。所做的改变在经济上和技术上都是可行的，可以做到成本效益的平衡，我们应该毫不延迟地采纳。寿命相对较短的甲烷，其气候效应还是可逆的，首要且最为紧迫的措施应是削减二氧化碳排放，其是导致气候变暖和相关极端天气频发的主要诱因，造成极地冰损，海平面上升，气候影响效应将达数千年。”

第 27 届联合国气候变化大会（COP 27）将于 11 月 7 日至 18 日在埃及的沙姆沙伊赫（Sharm-el-Sheikh）举行，会议前夕，WMO 公布的报告旨在促进 COP27 谈判代表能成为有效行动的决策者，以实现《巴黎协定》确定的目标，即将全球变暖增幅控制在相对于工业化前平均水平的 2 摄氏度以内，尽可能在 1.5 摄氏度以内。目前，全球平均气温较 1850-1900 年工业化前的平均水平高出 1.1° C 以上。

从世界气象组织报告提供的信息看，形成共识、建立规则和目标固然重要，但若没有可行的具体措施和监督机制，使各国共同采取有效行动，形成合力，减排和应对气候变化之路让将是艰难和曲折的。

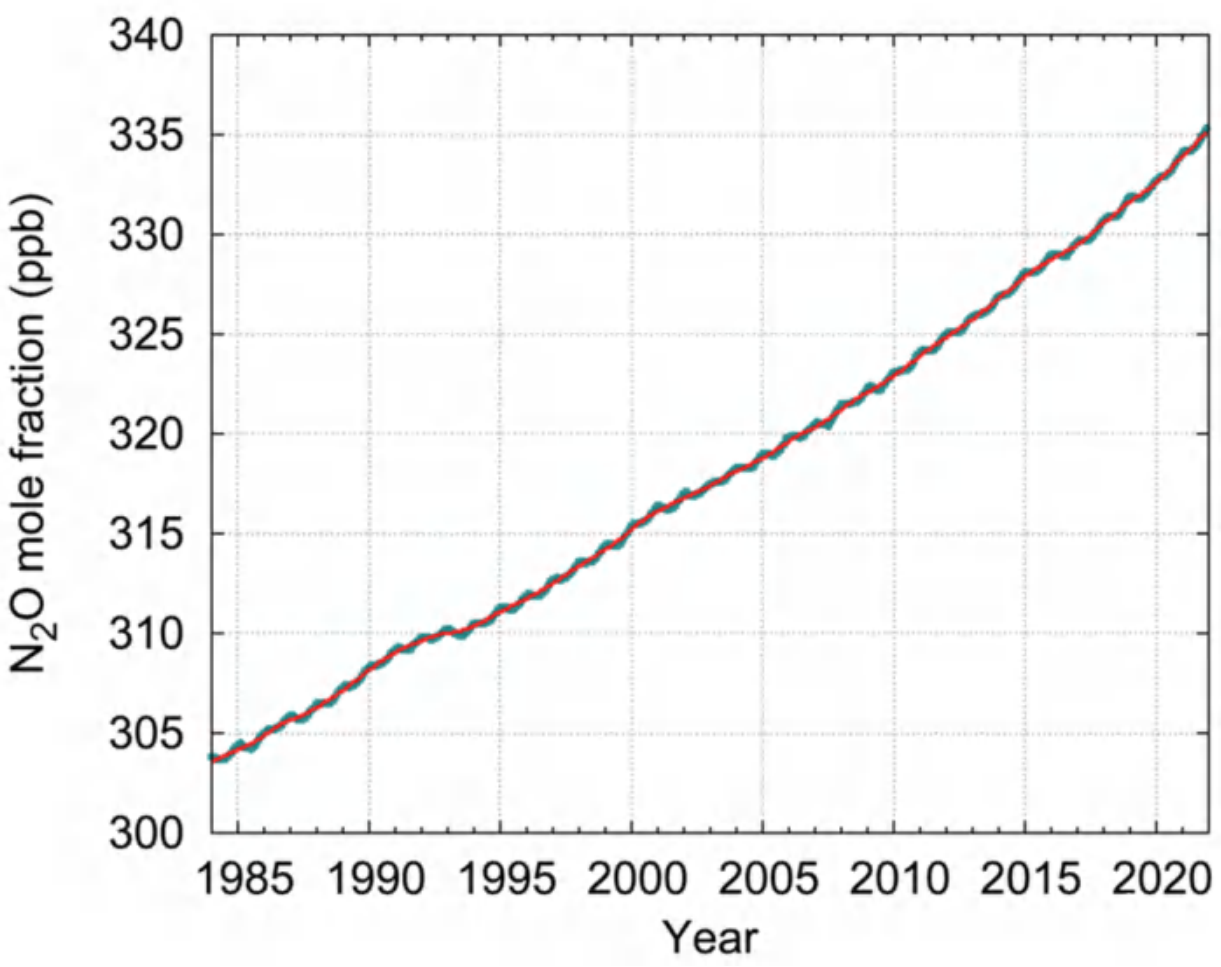

再探青藏高原十大关键地学科学问题

——《地质学报》百年华诞纪念

REVISITING THE TEN KEY GEOSCIENTIFIC PROBLEMS IN THE QINGHAI-TIBET PLATEAU

—— 《ACTA GEOLOGICA SINICA》100th Anniversary

作者：许志琴[1,2]，李广伟[1]，张泽明[2]，李海兵[2]，王岳军[3]，彭淼[4]，胡修棉[1]，易治宇[3]，郑碧海[1]

1. 南京大学内生金属矿床成矿机制研究国家重点实验室，南京大学地球科学与工程学院，南京大学大陆动力学研究院，江苏南京，210034；
2. 中国地质科学院地质研究所，北京，100037；
3. 中山大学，广东珠海，510275；
4. 中国地质大学（北京），北京，100083

内容提要：本文重新审视了青藏高原的关键科学问题，为解决板块构造理论的“登陆”难题提供新的线索，为理解板块汇聚边界的大陆岩石圈演化及其能源资源、地质灾害和全球环境效应提供新的思路。本文探讨了青藏高原如下十大关键地学问题：① 印度大陆北漂模型；② 印度－亚洲初始碰撞时限；③ 青藏高原的古特提斯造山作用；④古近纪喜马拉雅造山带的地壳缩短；⑤ 高喜马拉雅的深熔机制；⑥ 青藏高原隆升的时限和差异性；⑦ 构造－剥蚀－气候相互作用与南亚季风；⑧ 青藏高原关键矿产资源的分布

与成因；⑨ 青藏高原的活动断裂带与孕震机制；⑩ 碰撞后的印度板块何去何从———深部动力学过程。这些问题可以作为当前研究青藏高原大陆动力学演化的重点方向。

关键词：青藏高原；板块构造；大陆动力学

青藏高原是世界上最高、最大、最厚、最新的高原，是发展固体地球科学理论的最佳实验室。青藏高原研究从喜马拉雅开始已经有２００ 多年的历史，重新审视和探究青藏高原的关键科学问题，可以为研究板块汇聚边界的大陆岩石圈演化及其能源资源、地质灾害和全球环境效应提供新的重要信息，为解决板块构造理论的“登陆”难题做出贡献。

印度—亚洲碰撞是新生代以来最壮观的地质事件，导致喜马拉雅山脉的崛起、青藏高原的隆升、巨厚地壳的形成、青藏高原物质向东、东南和向西南的大逃逸、２０００km 范围亚洲大陆内部的弥散变形、环青藏高原的盆地系统和油气资源、南亚季风和亚洲内陆干旱化等。笔者提出青藏高原如下重大关键地学问题，作为研究青藏高原的新思考：① 印度大陆北漂模型；② 印度—亚洲初始碰撞时限；③ 青藏高原的古特提斯造山作用；④ 古近纪喜马拉雅造山带的地壳缩短；⑤ 高喜马拉雅的深熔机制；⑥ 青藏高原隆升的时限和差异性；⑦ 构造—剥蚀—气候相互作用与南亚季风；⑧ 青藏高原关键矿产资源的分布与成因；⑨ 青藏高原的活动断裂带与孕震机制；⑩ 碰撞后的印度俯冲板块何去何从———深部动力学过程。以此作为对《地质学报》１００周年华诞的纪念。

1. 印度大陆北漂模型

穿越时空的隧道，在中生代期间，印度大陆与欧亚大陆之间还是一片汪洋，称之为新特提斯洋。研究表明，三叠纪印度板块开始从冈瓦纳超大陆解体（Zhuetal.,2011;Metcalfe,2013,2017,2021；MaXuxuanetal.，2018，2021c），随后在白垩纪开始了北漂的里程，至 60 Ma 左右与欧亚大陆碰撞（Huetal.，2015）。由此，喜马拉雅山崛起，青藏高原隆升及大量物质向两侧逃逸，2000 km 范围亚洲大陆内部的弥散变形，在喜马拉雅造山带和藏南形成了地球上最厚的地壳（70 ～ 80km）（Zhao Wenjin et al.，1993；Yin An，2000；Schulte — Pelkum et al.，2005；Zhang Zhongjieet al.，2011）。印度大陆自早白垩世以来的北漂过程中还发生 90°的逆时针旋转运动，引起印度板块的古纬度变化（Besse et al.，

2002；张也等，2017)。

印度大陆的北漂存在两种不同的构造重建模型：大印度北漂（为大多数学者观点）和“大印度盆地”北漂(van Hinsbergen et al.,2012)（图1）。前者认为随着新特提斯洋盆的俯冲到闭合，北漂的大印度板块与欧亚大陆碰撞。后者提出白垩纪之前为 大印度板块的北漂，晚白垩世喜马拉雅微陆块（包含 特提斯喜马拉雅和高喜马拉雅）与印度主大陆分离，中间隔了大印度盆地，继后两陆块与大印度盆地同时北漂；50Ma 期间喜马拉雅微陆块首先与欧亚大陆软碰撞，25～20Ma 期间大印度盆地闭合致使印度主大陆与欧亚大陆硬碰撞（van Hinsbergen et al.，2012)。

在“大印度盆地北漂”模型的基础上，近年来又发展出一些新的两阶段碰撞模型（Yang Tianshui et al.，2015，2019；Yuan Jie et al．2021；Jadoon et al．2021)。Yuan Jie et al.(2021）根据从江孜和萨嘎地区特提斯喜马拉雅北带的古地磁数据限定“大印度”的北界，认为不存在“大印度盆地”陆壳，强调晚白垩世存在一个1000 km左右的“北印度洋”，是晚白垩世（约75～61 Ma）喜马拉雅微陆块与印度主大陆分离的结果，约 61 Ma 喜马拉雅微陆块与拉萨地体碰撞，53～48 Ma印度大陆与特提斯喜马拉雅碰撞。Jadoon et al.（2021) 根据巴基斯坦晚白垩世海相红层的古地磁数据，建立了一个类似的印度－亚洲多阶段碰撞模式。

对此，笔者认为印度大陆北漂过程的主要争论在大印度板块的大小。对于古地磁数据需要进一步 的物源分析来限定其与印度或是拉萨地体的亲缘性，才能使其大地构造位置判断具有说服力。另外，关于印度大陆在早白垩世—晚白垩世期间的大约 90°的旋转北漂过程如何引起特提斯喜马拉雅不同地区的纬度变化，以及是否引起印度大陆与特提斯喜马拉雅地体之间的“伸展”值得进一步研究。由于沿着喜马拉雅微陆块和印度主大陆北缘的低喜马拉雅之间存在主中央逆冲断裂带（MCT），一直没有发现代表洋壳残片的蛇绿岩或者伸展盆地的记录，两阶段碰撞模式至今仍为野外地质学家所质疑。此外，在讨论新特提斯洋

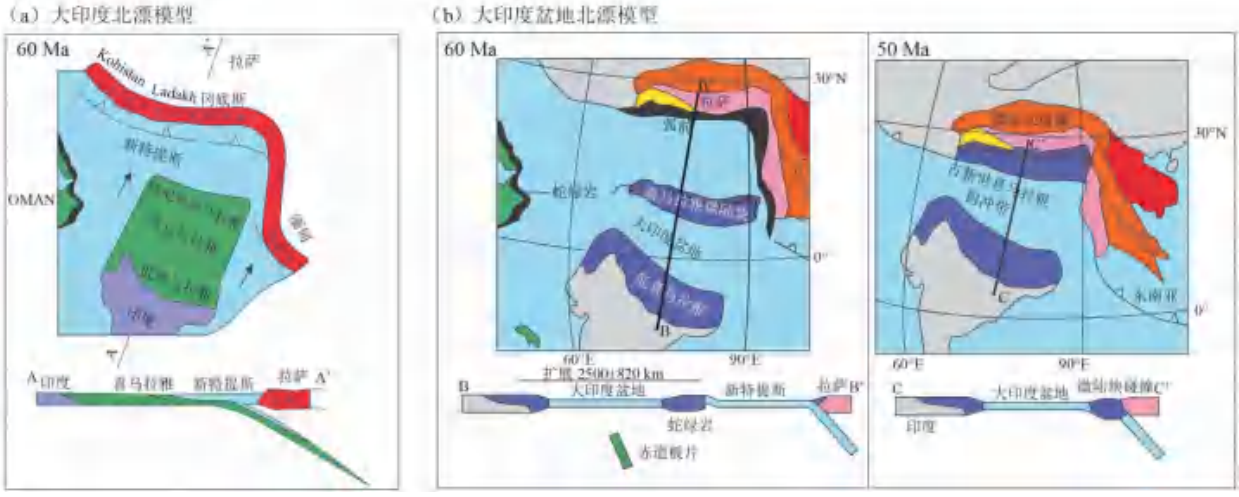

图1 印度板块重建和向北漂移的模型对比

（a）—大印度北漂模型显示具有广阔大陆边缘的单个印度板块，包括低喜马拉雅、高喜马拉雅和特提斯喜马拉雅，约50M a发生印度－亚洲碰撞；（b）—大印度盆地北漂模型将西藏－喜马拉雅微板块（高喜马拉雅和特提斯喜马拉雅）与主要的印度板块分开，中间有一个海洋，称之为“大印度盆地”，该模型涉及50M a的“软碰撞”和25～20M a的“硬碰撞”（据van Hinsbergen et al.，2012）

盆消减的过程中，还应考虑新特提斯洋—陆格局的复杂性，包括：① 在新特提斯洋盆消减过程是否存在洋内俯冲到洋—陆碰撞的转换？转换的时限和方式？② 印度—亚洲汇聚速率随时间和空间的差异性变化？

现代表洋壳残片的蛇绿岩或者伸展盆地的记录，两阶段碰撞模式至今仍为野外地质学家所质疑。此外，在讨论新特提斯洋盆消减的过程中，还应考虑新特提斯洋—陆格局的复杂性，包括：① 在新特提斯洋盆消减过程是否存在洋内俯冲到洋—陆碰撞的转换？转换的时限和方式？② 印度—亚洲汇聚速率随时间和空间的差异性变化？

2. 印度—亚洲初始碰撞时限

印度—亚洲大陆初始碰撞的时限问题一直存在争论。关键取决于人们如何定义“初始碰撞”，不同学者利用不同方法获得的初始碰撞时间差异很大（从 70Ma 到 34Ma）（Powell et al.，1973；Patriat et al.，1984；Le Fort，1987；王成善等，2003；Ding Lin et al.，2005；Aitchison et al.，2007；莫宣学等，2007；Garzanti，2008；黄宝春等，2010；Najman et al.，2010；van Hinsbergen et al.，2012；DeCelles et al.，2014；Wu Fuyuan et al.，2014；Hu Xiumian et al.，2015，2016a，2016b；Zhuang Guangsheng et al.，2015；丁林等，2017a；朱弟成等，2017）。制约初始碰撞精细时间的方法包括印度板块向北漂移减速时间的古地磁证据（Molar et al.，1975；Treloar et al.，1991；Klootwijk，1992；Ali et al.，2005；Najman et al.，2010；Copley et al.，2010；van Hinsbergen et al.，2012）、在印度—雅鲁藏布江缝合带和沿印度板块北缘的最后海相沉积时间的证据（Garzanti et al.，1987；Searle et al.，1987；Hu Xiumian et al.，2015，2016a）、沿缝合带最老的大陆沉积的时间（Searle et al.，1987；St—Onge et al.，2010；DeCelles et al.，2014）、与俯冲有关的亚洲南缘的岩浆弧中“I”型花岗岩岩基的岩浆作用的终结（Chung Sun—Lin et al.，1998a；St—Onge et al.，2010；马绪宣等，2021a；Ma Xuxuan et al.，2021b，2021c）以及沿印度板块北端的超高压变质作用的时限（Leech et al.，2005）等。

最近，古地磁研究提供印度—亚洲初始碰撞新时限，通过特提斯喜马拉雅地体的岗巴宗浦组（约 62 ～ 59Ma）褶皱检验、磁性矿物提取得到碎屑磁铁矿＋生物磁铁矿，证明古地磁结果为原生剩磁，指示古纬度为 6.6° ±3.5°N（Yi Zhiyu et al.，2011，2021；Zhao Qian et al.，2021）；同时根据拉萨地体林周盆地“典中组”砾石、Ar—Ar年代学、岩相学证明（64 ～ 60Ma）古地磁结果为原生记录，指示古纬度 6.7° ±4.4°N。根据特提斯喜马拉雅和拉萨地体最新古地磁（原生剩磁）数据对比，印度—亚洲初始碰撞时间不晚于 62±2Ma，初始碰撞位置位于赤道湿润带以内（6.7° ±4.4°

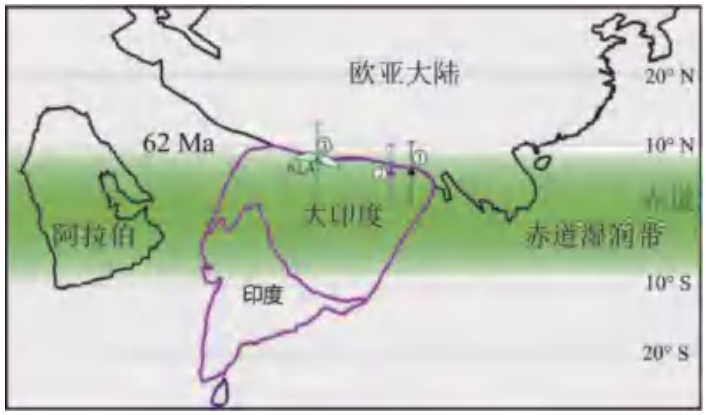

图 2　印度和欧亚大陆碰撞时限图示（据 Yi Zhiyu et al.，2021）

（数据分别引自① Yi Zhiyu et al.，2021；② Yi Zhiyu et al.，2011；③ Martinet al.，2020；KLA—科西斯坦拉达克弧）

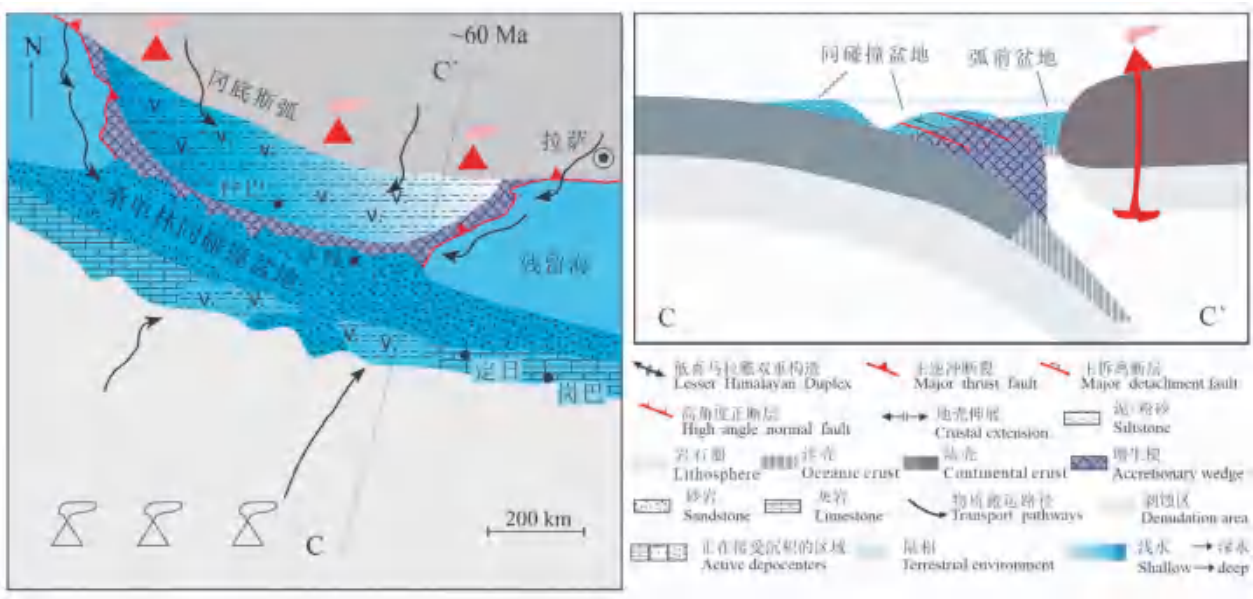

图 3　西藏萨嘎地区桑单林同碰撞时期的海沟盆地的平面图和剖面图（引自 Hu Xiumian et al., 2015）

在桑单林沉积上部发现来自印度和亚洲物源的交互沉积，为初始碰撞事件（59 ± 1Ma）产物

N）（Yi Zhiyu et al.，2021）（图2）。

另外，根据大陆初始碰撞时间的三种常用定义：① 以洋壳消失、俯冲板片的陆壳进入上覆活动大陆边缘海沟的“同碰撞盆地”作为初始碰撞时间；② 以两个大陆之间海洋消失的时间作为初始碰撞的时间；③ 以大陆之间发生强烈构造变形作用的时间作为初始碰撞的时间，只有①代表了实际的初始碰撞时间。最近对同碰撞盆地的研究提供了印度－亚洲初始碰撞的新证据：在西藏萨嘎地区桑单林剖面上部（桑单林组）发现来自印度和亚洲物源的交互沉积，为同碰撞时期的海沟盆地初始碰撞事件的产物，初始碰撞被精确限定在 59±1Ma（Hu Xiumian et al., 2015）（图3）。

需要指出的是：上述新的初始碰撞时间的证据主要取自冈底斯－喜马拉雅弧形带的中段。沿冈底斯－喜马拉雅弧形带的走向，印度－亚洲初始碰撞的时间是否一致还需要深入研究，特别是东－西构造结尚未找到典型同碰撞时期的海沟盆地，即初始碰撞事件的证据，仅用最后海盆的结束时间和超高压变质带的形成时间尚不能确定初始碰撞的时限。

3. 青藏高原的古特提斯造山作用

特提斯是地球显生宙期间位于北方劳亚超大陆和南方冈瓦纳超大陆之间的巨型大洋，它经历了一系列的洋盆消减、地体碰撞以及增生－碰撞造山作用，并最终于新生代闭合而造就了现今近东西向展布的巨型特提斯造山带。追溯特提斯洋的演化历史，是重建青藏高原形成过程的重要基础。Sengör（1979）曾强调，劳亚超大陆和冈瓦纳超大陆之间在晚古生代发育古特提斯洋，由于该大洋于中生代早期的消减和萎缩，而在冈瓦纳大陆以北发生扩张形成新特提斯洋。Sengör（1979，1987，1989）认为当时南、北大陆之间存在两个大洋（古特提斯洋和新特提斯洋）和一个夹持其间的基墨里（Cimmerian）大陆，基墨里大陆由包括巴尔干－马来西亚半岛之间的伊

图 4　特提斯格架一级古地理 / 古构造要素及其现今地理位置（据 Sengöret al.,1987 修改）

1—劳亚大陆；2—冈瓦纳大陆；3—基墨里大陆；4—其他区域；5—古特提斯缝合带；6—新特提斯缝合带

朗— 土耳其—北帕米尔—松潘甘孜—印支地体所组成，为三叠纪从冈瓦纳超大陆分裂出来的大陆拼贴体，于晚三叠世—中侏罗世与北方的劳亚大陆碰撞，形成由超级造山杂岩组成的基墨里造山带（Sengör，1979，1987；Boulin，1981；Audley—Charles，1984；Golonka，2006；Li Haibin et al.，2009）（图 4）。但是根据冷水和暖水动物群的分布，越来越多的研究者将位于青藏高原中部的龙木错—双湖—昌宁—孟连缝合带作为含冷水动物群的基墨里大陆与含暖水动物群的华夏陆块的分界线，将原来的基墨里大陆解体为南北两部分，南侧为由西基墨里、南羌塘和滇缅泰（Sibumasu）地体拼贴组成的基墨里大陆，北侧则由北羌塘、松潘甘孜、思茅—印支地体拼贴而成华夏陆块之南部（图 5）（Metcalfe，2006，2013；许志琴等，2012；Wang Qing et al.，2021）。

法国学者 Fromaget（1927，1952）曾在研究越南地质时提出印支造山作用的概念，把晚二叠世— 中晚三叠世的造山作用称为印支运动，之后许多学者强调越南—滇西的印支运动在中国大陆构造演化的重要性（孟宪民，1937；黄汲清，1945；任继舜，1984）。近 20 年来东南亚古特提斯研究取得新的进展，特别是东南亚陆块的东、西两条缝合带所反映的古特提斯洋盆开合及其碰撞造山过程取得了新的认识（Sone et al.，2008；Metcalfe，2013；Wang Yujun et al.，2018；Tran et al.，2020）。东南亚陆块的东侧缝合带即金沙江—哀牢山—松马缝合带，为华夏陆块中的思茅—印支地体与华南陆块的边界，反映了古特提斯的分支洋盆（或弧后盆地）的关闭，两地体碰撞时间约为 247 Ma，同碰撞和后碰撞造山事件分别限定在 247 ～ 237 Ma 和 237 ～ 200 Ma（Wang Yujun et al.，2018）。西侧缝合带为昌宁—孟连缝合带，作为基墨里大陆的滇缅泰地块和思茅— 印支地体之间的古特提斯主洋盆闭合界线，两地体的碰撞发生在约 237 Ma，同碰撞和后碰撞的造山事件分别发生在 237 ～ 230

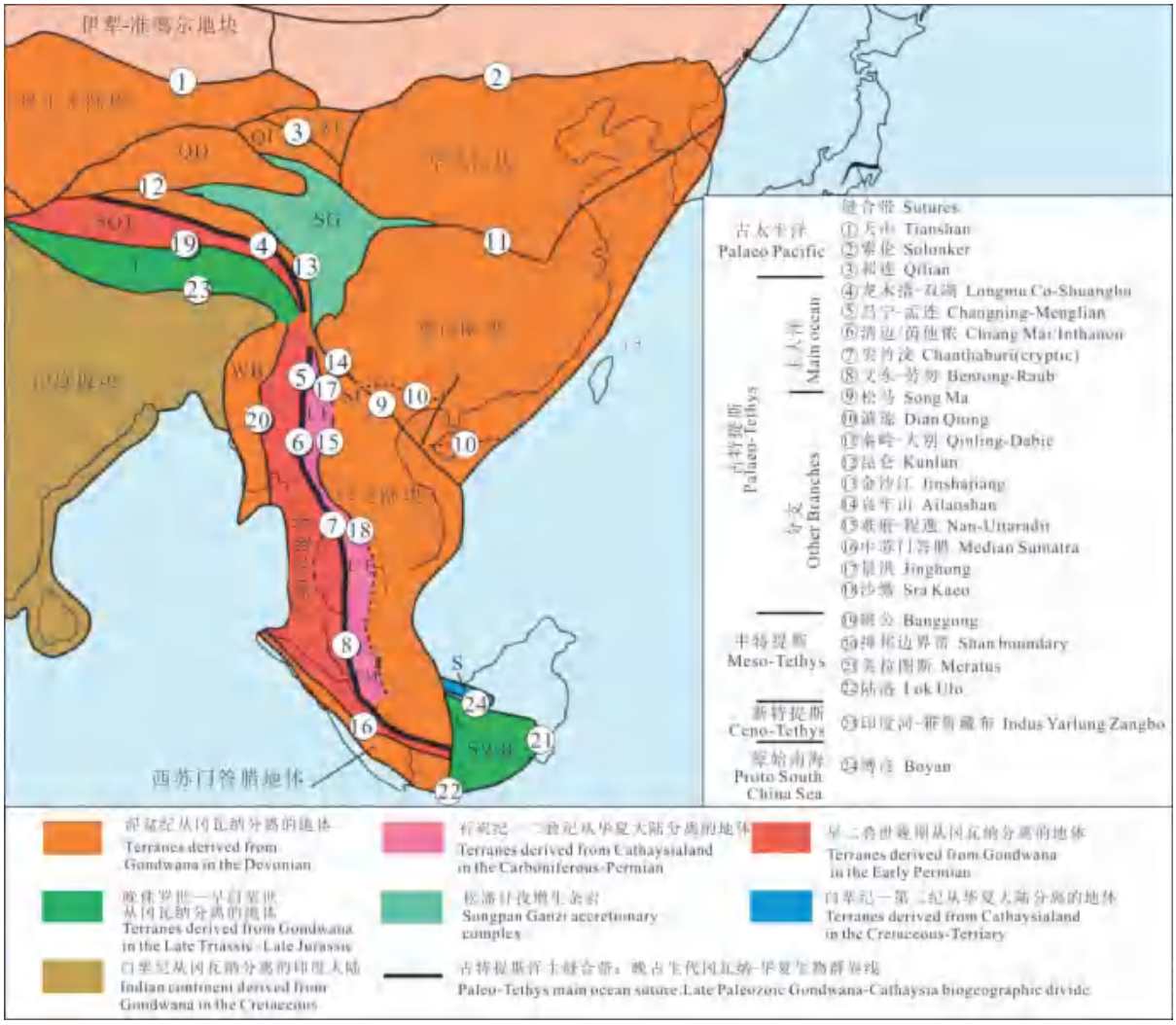

图 5　东亚和东南亚的主要大陆地体和缝合带的分布图（据 Metcalfe，2013）

WS—西缅甸地体；SWB—西南婆罗州地体；S—塞密塔地体；L—拉萨地体；NQT—北羌塘地体；SQT—南羌塘地体；QS—昌都－思茅地体；SI—思茅地体；SG—松潘－甘孜增生杂岩；QD—柴达木地体；AL—阿拉善地体；KT—Kurosegawa地体；LT—临沧岩浆弧地体；CT—尖竹汶岩浆弧地体；EM—东马来亚地体；QI—祁连地体

Ma 和 230 ～ 200 Ma（图 6）（Wang Yujun et al.，2018）。因此，基墨里造山运动不仅涉及基墨里陆块与印支地体，也叠置了印支地体和华南陆块之间的早期印支造山带。因此 Tran et al.，（2020）提出，Fromaget（1952）依据越南地质现象所提出的印支运动并不适合发生在滇缅泰和思茅－印支地体之间的晚三叠世—侏罗纪的碰撞后造山事件，建议根据地域将晚二叠世—中晚三叠世的印支运动改名为“跨湄公河造山运动”（Trans—Meigonghe orogen）。

上述表明：东南亚地区基墨里大陆的滇缅泰地体与华夏陆块碰撞造山的时限与基墨里造山事件的时间重合，而东南亚印支地体与华夏陆块间的造山时间从印支运动开始，其结束时间与基墨

里造山事件相当。因此，笔者认为在东南亚基墨里大陆与印支、华南陆块之间所反映的基墨里造山事件是广泛和强大的。但东南亚地区代表古特提斯造山运动的印支造山是否存在着地域性和时域性差异值得探讨，它和基墨里造山事件究竟什么关系，是否代表基墨里造山运动的前身也有待进一步查明。

作为华夏大陆组成部分的松潘－甘孜地体被北部的东昆仑－柴达木地体、东南部的华南陆块和南部的北羌塘地体所围限，是由北侧东昆仑－

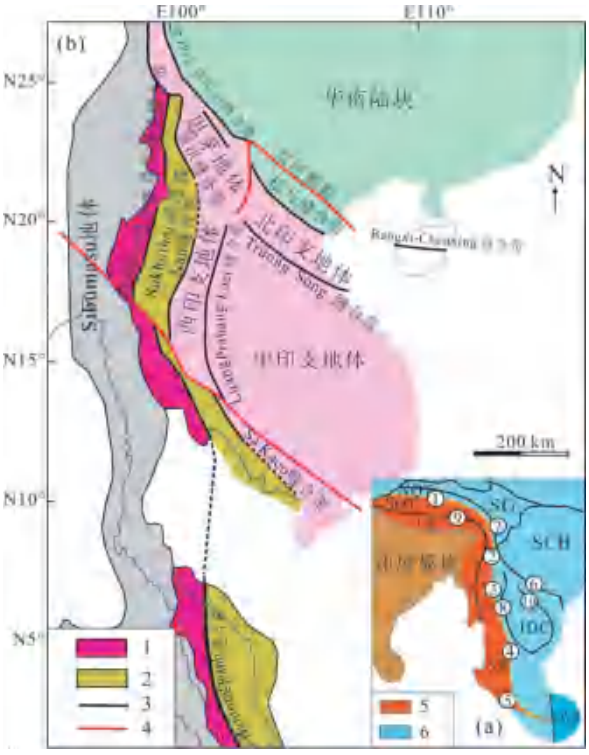

图 6　东南亚的大地构造背景（ a ）及主要陆块示意图（ b ）（据 Wang Yujun et al.，2018 修改）

①—龙木错－双湖缝合带；②—昌宁－孟良缝合带；③—Inthanon 缝合带；④—景洪－Nan－Sa Kaeo缝合带；⑤—Bentong－Raub 缝合带；⑥—松马缝合带；⑦—金沙江－哀牢山缝合带；⑧—Luang Prabang－Loei缝合带；⑨—班公湖－怒江缝合带；⑩—Truong Son 缝合带；NQT—北羌塘地体；SQT—南羌塘地体；LS—拉萨地体；SB—滇缅泰地体；SG—松潘－甘孜地体；SCB—华南陆块；IDC—印支陆块；SWB—西南婆罗州地体；1—古特提斯主要缝合带；2—古特提斯主要岛弧带；3—古特提斯其他缝合带；4—新生代断裂；5—高纬度冷气候的冈瓦纳型动植物群；6—低纬度暖气候的华夏型动植物群

图 7　晚三叠世松潘－甘孜地体所在的古地理位置（据 Metcalfe，2006）

NC—华北陆块；SC—华南陆块；Ⅰ—印支陆块；EM—东马来地体；WS—西苏门答腊地体；S—滇缅泰地体；SG—松潘－甘孜地体；WB—西缅甸地体；QI—羌塘地体；L—拉萨地体；WC—西基墨里大陆

阿尼玛卿和南侧金沙江古特提斯缝合带所限定、由三叠纪巨厚（5～15km）深海浊积岩组成的三角形增生杂岩地体（许志琴等，1992）。前人对松潘－甘孜深海盆地的构造属性提出了不同模式，如：弧后盆地（Klimetz，1983；Sengör，1987；Watson et al.，1987；Gu Xuexiang，1994），前陆深海／残余洋盆（Nie Shangyou et al.，1994；Zhou Da et al.，1996；Weislogel et al.，2006），陆间裂谷盆地（McElhinny et al.，1981；Chang Edmend，2000；Meng Qingren et al.，2000）等。

许多学者将松潘－甘孜地体划入印支造山带范围（Ren Jishun，1984；Xu Zhiqin et al.，1992，2012；Harrowfield et al.，2005）。研究表明，在中—晚三叠世古特提斯洋盆闭合的基础上，松潘－甘孜晚三叠世增生造山楔以强烈地壳缩短和加厚、228～180Ma 大量花岗岩侵位并伴随锂金属元素的超常富集为特征（Zhang Hongfei et al.，2006，2007；Yuan Chao et al.，2010；Xu Zhiqin et al.，2020）。与其他刚性地体（或陆块）之间的硬碰撞造山不同，由三叠纪

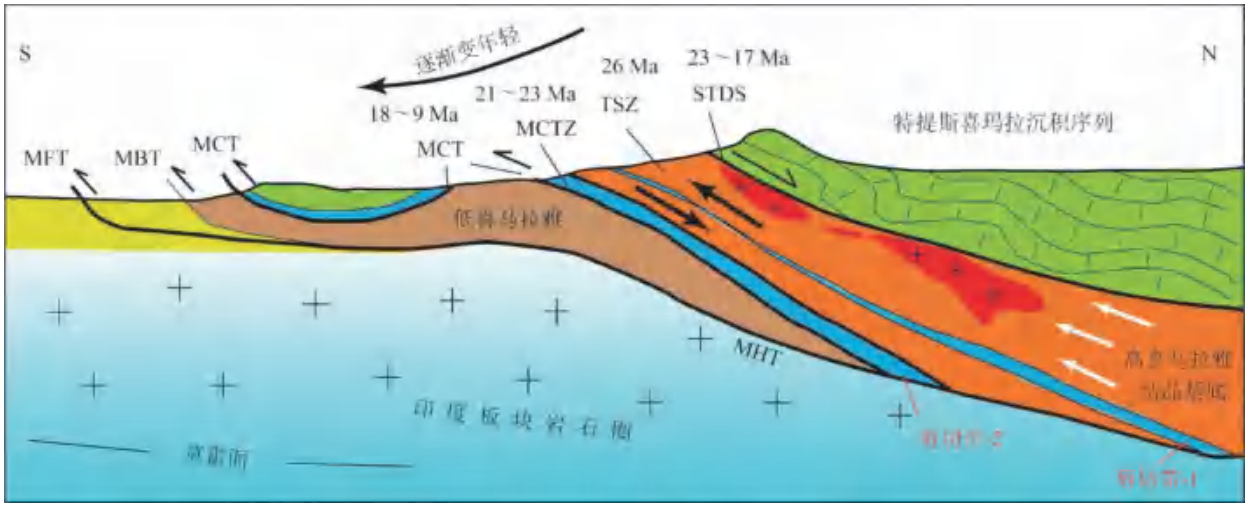

图 8　喜马拉雅构造剖面（修改自 Carosi et al., 2010）

STDS—藏南拆离系；MCT—主中央逆冲断裂带；MBT—主边界逆冲断裂；MFT—主前锋逆冲断裂；TSZ—Toijem逆冲剪切带；MHT—主喜马拉雅逆冲断裂

地层组成的松潘－甘孜地体与周围刚性陆块的“软碰撞”造山（图 7）发生的时限为晚三叠世—早中侏罗世，晚于印支运动，与基墨里造山作用的时限相当。

研究表明，东昆仑－阿尼玛卿缝合带向东与秦岭地体的勉略缝合带连接（Li Chunyu et al.，1978，1982；Zhang Guowei et al.，1995），并通过 NE—SW 向“宁陕－湘河”左行走滑剪切带与东秦岭－大别－苏鲁地体的超高压变质带的俯冲前缘相连（许志琴等，2015a）。大别－苏鲁造山带超高压变质作用的时间为 240 ～ 225Ma，超高压变质岩从高压榴辉岩相到角闪岩相的折返时间为 225 ～ 200Ma（Edie et al.，1994；Ayers et al.，2022；Li Shuguang et al.，1993，2003；Liu Fulai et al.，2011；Xu Zhiqin et al.，2006；Liu Fulai and Liou，2011;郑永飞，2008）。因此，华南与华北陆块的陆陆碰撞时间应早于 240Ma，其碰撞造山作用的初始时限与印支运动相当，结束时间与基墨里造山运动相当。因此，一些作者推测古特提斯北支洋盆（即东昆仑－阿尼玛卿－勉略－秦岭 / 大别 / 苏鲁缝合带）具有东早西晚的剪式洋盆闭合形式，致使整个中央造山带的碰撞造山作用呈现东早、西晚的穿时特征。

由于新生代造山作用是在古特提斯造山运动的废墟上建立，因此重塑古特提斯完整独立的造山体系十分困难。青藏高原集“始特提斯”、“古特提斯”和“新特提斯”为一体，重新审视古特提斯造山作用，特别考虑造山作用的地域性和时域性的差异对理解青藏高原的形成演化十分重要。正如欧洲的“加里东”和“华力西”造山作用并不适用于中国大陆的造山带一样，印支造山作用和基墨里造山作用对中国大陆的影响需要通过全球对比，进行检验。

4. 古近纪喜马拉雅造山带地壳缩短的机制

喜马拉雅造山带自北向南由特提斯喜马拉雅（THS）、高喜马拉雅（GHS）、低喜马拉雅（LHS）和次喜马拉雅（SHS）等四个构造单元组成，各单元之间的边界依次为藏南拆离系（STD）、主中

央逆冲断裂（MCT）、主边界逆冲断裂（MBT）和主前锋逆冲断裂（MFT）（图 8）。Vanney et al.（1996）对尼泊尔中部 KaliGandaki 剖面的高喜马拉雅开展了系统的构造变形、岩石学、变质作用和年代学研究，把喜马拉雅造山带的演化分成三个阶段：在始新世早期—中期，特提斯喜马拉雅沉积岩系发育上盘向南的褶皱冲断带，经历了低级变质作用，这一薄皮构造可能受控于特提斯喜马拉雅古生代地层中主拆离断层的逆冲推覆；始喜马拉雅期（Ehoimalayan episode）高喜马拉雅埋俯冲到特提斯喜马拉雅之下，以始新世中期－渐新世的蓝晶石相进变质作用为特征，埋深超过 35km；新喜马拉雅期（Neohimalayan episode）高喜马拉雅在主中央逆冲断裂和藏南拆离系的控制下快速折返，以渐新世—中新世的退变质作用为特征，新喜马拉雅期的峰期变质作用在 23 ～ 21Ma。

喜马拉雅古近纪的变形记录常被中新世以来的变质－变形强烈叠加或抹去，根据主中央逆冲断裂和藏南拆离系在 24 ～ 16Ma 具有相反的运动学指向和同期构造活动，前人提出了不同的高喜马拉雅挤出模式，包括：楔状挤出（Burchfiel and Royden，1985）、地壳隧道流（Nelson et al.，1996；Chemenda et al.，2000；Beaumont et al.，2001）、构造楔（Yin An，2006；Webb et al.，2007）和双重构造（He Dian et al.，2016）等。

沿特提斯喜马拉雅褶皱冲断带面理生长的伊利石或淡色花岗岩的 40Ar / 39Ar 年龄测定表明，特提斯喜马拉雅褶皱冲断带的形成年龄在 56 ～ 45 Ma（Ratschbacher et al.，1994；Wiesmayer et al.，2002）。因此，藏南拆离系作为中新世特提斯喜马拉 雅和高喜马拉雅的边界，无论从时间、运动学和驱动力上都无法解释上盘特提斯喜马拉雅的始新世地壳缩短。上述基于中新世高喜马拉雅折返的构造模型不能适用始喜马拉雅期的地壳缩短和深熔作用。

近年来笔者在喜马拉雅造山带东部的研究表明：始喜马拉雅期的地壳缩短受到特提斯喜马拉雅底部的滑脱断层（特提斯喜马拉雅滑脱带，Tethyan Himalayan Décollement，THD）制约（图 9）。特提斯喜马拉雅滑脱带约有 4 km 厚，发育在早古生代变质地层中，伴随高级变质作用和局部熔融，形成于 50 ～ 17Ma，具有上盘向南的剪切指向，并控制了特提斯喜马拉雅单元的地壳缩短和加厚。在特提斯喜马拉雅滑脱带的顶部叠置了上盘向北剪切的藏南拆离系，表明特提斯喜马拉雅滑脱带是藏南拆离断层的前身，也是特提斯喜马拉雅和高喜马拉雅在始新世—渐新世的构造边界。这是对喜马拉雅造山带早期构造格架的新解释，对认识印度－亚洲碰撞早期板块边界的构造变形具有重要意义。特提斯喜马拉雅滑脱带的向西延展是值得进一步研究的问题，将有助于我们理解喜马拉雅造山带沿走向的构造差异。

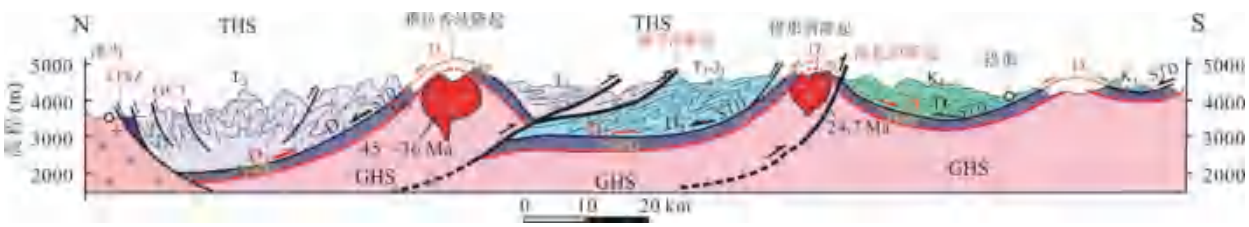

图 9　喜马拉雅造山带东部的南北向构造剖面

GHS—高喜马拉雅结晶基底；THD—特提斯喜马拉雅滑脱带；STD—藏南拆离系；ITSZ—雅鲁藏布江缝合带；GCT—大反冲断裂；THS—特提斯喜马拉雅

5. 高喜马拉雅深熔作用的成因

作为地壳深熔作用产物的淡色花岗岩，广泛出露在高喜马拉雅上部（Dietrich and Gansser，1981；Le Fort et al.，1987；Burchfiel et al.，1992；Guillot et al.，1994；Hodges et al.，2000；吴福元等，2015）和特提斯喜马拉雅底部（Xu Zhiqin et al.，submitted）。长期以来，喜马拉雅淡色花岗岩被认为主要形成于 23 ～ 22 Ma 到 13 ～ 12 Ma，最年轻（小于 4 Ma）的出露在东、西构造结。但是，特提斯喜马拉雅岩系里近东西向展布的北喜马拉雅片麻岩穹隆中，发现了早于 40Ma 淡色花岗岩，引起了广泛关注（Zeng Lingsen et al.，2011；吴福元等，2015）。

高喜马拉雅淡色花岗岩究竟如何形成？Le Fort et a.（1987）曾提出“熨斗模式”，认为由于高喜马拉雅单元底部主中央逆冲断层的逆冲致使下部冷的低喜马拉雅单元产生变质作用，释放流体而导致高喜马拉雅局部熔融（图 10）。但此模式无法解释为什么淡色花岗岩主要产在高喜马拉雅单元的上部，也无法解释早期淡色花岗岩的形成。

大多数研究认为，高喜马拉雅结晶岩系变泥质岩的深熔作用形成了喜马拉雅淡色花岗岩（Le Fort et al.，1987；Guillot et al.，1995；Harris et al.，1995；Patiño — Douce et al.，1998；Aoya et al.，2005；Guo Zhengfu et al.，2012；Zeng Lingsen et al.，2012；Weinberg，2016）。一系列淡色花岗岩成因模式被提出，如：高 Sr / Y 淡色花岗岩形成于喜马拉雅加厚下地壳的局部熔 融（Zeng Lingsen et al.，2011）；沿藏南拆离系母岩浆的高分异形成（吴福元等，2015）、软流圈地幔上涌形成以及变基性岩石部分熔融的贡献（Hou Zengqian et al.，2012）。

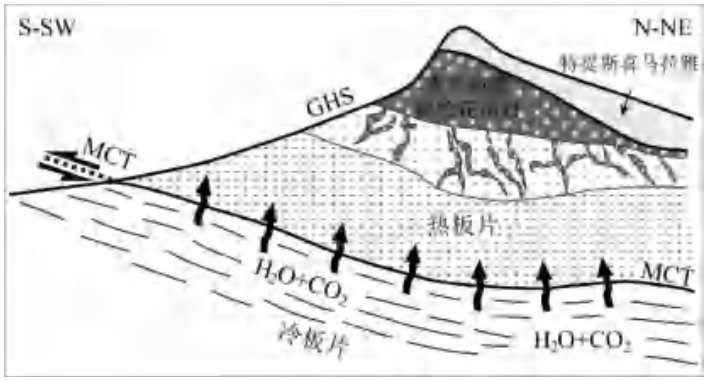

图 10　高喜马拉雅（GHS）底部逆冲断层（MCT）产生的熨斗模式：由于高喜马拉雅单元底部主中央逆冲断层的逆冲致使下部冷的低喜马拉雅单元产生变质作用，释放流体而导致高喜马拉雅局部熔融（据 Le Fort et al.，1987）

前人提出了三种不同的地壳部分熔融机制：增压过程中的进变质加热熔融（Visonà et al.，2002；Groppo et al.，2013），折返过程中的降压熔融（Harris et al.，1994；Patiño — Douce et al.，1998；Guo Zhengfu et al.，2012），以及注水熔融（Knesel et al，2002；Weinberg，2016；Gao Li'e et al.，2017）。

除了熔融机制不同之外，原岩类型和部分熔融程度的不同以及熔体混合都会导致喜马拉雅淡色花岗岩的化学成分发生变化。研究表明，东喜马拉雅构造结的泥质、长英质和基性岩石均经历了不同程度的部分熔融。根据地球化学成分，具有不同 87Sr / 86Sr 初始同位素比值的喜马拉雅淡色花岗岩起源于两种不同的原岩：二云母淡色花岗岩起源于变质杂砂岩（87Sr / 86Sr）i ＜ 0.752 和 εNd ＜ 15），电气石淡色花岗岩起源于变泥质岩（87Sr / 86Sr）i ＞ 0.752 和 εNd ＞ 15）（Guillot et al.，1995），而始新世的高 Sr / Y 花岗岩可能是喜马拉雅造山带加厚下地壳中角闪岩部分熔

融的产物（Zeng Lingsen et al.，2011；Hou Zengqian et al.，2012）。此外，Gou Zhengbin et al.（2016）认为电气石－白云母淡色花岗岩是白云母脱水熔融形成的，而白云母－黑云母淡色花岗岩是高喜马拉雅结晶岩系中泥质和长英质麻粒岩进变质过程中黑云母脱水熔融的产物。在晚渐新世到中新世，高喜马拉雅的变泥质岩、变杂砂岩和花岗片麻岩均发生了部分熔融，由于深熔源区占主导的岩性发生变化，导致高喜马拉雅淡色花岗岩的地球化学特征随时间变化（Ji Min et al.，2021）。

变质作用与部分熔融关系的研究表明，约45～23Ma的进变质作用发生在中压和高压麻粒岩相条件下（Searle et al.，1992；Ding Lin et al.，1999；Hodges et al.，2006；Zhang Zeming et al.，2010），23～14Ma的退变质作用发生在角闪岩相条件下（Searle et al.，1992；Walker et al.，1999；Hodges，2000）。Zhang Zeming et al.（2010）认为，在始喜马拉雅进变质和新喜马拉雅退变质早期，高喜马拉雅结晶岩系经历了长期持续的高温变质和脱水熔融（包括泥质

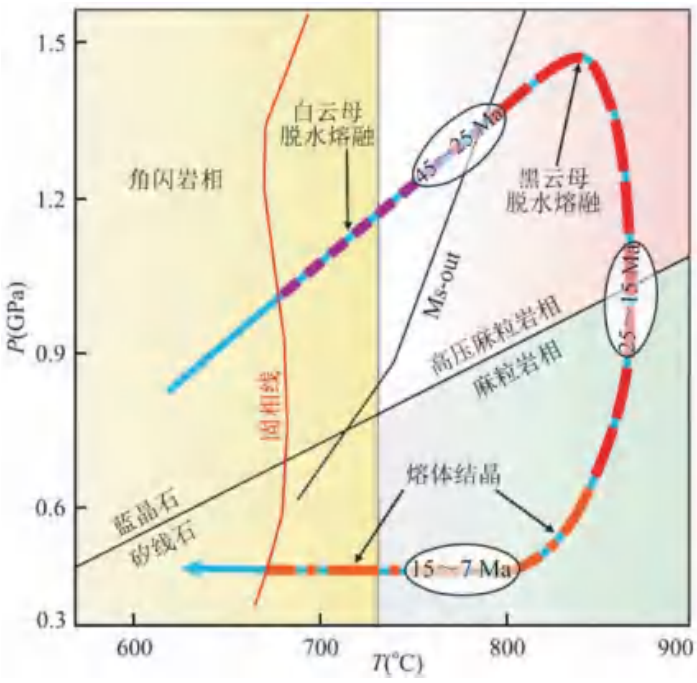

图 11　喜马拉雅高温变质、深熔和熔体结晶的P－T轨迹（据 Zeng Lingsen et al.，2010）

麻粒岩的白云母和黑云母脱水熔融，基性麻粒岩的角闪石脱水熔融），熔体混合、岩浆混染和分离结晶作用形成了复杂的S＋I型花岗岩。因此，高喜马拉雅深熔作用很可能是长期大陆俯冲、地壳加厚、持续高温变质和脱水熔融的结果（图 11）。

6．青藏高原隆升的时限和差异性

由于印度－亚洲的新生代陆陆碰撞，形成了平均海拔近 5000 m 的青藏高原，并造就了“世界屋脊”之称的喜马拉雅山链。解析青藏高原的隆升剥露历史，对于揭示碰撞造山的运动学过程和动力学机制有着重要的意义。同时，高原的隆升剥露过程也深刻影响到了全球和区域气候、海洋化学的变化以及生物演化（Burbank et al.，1993；An Zhisheng et al.，2001；Tapponnier et al.，2001；Molnar et al.，2010；Spicer，2017；Deng Tao et al.，2019）。长期以来，前人对于青藏高原隆升过程和动力学机制开展了大量的研究，存在不少争议。早期研究阶段根据古生物化石（高山栎，三趾马等；施雅风等，1964；李吉均等，1979）、钾质火山岩活动时间（Turner et al.，1993）、断裂活动（Harris et al.，1995）等判断青藏高原隆升形成时间为 13～3Ma。随后，Chung Sun—LinHarris et al.，1995.（1998b）提出青藏高原的东西隆升差异性，东早（约 40Ma）而西晚（约 20Ma）。Tapponnier et al.（2001）提出了在

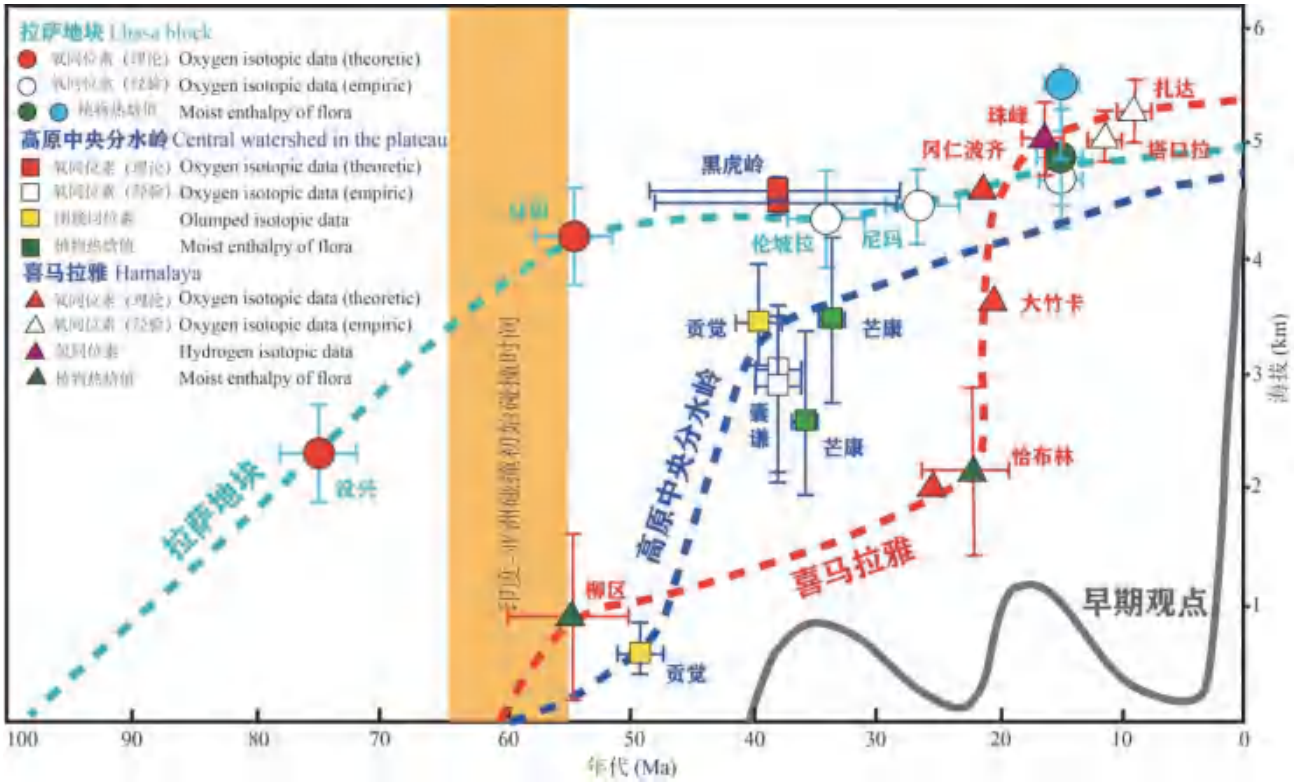

图 12　青藏高原不同地质单元的隆升曲线图（修改自丁林，2021[1]）

印度－亚洲初始碰撞之后，青藏高原逐渐由南向北生长；之后的氧同位素古高程研究结果为该模型提供了佐证（Rowley et al.，2006）。Wang Chengshan et al.（2008）根据沉积记录和低温热年代学数据提出高原是由中部向外不断扩展而形成，得到不少学者认同（Rohrmann et al.，2012；Li Yalin et al.，2015；Li Guangwei et al.，2016）。但是，近年在青藏高原中部班公－怒江缝合带地区的尼玛、伦坡拉盆地发现的古鱼类等动植物化石（Wu Feixiang et al.，2017；Deng Tao et al.，2019）指示青藏高原中部在约 26Ma 之前仍然处于相对较低海拔（至少＜ 2500 m）。Ding Lin et al.（2014）以及 Fang Xiaomin et al.（2020）提出青藏高原中部在始新世—渐新世期间呈现“两山夹一谷”的形态。最近丁林（2021）[1]根据同位素和植物化石总结了青藏高原隆升演化历史，显示出高原各块区的隆升差异性（图 12）。

综上所述，关于青藏高原隆升过程的争论，目前主要问题集中在：① 青藏高原是均匀整体还是差异性抬升，各块体的具体隆升过程如何？ ② 青藏高原是否是由中部向南北扩展而形成？ 中北部的松潘－甘孜、昆仑等地体是否存在早期（白垩纪）高原？ ③ 喜马拉雅是从中新世渐进式隆升还是在晚期（上新世）才隆升的？而造成上述诸多争论，则主要由于研究区域和古高程估算方法的不同。早期有不少学者利用构造或岩浆等替代性指标研究高原隆升，但随着研究深入，由于各自成因的多解性，其可靠性有待商榷。如 Harrison et al.（1995）提出青藏高原（包含喜马拉雅地区）东西向伸展主要在 9 ～ 7 Ma 期间，认为当时高原已隆升到最大高度，由于重力失稳而开始垮塌。

但是印度－亚洲的南北向挤压亦可在喜马拉雅地区形成东西向伸展，因此用伸展断裂的活动作为高原隆升指标有所欠缺。同样，钾质岩浆活动由于成因多解性，也不能作为高原古海拔的可靠指标（Turner et al.，1993；Chung Sunlin et al.，1998b；王成善等，2009）。也有不少学者利用山前盆地（Najaman et al.，2010）和海底冲积扇开展高原隆升研究（McNeill et al.，2017；Zhou Peng et al.，2020）。再如，探讨剥蚀速率的热年代学（Thiede et al.，2013）的方法直接反映 的是岩石温度变化速率，应用于隆升时，还应注意转换对接条件和其他观测数据的限定。

值得注意的是，近年来很多直接限定古高程的方法不断发展，例如：古环境分析（特定动物化石或组合分析、古植物化石组合分析、稳定同位素法）、植物结构和形态分析（叶边分析法、CLAMP 法）、定量同位素分析法（氢、氧同位素、“团簇同位素”温度计法）、火山熔岩的封闭气孔形态等，但由于各种方法的局限性以及采样的差异性，经常出现不同方法或不同地区（甚至同种方法对同一地区）估算的高原隆升高度存在不小差别（图 12、13）（Huntington et al.，2015；Ding Lin et al.，2017b；Li Lin et al.，2019；Chen Chichao et al.，2020；Spicer et al.，2020）。因此，要精细刻画青藏高原隆升与剥蚀的过程，还需加强多地区详细调查以及新技术方法的开发和改进，并加强多种手段相结合、相互验证，区分局部效应和整体效应，进而综合探讨青藏高原的隆升历史，为探讨青藏高原隆升的动力学机制提供可靠依据。

（转载于《地质学报》2022 年第一期
剩余部分下期发布）

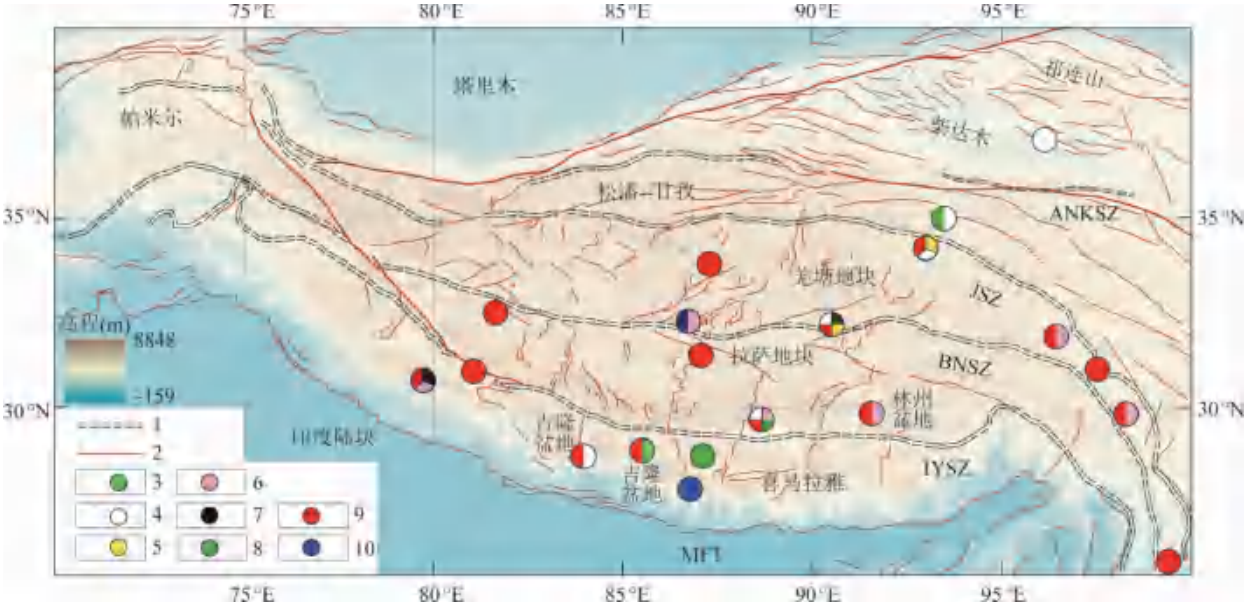

图 13　青藏高原古高程研究的相关盆地分布图以及相关分析方法
（数据来自 Li Lin et al.，2019；Chen Chichao et al.，2020 及其参考文献）

MFT—主前锋断裂；ANKSZ—阿尼玛卿－昆仑缝合带；JSZ—金沙江缝合带；BNSZ—班公怒江缝合带；IYSZ—印度－雅鲁藏布江缝合带；数据引自Li Lin et al（2019），Chen Chichao et al（2020）等以及其文中参考文献；1—缝合带；2—活动断裂；3—牙齿化石 $\delta^{13}C$；4—植物蜡正构烷烃 δD；5—孢粉组合；6—碳酸结核团簇同位素；7—哺乳动物化石；8—植物叶相；9—$\delta^{18}O$碳酸结核 / 牙齿化石；10—δD热液蚀变含水矿物

北京市海淀外国语实验学校京北校区单井循环地源热泵系统工程

入选国家节能中心典型案例

SINGLE-WELL CIRCULATION GROUND SOURCE HEAT PUMP SYSTEM PROJECT AT BEIJING HAIDIAN FOREIGN LANGUAGE EXPERIMENTAL SCHOOL, BEIJING NORTH CAMPUS

A Case Study by the National Energy Conservation Center

作者：马晓芳（特约记者） 李艳超（专业总工程师）

在国家发展改革委员会下属单位国家节能中心组织的“第三届重点节能技术应用典型案例”评选中，恒有源科技发展集团有限公司申报的“北京市海淀外国语实验学校京北校区单井循环地源热泵系统工程”，经过初评、答辩、现场核查等多个环节筛选，最终成功入选。从国家节能中心官网发布的《关于第三届重点节能技术应用典型案例最终入选典型案例名单的通告》可以看到，全国最终确定的 16 个重点节能技术应用典型案例中，恒有源“北京市海淀外国语实验学校京北校区单井循环地源热泵系统工程”极具代表性：不仅代表了节能前沿科技，也代表了节能应用发展的未来。

北京市海淀外国语实验学校京北校区位于冬奥之城张家口市，距离北京市 80 公里，该校区是海淀外国语实验学校新建的 12 年一贯制国际化学校，是北京 2022 年冬奥会和冬残奥会奥林匹克教育示范学校及国家体育总局为奥运储备中国国少队人才的冰雪项目基地。校区占地 660 亩，可容纳 5000 余名学生和教职工同时生活、学习。

校区总规划建筑面积 30 万平方米，分为三期建设，截止目前一期、二期 10 栋建筑总计 14 万平米已经投入使用，三期正在建设中。

目前，北京市海淀外国语实验学校京北校区共有 10 栋建筑，为适应校园面积比较大、建筑物分散、地表高程差比较大、各建筑使用时间及频率不一等特点，系统应用恒有源“单井循环换热地能采集技术”，采用地热能集中采集、分布式冷热源站独立供能的恒有源浅层地热能分布式冷热源系统实现了项目全部供暖、制冷、生活热水的清洁能源供应，较传统冷热源系统节能 60%。

秉持冬奥精神 节能环保打造学生宜居宜学良校

成立于 1999 年的北京市海淀外国语实验学校，经过二十多年的发展已成为海淀外国语，在国内外有多个校区。北京市已建立“两校一园多址”，“两校”指的是北京市海淀外国语实验学校和北京市海淀国际学校，“一园”指的是北京市海淀外国语实验学校附属幼儿园（海淀 / 京北 / 朝阳园），而“多址”指的是海淀和京北两个校区：海淀校区位于北京市海淀区，京北校区坐落在首都北部生态新区，位于河北怀来和延庆两处，与冬奥场馆也是相距咫尺。

海淀外国语学校京北校区一期项目坐落在张家口市怀来县北辛堡镇原乡，建设校区共 6 栋楼，包括 1# 小学部、2# 中学部、3# 海外剧场、4# 综合体育中心、5# 冰雪中心、滑雪大厅等，供暖冷总建筑面积 59292.93 ㎡。自 2019 年 9 月起投入使用。

京北校区在建筑设计十分人性化，学生的宿舍、教室、食堂、室内篮球场、游泳馆等场所是彼此相通的，很好地避免了孩子们运动完后一身大汗地在户内外不同温差中切换的情况。不仅如此，学校还为每栋宿舍楼都配备了中央空调和新风系统，冬暖夏凉。京北校区设施齐备，不仅包括各校区都有的动物园、游泳馆、大型室内运动场馆，还针对学校区位特色增加了独有的冰雪特色项目，设置了冰雪运动中心、滑雪练习场、网球馆、羽毛球馆、击剑馆、大型剧场等场馆。

保证京北校区室内环境四季恒定，除了建筑设计外还有一个必不可少的因素：恒有源单井循环换热地能采集技术。以“单井循环换热地能采集技术”为核心的恒有源地能热泵环境系统早在 2000 年就已经成为北京海淀外国语实验学校的供暖冷系统，并达到了良好的使用效果。该学校地处张家口市怀来县，空气清新，自然环境优越，但供暖期时间长，冬季气温低，为了保证项目正常供暖，并减少供暖系统的碳排放，达到清洁绿色供暖，项目继续采用了恒有源地能热泵环境系统作为项目的供暖系统，实现项目低碳、低成本供暖冷运行，为冬奥之城绿色发展做出贡献。

利用浅层地热按需供能 冬暖夏凉 24 小时热水

海淀外国语学校本部校区已经使用恒有源浅层地热能技术近 20 年，数据和使用过程让学校师生充分感受到了恒有源单井循环换热地能采集技术带来的巨大优势：冬供暖夏降温，低碳环保，24 小时热水。作为浅层地热能行业的领军企业，恒有源集团在建设北京市海淀外国语京北校区时更是秉承“一切为了孩子”的理念，集中公司上下合力，利用浅层地热为孩子们的每个春夏秋冬护航。

北京市海淀外国语京北校区项目一期的小学部、中学部、海外剧场、综合体育中心、滑雪厅、综合体育中心，二期的初中国际部、高中国际部、幼儿园、后勤办公楼等共计 10 栋建筑约 14 万平米已经投入使用，三期正在建设中。

该项目建筑分布东西跨度超过 1000 米，南北

跨度超过 800 米，地势高差超过 60 米，建筑周边采集井设置位置紧张。方案采用了恒有源分布式浅层地热能冷热源系统作为项目的冷热源方案。恒有源分布式浅层地热能冷热源系统由单井循环换热地能采集井、浅层地热能集中换热站、分布式冷热源站及建筑内供暖冷末端组成。

项目利用多套单井循环换热地能采集井集中采集浅层地热能，利用一次采集管网将浅层地热能输送至浅层地热能集中换热站，由二次换热管网将浅层地热能分配至分布式冷热源站，分布式冷热源站内设置能量提升三次管网，提升至到达供暖冷需求的温度品位，由四次管网输送至建筑内供暖冷末端系统，完成供暖冷过程。

根据项目分期建设的需求，项目一期二期各设置一套恒有源分布式浅层地热能冷热源系统，其中一期设置地能采集井 22 套，集中换热站 1 座，分布式冷热源站 4 个；二期设置地能采集井 28 套，集中换热站 1 座，分布式冷热源站 3 个。

恒有源分布式浅层地热能冷热源系统应用于该项目的优势：

1、集中采集浅层地热能，实现按需供能

项目建筑的用能多少、使用频率等各不相同，采用集中采集浅层地热能的方式，通过设置采集井循环水回水的温度而调整其循环流量，实现按需取能，用多少、取多少、采多少，节约采集水泵电耗。

2、二次网闭式循环输送浅层地热能，降低输送能耗

项目建筑物分布高差达 60 米，若采用常规的恒有源地能热泵环境系统，需要将采集井的循环水直接输送至每个冷热源站中，每个采集水泵需要克服由于地势高差带来的 60 米静水压差，总采集水泵电功率需要 1250kw。方案采用设置集中换热站的方式后，每口采集井的循环水只需要输送至集中换热站即可，而集中换热站设置在地能采集井附近，大幅降低的了采集井需要克服静水压差，总采集水泵电功率只需 750kw。由于设置集中换热站，需要增加设置二次管网输送循环泵，循环泵总功率为 200kw，在扣除增加的二次管网输送循环泵功率后，总的采集系统电功率也较常规系统减少了 24%。同时，二次管网输送循环泵采用变频控制，能够进一步的降低运行时的能耗。

3、二次管网输送低温地热能，减少热量损失

采用常规的恒有源地能热泵环境系统时，地能采集井循环水的供水温度为 15℃，采用设置集中换热站的方式后，由集中换热站输送至每个冷热源站的二次水供水温度降至 13℃，按照管道埋深位置冬季土壤温度为 0℃计算，热量损失可减少 13%。

4、分布式冷热源站按需设置，与建筑冷热量需求高度贴合

根据每个建筑的冷热负荷情况，合理设置分布式冷热源站内热泵机组的装机容量，并考虑部分负荷时的运行情况，采用多台机组、每台机组多机头设置，能够实现建筑供能量与建筑需求量的高度贴合，避免大马拉小车情况的同时，进一步降低现系统运行能耗。

每年节电成果显著

节能环保是恒有源单井循环换热地能采集技术的巨大优势，北京市海淀外国语实验学校京北校区运行以来的各项数据正说明了这一点。项目 2021-2022 年供暖季总能耗为 259.03 万 kWh 电能，折合 318 吨标煤。与采用电锅炉供暖比较，可节能约 800 吨标煤，可减少 CO_2 排放 1976 吨，减少 SO_2 排放 16 吨，减少粉尘排放 8 吨。

项目每年夏季制冷总用电量为 50.89 万度，

比传统中央空调系统节电量约为 17.11 万度电。因不采用冷却塔，没有水的蒸发损失，每年节水 396 吨。

经过运行分析计算，该项目耗电量平均为冬季供暖和热水 38.2kW · h/ ㎡（含 1400 人的生活热水），夏季 8.6 kW · h/ ㎡（夏季余热回收免费制热水和辅助制冷），全年供暖、制冷和提供生活热水共耗电量为 46.8kW · h/ ㎡，按照居民电价 0.52 元 / kW · h 计算，全年运行费用为 24.4 元 / ㎡（146 天供热，200 天热水，365 天泳池加热，90 天制冷）。

该项目利用单井循环换热地能采集技术采集地表下百米以内深度的土壤、砂石、地下水中蕴含的低于 25°C的低温热能，与成熟的热泵技术相结合，为建筑物供暖、制冷、提供生活热水。技术使用过程中没有水的消耗，对地下水无污染，不会产生潜在地质灾害，是土壤源热泵的一种。

系统制冷产生的热量可直接通过热泵机组实施热回收用作制备生活热水或用于泳池池水加热，实现系统能量的循环利用。同时，项目实现了原创技术的完全市场化，参考以往类似项目实际运行情况并结合本项目特点，在没有获得任何项目相关补贴的情况下，可实现项目的低成本运营。年均运行费用 24.4 元 / ㎡，较张家口市 2018 年发布执行的张家口市非居民（学校）供热价格 44.1 元 / ㎡（建筑平米）节约 44.7%。

浅层地热能多项优势促环保

恒有源浅层地热能分布式冷热源系统由单井循环换热地能采集井、浅层地热能集中换热站、分布式冷热源站及建筑物室内的末端系统组成。项目设置多口单井循环换热地能采集井集中采集浅层地热能，利用一次采集管网将浅层地热能输送至集中换热站，由二次换热管网将浅层地热能分配至分布式冷热源站，分布式冷热源站内设置能量提升三次管网，提升至供暖冷需求的温度品位，由四次管网输送至供暖冷建筑物室内的末端系统，完成供暖冷过程。

恒有源浅层地热能分布式冷热源系统优势：

1、集中采集浅层地热能，利于系统检修维护；

2、二次管网输送送低温地热能、减少热量损失；

3、分布式冷热源站根据建筑的用能需求、使用频率等特点设置，保证运行灵活，实现按需取能，用多少、取多少、采多少，节约用能；

项目的核心技术为单井循环换热地能采集技术，该技术是一项我国原创的先进的适用于多种地质条件的浅层地热能采集技术。它以循环水为介质采集浅层地下温度低于 25°C的热能，可以实现地下水就地同层全部回灌。根据适用的不同地质条件，分为适用于强透水地质的无换热颗粒采集井和弱透水地质的有换热颗粒采集井。采集井由加压回水区、密封区、抽水区组成，以水为介质，从抽水区将采集到的热量进入换热器，将换热以后的介质通过加压回水区循环到抽水区，封闭循环换热，达到取热不耗水的目的，能够安全、高效、省地、经济的采集浅层地热能，为大规模安全开发利用清洁可再生能源为建筑供暖冷提供了有利的技术支撑，该技术适用于新建、改扩建的各种公建、民建、农户等建筑的供暖冷，能够进一步促进建筑节能低碳运行，实现更高的经济效益和环境效益。

单井循环换热地能安全高效

单井循环换热地能采集技术是一种安全、高效、省地、经济地采集浅层地热能的应用技术，早在 2000 年就已成功运用，经过 20 多年来技术发展与更新，目前已经成为一项先进的适用于多

种地质条件的浅层地热能采集技术。单井循环换热地能采集井利用压差得到温差，循环换热采集岩土体中的地热能。地热能采集利用全过程不消耗也不污染地下水，对地下水是安全的，避免了潜在地质灾害。

单井循环换热地能采集井按结构分为有换热颗粒地能采集井和无换热颗粒地能采集井两种形式。有换热颗粒地能采集井适用于弱透水地层，井深 40-100 米，单井地热能采集量 100-300kW；无换热颗粒地能采集井适用于强透水地层，井深 60-100 米，单井地热能采集量 15-500kW。

单井循环换热地能采集井是我国原创的自主知识产权技术，经中科院文献情报中心国内外双向查询为原创技术，具有多项国际发明专利，省部级鉴定国际先进水平。2012 年 12 月，由恒有源科技发展集团有限公司参编的北京市地方标准《单井循环换热地能采集井工程技术规范》（DB11/T935-2013）被北京市质量技术监督局批准发布。经过多年的推广实施，已经应用至超过 2100 万平方米建筑的供暖冷中，成为降低建筑运行碳排放的重要技术措施，为早日实现双碳目标贡献力量。是解决建筑供暖冷的重要低碳路径。

恒有源单井循环换热地能采集还有多个技术优势：

1、高效

单井循环换热地能采集井是以地下水为介质，采用与地下土壤砂石直接换热的小温差方式采集浅层地热能，大幅减小了传热温差，提高了换热井的供水温度，从而提高了整个供热（冷）系统的能效；

2、安全环保

地热能采集利用全过程不消耗也不污染地下水，对地下水是安全的，避免了潜在地质灾害。

3、省地

其换热效率为传统土壤源方式的 20-100 倍，单井成井后地面仅占一个检修井盖面积，占地面积为传统方式的 1/（20-100），为浅层地热能在土地紧张建筑密集的城市中心区应用提供了技术支持；

4、适用性广

地能采集井分为有蓄能颗粒地能采集井和无蓄能颗粒地能采集井，可适用于不同地质情况，可设计性强，适用范围广。

5、施工周期短

根据项目冷热量需求设定采集井数量，单井施工周期 3-7 天，可实现多井同步施工，可大大缩短工期。

浅层地热能分布广、蕴藏丰富、温度恒定，结合先进的单井循环换热地能采集技术为建筑物供暖冷已应用多年，实例证明其完全可以作为供暖冷的替代能源。恒有源地能热泵环境系统可设计性强，可以根据项目的规模、建筑分布特点、使用规律等进行专项的设计，该项目就是典型案例。恒有源分布式浅层地热能冷热源系统实现了项目全部供暖、制冷、生活热水的清洁能源供应，较传统冷热源系统节能 60%。恒有源地能热泵环境系统运行过程中节能量显著，能够大幅降低系统的碳排放，促进实现人与环境和谐共生。

纵观现行多种供暖形式，浅层地热能节能、高效、无污染的独有特点，成为供热行业助力“双碳”目标的优势选项。因此，需要不断加大浅层地热能行业的科技研发力度，努力提升浅层地热能清洁供暖的占有率，以事实和数据作为有力支撑力促浅层地热能成为供暖替代能源的首选，积极推进新时代供暖能源转型。独行者速，众行者远，为碳中和、碳达峰目标的实现，身为清洁能源企业理所应当积极贡献智慧和力量，恒有源有责任有义务致力于全面推动首选浅层地热能作为供暖替代能源，全力为习近平主席惦记的亿万百姓暖冷大事而奋斗。

A PRELIMINARY STUDY ON THE COUPLING HEATING (COOLING) SYSTEM OF HYDROGEN ENERGY AND SHALLOW GEOTHERMAL ENERGY

Author: Liu Baohong (Vice President of Heng Youyuan Technology Development Group)

1.Summary

Hydrogen energy is a clean and efficient secondary energy with abundant resources, wide source variety, and high energy value of combustion. It is clean and pollution-free, consists of various forms of utilization, and can be used as an energy storage medium among many other advantages. Shallow geothermal energy is a clean and renewable energy. It refers to the low-temperature geothermal resources in the shallow crustal rock and ground water with a temperature lower than 25°C within the depth of 200 meters below the surface and beholds great value of development and utilization under current technical and economic contexts. It has the advantages of having huge reserves, rapid regeneration, wide distribution, moderate temperature, and consistent stability, often boasted as an inexhaustible huge “green energy treasure house.” The shallow geothermal energy heat pump system is driven by hydrogen fuel cell power generation, and a clean power supply for heating. Cooling and domestic hot water supply system can be built independently to form a low cost, efficient and clean distributed comprehensive energy utilization system. In this paper, the technical scheme of the coupled heating (cooling) system of hydrogen energy + shallow geothermal energy is proposed. The influences of different coupling modes on the initial investment, operating cost and user burden are discussed, and the coupling modes and proportions are determined and optimized. The coupled heating (cooling) system of hydrogen energy + shallow geothermal energy is suitable for the areas without power conditions, especially for the vast rural areas lacking electricity. It can reduce the heating cost, improve the reliability of heating, and realize energy saving, environmental protection, saving and affordable for residents in the heating field.

2.Purpose of research

In 2020, China included hydrogen energy in its 14th Five-Year Plan and Vision 2035, which will help achieve the country's strategic goal of "carbon peak and carbon neutrality." In particular, China has a vast territory and abundant renewable energy resources such as solar energy, wind energy and tidal energy. Its installed capacity of renewable energy ranks first in the world, and it has great potential in the supply of clean and low-carbon hydrogen energy.

At present, the top-level design of hydrogen energy industry has begun in China. The local government and enterprise are actively involved in the layout of hydrogen energy, and the hydrogen energy technology chain is gradually nearing completion and optimization, with the hydrogen energy industry chain gradually being formed. A "Hydrogen China" strategy has emerged. The coupled heating (cooling) system of hydrogen energy and shallow geothermal energy can realize distributed cold, hot and electric power supply, which can adjust the peak of the power system and improve the reliability of the power supply. It can also be used as a clean and renewable comprehensive energy for building heating (cooling) and domestic hot water, which can play an irreplaceable role in the future building heating field. Evidently, hydrogen + shallow geothermal energy coupled heating system can solve the intermittent problems brought by large-scale new energy access, clean heating network, environmental pollution and carbon emission reduction problems, and will greatly promote the rapid development of new energy in our country, promote energy transformation, and meet the needs of national economy and social development.

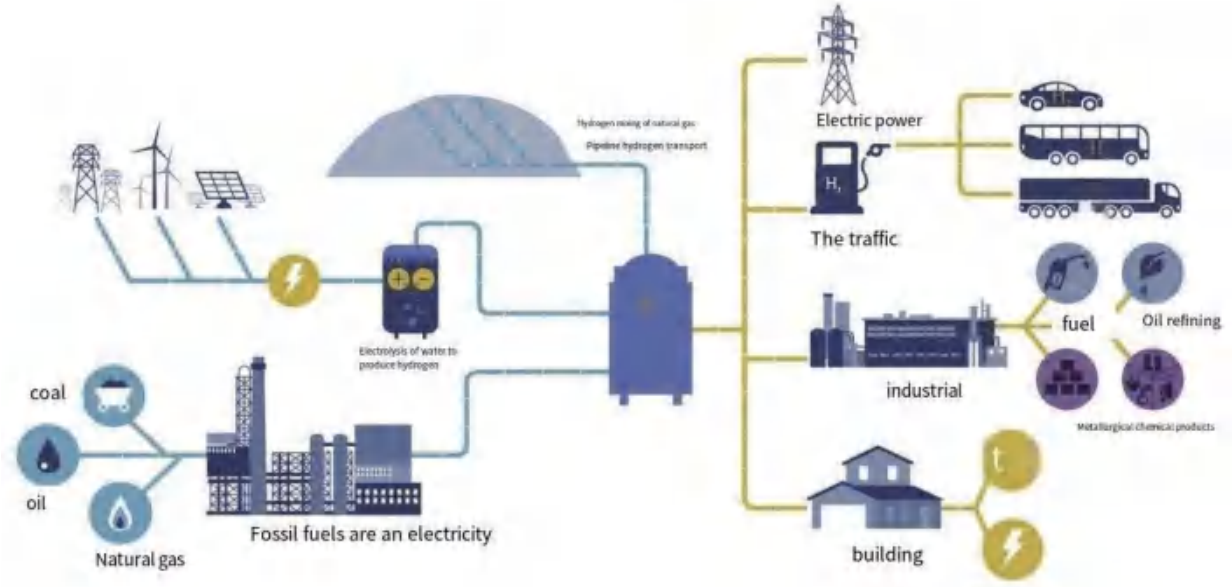

Schematic diagram of the whole industrial chain of hydrogen energy with green hydrogen as the core

3.Hydrogen + shallow geothermal coupled heating (cooling) system

3.1 Hydrogen energy + shallow geothermal energy coupling heating system

The coupled heating system of hydrogen energy and shallow geothermal energy can form a completely independent, continuous and stable off-grid power supply, heating, cooling and hot water supply system. According to the adaptability of the product and the characteristics of the system, it can be divided into distributed power generation household heating (cold) system and distributed power generation central heating system.

3.1.1 Distributed generation household heating system

3.1.1.1 Hydrogen-powered domestic CHP fuel cell + household heating system coupling

Similar to the gas + ground energy heat pump triple supply system, hydrogen energy and fuel cells can also be coupled to the building energy supply. The fuel of the fuel cell system is city gas, specifically natural gas, gas, LPG, etc.

The triplex power supply system coupled with hydrogen household CHP fuel cell + household heating system is composed of six parts: fuel processing subsystem, fuel cell system, power electronics subsystem (power supply), waste heat recovery subsystem, coupled hot water system, coupled heating (cooling) system. First, the fuel processing subsystem reorganizes gas into hydrogen, which is delivered to the fuel cell system to generate electricity. Secondly, the power electronics subsystem converts the direct current generated by the fuel cell into alternating current, which is used by the home-heating system of the ground energy heat pump or incorporated into the power grid. Then, the waste heat recovery subsystem can recover and store the waste heat generated by fuel cell power generation for heating and heating water. Finally, according to the cold and hot demand of the building in winter and summer, the coupled hot water

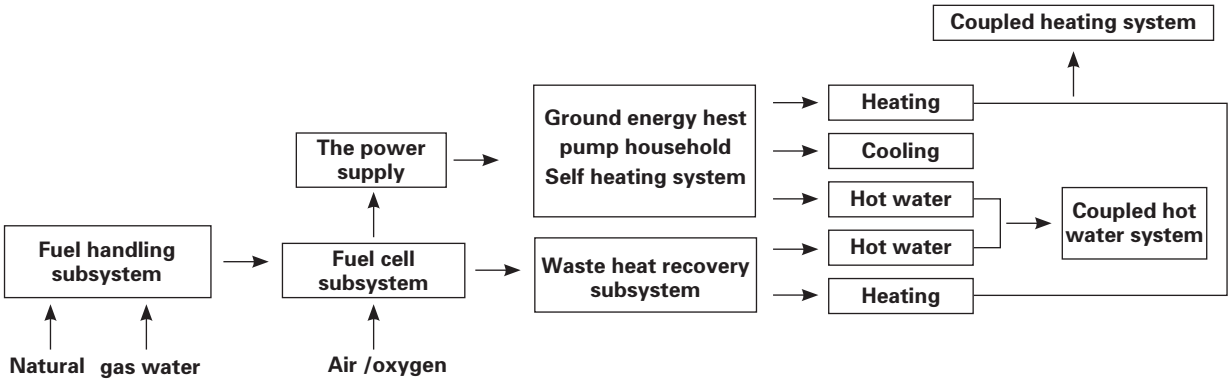

Schematic diagram of coupled household heating system

system and the coupled heating (cooling) system are composed.

3.1.1.2 Optional equipment at home and abroad

① Fuel cell equipment

In Europe, America, Japan and other developed countries, under the strong support of the government, the fuel cell building energy supply system has entered the stage of commercial application. SOLIDPOWER, a German company, is a pioneer in the small SOFC fuel cell industry and has strong technological innovation capability. Its core product, BlueGEN, claims the most efficient m-CHP equipment in the world, with more than 1,000 installations worldwide. BlueGEN uses natural gas power generation as a fuel source to supply energy, with the input of 2.5kW fuel, output of 1.5kW electricity and 0.6kW heat, with a comprehensive efficiency of 85%. Japan is committed to developing distributed energy systems. With more than 200,000 home fuel cell systems in operation, Japan has the most extensive use of fuel cells in the world. Japan's domestic fuel cell energy supply system uses urban gas as fuel and mainly consists of a fuel cell and a heat storage tank. The fuel cell is used to generate electricity and the tank is used to recover waste heat. Mainstream products on the market include Panasonic, Aisin Seiko and Toshiba, etc. The specific parameters are shown below.

ENE-FARM SERIES

Manufacturer		Aixin Precision Machine	Panasonic	Toshiba
Fuel Cell Type		Solid Oxide	Polymer Electrolyte	Polymer Electrolyte
Power Output		700W	700W	700W
Hot water storage capacity		90L 70°	140L 60°	200L 60°
Efficiency	Power generation efficiency	46.5% (net thermal efficiency)	39.0% (net thermal efficiency)	39.0% (net thermal efficiency)
	Total efficiency	90.0% (net thermal efficiency)	95.0% (net thermal efficiency)	95.0% (net thermal efficiency)
Durability (in years)		10	10	10

Schematic diagram of coupled household heating system

② Ground energy heat pump household heating equipment

Ground energy heat pump household heating equipment has been widely popularized and applied. According to the form of the end system, it can be built into a ground energy heating and cooling all-in-one equipment, with the end terminal composed of cold and hot air type, and with ground energy heating and cooling all-in-one household hot water system.

The equipment is low-power distributing at 220V, with the end terminal of hot (cold) wind type. Heating speed is fast, with divided configuration and use, and users can open the room equipment at will, maximizing energy-saving needs.

2) Geothermal heat cooling household water heater products

Geothermal energy household water heater equipment is low-power distributing at 220V, with the end terminal of hot (cold) water type, and can be combined with floor radiation heating, radiator, fan coil end systems.

3.1.1.3 Characteristics of Coupling Heating system

Geothermal heat and cooling integrated machine frequency conversion products

Serial no.	Working Medium	Product Series	Specifications and Models		Cold Regions【Note 1】	Cold Regions 【Note 2】		Regions with cold winters and hot summers【Note 3】		Reference heating area (㎡)
					Heat product ion (kW)	Heat production (kW)	Cooling capacity (kW)	Heat production (kW)	Cooling capacity (kW)	
1	R410A	Geothermal heat & cold all-in-one machine (frequency conversion)	2P Frequency conversion one-driven-two	Cabinet DNV-I-56AN2	5.0	5.6	5.6	6.2	5.6	⩽ 60 (single room ⩽ 30)
2			2P Frequency conversion one-driven-two	Wall-Suspending DNV-I-56AN2	5.0	5.6	5.6	6.2	5.6	⩽ 60 (single room ⩽ 30)
3			3P Frequency conversion one-driven-three	DNV-I-75AN3	6.8	7.6	7.6	8.3	7.6	⩽ 90 (single room ⩽ 30)
4			3P Frequency conversion one-driven-three	DNV-I-75AN3	6.8	7.6	7.6	8.3	7.6	⩽ 90 (single room ⩽ 30)

One–drive–three frequency converter (internal cabinet and wall–suspending machines can be matched at will)

One–drive–two frequency converter (internal cabinet and wall–suspending machines can be matched at will)

Features: Each household is an independent energy utilization system, independent of power grid operation, reducing energy transmission investment and operation costs; Flexible operation, environmental protection without harmful substance emissions.

Development prospect: It can be distrib-

Serial no.	Working Medium	Product Series	Specifications and Models		Cold Regions【Note 1】	Cold Regions 【Note 2】		Regions with cold winters and hot summers【Note 3】		Reference heating area (㎡)
					Heat product ion (kW)	Heat production (kW)	Cooling capacity (kW)	Heat production (kW)	Cooling capacity (kW)	
1	R410A	Ground Energy Heat Pump Boiler	3P Ground Energy Heat Pump Boiler	DNS-II-75A	7.2	8	6.4	9.4	6.4	⩽ 130
2			6P Ground Energy Heat Pump Boiler	DNS-II-150A	14.4	16	12.8	18.8	12.8	⩽ 260
3			9P Ground Energy Heat Pump Boiler	DNS-II-225A	21.6	24	19.2	28.2	19.2	⩽ 390

Note 1: Heat production in cold regions refers to the stable heat supply of the heat pump when the extreme outdoor temperature is -48.5°C and the shallow geothermal energy temperature is about 9°C in Harbin, Changchun, Shenyang, Hohhot and other areas.

Note 2: Heat production in cold areas refers to the stable heat supply of heat pumps in Yan 'an, Beijing, Tianjin, Shijiazhuang, Jinan, Taiyuan,

Zhengzhou, Xi 'an and other areas when the extreme outdoor temperature is -25°C and the shallow geothermal energy temperature is about 15°C .

Note 3: Heat production in cold winter and hot summer areas refers to the stable heat supply of the heat pump when the extreme outdoor temperature is -12°C and the shallow geothermal energy temperature is about 19°C in Shanghai, Nanjing, Hangzhou, Hefei, Wuhan, Nanchang, Fuzhou, Changsha and other areas.

uted to realize the single household self-use and the combination of generation and use, clean and pollution-free, which is the most ideal way of user end energy use.

3.1.2 Distributed generation central heating system

3.1.2.1 The hydrogen fuel cell power station coupled with the ground energy heat pump central heating system

Hydrogen energy has a high energy density and can achieve orders of magnitude increase in energy storage capacity compared with traditional energy storage methods. The waste wind power generation, photovoltaic power generation and other renewable energy can produce hydrogen at a low cost, complete the transformation of electric-hydrogen-electric cycle, and realize a more controllable, stable and secure supply of renewable electricity. Domestic hydrogen fuel cell power station application technology is mature, has been successfully used in traffic, emergency power and other scenarios. The coupling system of hydrogen fuel cell power station and ground energy heat pump central heating system can provide heating, cooling and hot water for large area buildings or buildings.

3.1.2.2 Optional equipment at home and abroad

1.Hydrogen fuel cell power station equipment

In 2013, Germany completed the first commercial h2-herten multi-energy complementary project to produce hydrogen from wind power. The project is capable of producing 250MW·h of electricity per year and nearly 6,500 kg of hydrogen, some of which is used in fuel cells to generate enough electricity for a nearby office building. Similarly, France has completed the MYRTE power generation project in Corsica, with a 560kW

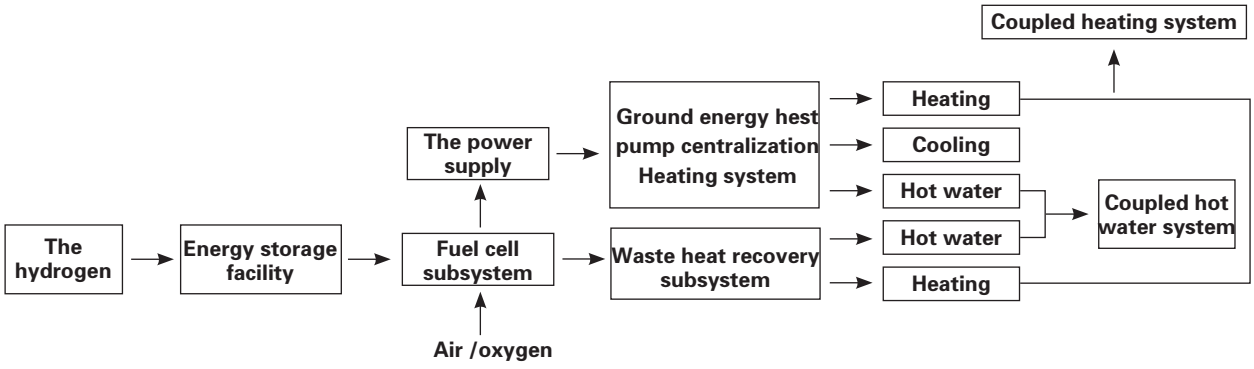

Schematic diagram of coupled central heating system

photovoltaic plant, a 50kW water electrolysis plant and a 100kW PEMFC fuel cell.

Domestic hydrogen fuel cell power station technology is very mature, and is widely used in automobile, emergency power and other scenarios. Shanghai Hengjin Power 100kW hydrogen fuel cell power station equipment related parameters are as follows:

The parameters of 100kW independent hydrogen fuel cell power station are as follows:

2.Shallow geothermal energy central heating equipment

Ground energy heat pump central heating product specifications and models are more, from scroll compressor to screw compressor, centrifuge and so on have corresponding specifications, a single heat pump host can meet the heating needs of thousands or even tens of thousands of square meters of

Schematic diagram of hydrogen power generation system

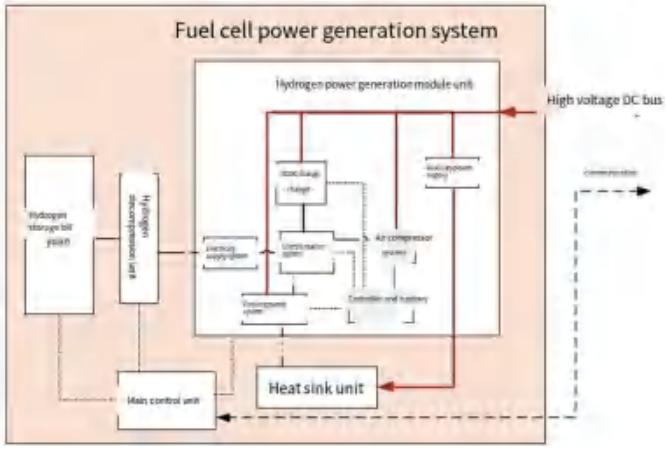

Hydrogen power generation module unit (reactor module) 1150*660*476mm

Hydrogen power generation module unit (integrated module) 1135*660*591mm

category	project	parameter
Hydrogen energy source Power generation system	model	HAWS3OK/60K/130K-A01
	type	PEM
	Rated output power (kW) Maximum output power (kW)	37/68/131 41/74/143
	Rated voltage (V)	87/174/348
	Starting temperature range (C) Maximum reactor operating temperature (C) Cumulative continuous life (hrs) Working years (years) Reactor specific power (kW/kg) Reactor power density (kW/1)	-15 85 3000 Ten years 2. 20 2. 65
	Starting battery (kWh)	3
	The efficiency of	53%
	Reactor startup time (no startup battery)	15s
	Power density per unit area (W/cm2)	0. 58
	Rated single chip voltage (v)	0. 65

scale buildings, common ground energy heat pump host single heat production from 10kW-2000kW.

3.1.2.3 Features of coupled heating system

Functions of coupled heating system: central heating, cooling and hot water supply for one building or multiple buildings.

Features: One building or multiple buildings is an independent energy utilization system, independent of power grid operation, environmental protection without harmful substance emissions; Hydrogen energy device equipment is placed in the public area of the building, combined with domestic development technology, the specific implementation of safety performance is easier to meet.

Development prospects: regional buildings can be distributed to realize self-use and combination of development and use, clean and pollution-free, which is a new distributed comprehensive energy utilization mode.

3.2 Cost and economic and environmental benefits of hydrogen energy + shallow geothermal energy coupling heating system

3.2.1 Initial Investment

① Hydrogen-powered household CHP fuel cell + household heating system coupling

More than 5,000 households in the 2020 Olympic Village in Tokyo, Japan, are powered by the hydrogen household combined heat and power fuel cell system. The total cost of each household equipment is about 1.4 million yen, equivalent to 88,400 yuan. The corresponding investment for 100 m^2 buildings which contains self- heating systems is about 25,000 yuan; The total investment of the cou-

pling system is about 113,400 yuan/household. With reference to BlueGEN equipment parameters, each household is equipped with hydrogen household cogeneration fuel cells with power of 1.5kW, coupled shallow geothermal energy household heat pump system can heat 6kW, plus power generation heating water load of 0.6kW, the maximum hourly household heat supply of 6.6kW. The investment of hydrogen household combined heat and power fuel cell system is calculated as 58,900 yuan /kW based on generation power and 13,400 yuan /kW based on coupling heating power. The investment of the shallow-layer geothermal energy household heat pump system is calculated by the coupled heating power of RMB 3,800 /kW; The total investment of the coupling system is 17,200 yuan /kW.

(2) Coupling of hydrogen fuel cell power station and ground energy heat pump central heating system

The cost of hydrogen fuel cell system is about 10,000 yuan /kW, and the market price of a complete set of 100kW hydrogen fuel cell power station is about 1.8 million yuan. According to the relevant parameters of the 100kW hydrogen fuel cell power station equipment of Shanghai Hengjin Power, the heating power of the ground energy heat pump system is 400kW, and the heating water load of the power generation is 60kW. The total heating power is 460kW, which can be used to heat 9000 square meters of buildings. The investment of the ground energy heat pump system is about 2 million yuan (excluding the heating terminal system), the total investment of the coupling system is about 3.8 million yuan, and the total investment of the coupling system is 82,600 yuan /kW.

3.2.2 Operation cost

Operating costs are influenced by hydrogen production cost, system power generation efficiency, etc. The main factor is hydrogen production cost. First, the cost of hydrogen production is high. At present, the cost of hydrogen production and transportation and filling cost is almost 1:1. The cost of coal hydrogen is about 2 yuan/cubic meter, and it becomes 4 yuan/cubic meter at the hydrogenation station. Additionally, the market price of hydrogen is 70 yuan/kg, and the energy price is relatively high. The operation cost is calculated and compared according to the hydrogen energy cost after industrialization development of 10 yuan/kg.

When the cost of hydrogen energy is 10 yuan/kg, the operation cost of the coupled heating system of hydrogen energy household CHP fuel cell + household heating system is 4150 yuan, which is 23.9% cheaper than the electric heating system, but 29% higher than the hydrogen boiler system and 67% higher than the geothermal energy heat pump system..

3.2.3 Comprehensive energy efficiency

Integrated energy efficiency is affected by hydrogen production technology, fuel cell

Heating System	Equipment Heating Capacity	Energy Consumption During One Heating System	Unit Price of Energy	Operating Cost (Yuan)
Electric Heating System	6kW	Electric Power Consumption 10500kWh	Electricity price of 0.52 yuan/KWH	5460
Geothermal Heat Pump System	5460	Electric Power Consumption 2625kWh	Electricity price of 0.52 yuan/KWH	1365
Hydrogen Boiler System	6kW	In 3233m^3 of hydrogen, 293.8 kg	Hydrogen at 44 Yuan/kg	12927.2
			Hydrogen at 10 Yuan/kg	2938
Hydrogen-powered household CHP fuel cell + household heating system coupling	6.9kW	In 4565m^3 of hydrogen, 415 kg	Hydrogen at 44 Yuan/kg	18260
			Hydrogen at 10 Yuan/kg	4150

power generation efficiency and integrated heat conversion efficiency. The coupling heating (cooling) system efficiency with shallow geothermal energy after power supply is shown in the figure below.

1) Hydrogen-powered household cogeneration fuel cell + household heating system coupling uses hydrogen-powered fuel cell power generation technology based on natural gas, gas, etc. Specifically, it is "natural gas/coal → natural gas/coal gasification hydrogen production (reforming efficiency of natural gas is 65%) → hydrogen storage (efficiency is 90%) → hydrogen fuel cell power generation (efficiency is 60%) + power generation heat generation (efficiency is 24%) → ground energy heat pump system heating."

Total heating efficiency 65% × 90% × (60%+24%) ×400%=196%;

Total refrigeration efficiency 65%×90% ×60%×500%=175%.

2) The coupling of hydrogen fuel cell

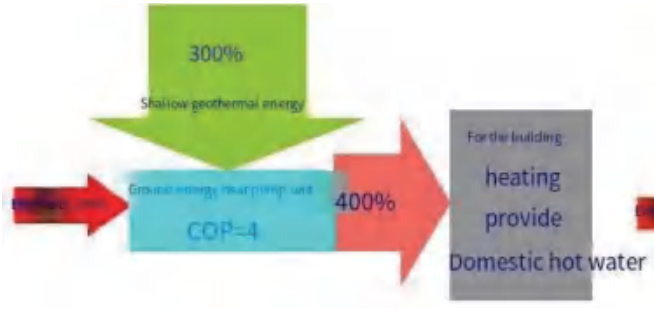

Winter energy balance diagram

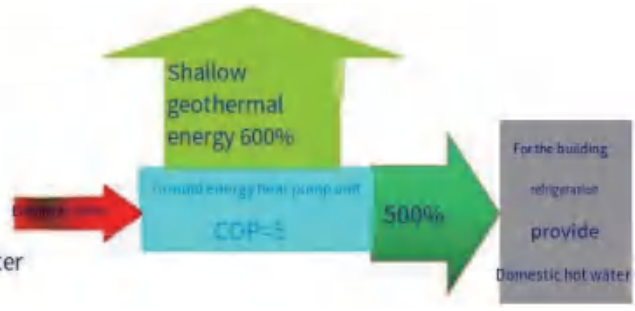

Summer energy balance diagram

power station and ground energy heat pump central heating system is based on renewable clean wind power generation, photovoltaic power generation → electrolytic water hydrogen production electrolytic water efficiency 60%) → hydrogen storage (efficiency 90%) → hydrogen fuel cell power generation (efficiency 50%) + heat generation (efficiency 30%) → ground energy heat pump system heating.

Total heating efficiency 60%×90%×(50%+30%) × 400%=172%;

Total cooling efficiency 60%×90%×50% × 500%=135%.

3.2.4 Analysis of energy saving in operation

Based on the analysis of 10500kWh heating load of 100 m^2 building in winter in Beijing area, The power generation is considered according to the national standard coal consumption of power supply of thermal power plants with 6000 kW or above, the calorific value of hydrogen fuel is 32,352 kcal/kg, the calorific value of 2.4m³ hydrogen is equivalent to the calorific value of 1kg standard coal, 1m³ hydrogen (11m³ hydrogen weighs 1kg) generates 1.5 degrees of electricity, the power generation efficiency is 60% according to BlueGEN equipment parameters, and the power generation efficiency is 60%. The hot

Heating System	Mode of Energy Conversion	Equipment Heating Capacity	Heating System Efficiency	Efficiency after Energy Delivery Loss	Energy Consumption in One Heating System	Converted to Standard Coal (kg)	Energy Saved (%)
Electric Heating System	Electricity delivered through centralized grid to each household and converted into heat	6 kW	1	0.6	Power Consumption 10500 kWh	5460	0
Geothermal Heat Pump System	Power generation centralized to transport electric energy to drive the heat pump	6 kW	4	2.4	Power Consumption 2625 kWh	1365	75.0
Hydrogen Boiler System	Hydrogen is burned and converted into heat energy	6 kW	0.95	0.8	Converts to 3233 m^3, 293.8 kg of Hydrogen	1683.9	69.2
Hydrogen-powered household CHP fuel cell + household heating system coupling	Heat pump is driven by hydrogen power generation	6.9 kW	2.3	2.3	Converts to 4565 m^3, 415 kg of Hydrogen	827.0	84.9

water efficiency is 24%. Hydrogen compression (3% loss ~ 6 percent), transportation (lost 2 percent ~ 3%), retail (10% loss), and overall energy transportation (15% loss).The energy consumption and energy saving analysis of different heating methods are as follows:

The above analysis shows that in the electric heating system, geothermal heat pump system, hydrogen boiler system, hydrogen household combined heat and power fuel cell + household heating system coupled heating system, The energy- saving efficiency in descending order is geothermal energy heat pump system > hydrogen household combined heat and power fuel cell + household self-heating system coupling heating system > hydrogen boiler system > electric heating system. The energy saving of hydrogen household combined heat and power fuel cell + household self-heating system coupling heating system is 15.7% higher than that of hydrogen boiler..

3.2.5 Environmental benefits

1.Hydrogen-powered household CHP fuel cell + household heating system coupling adopts the hydrogen-powered fuel cell power generation technology route based on natural gas and gas, etc. In the whole process, only the hydrogen energy production process will produce CO2 emission. CHP fuel cell and ground energy heat pump system are both zero-pollution and zero-emission processes. For each Kg of hydrogen produced, the CO2 emission of natural gas reforming technology is 9Kg, and that of coal gasification technology is 12Kg.

2.The coupling of hydrogen fuel cell power station and ground energy heat pump central heating system adopts the route of generating hydrogen based on renewable clean wind power and electrolytic water for photovoltaic power generation. As wind power and photovoltaic power generation are used as clean power sources, there is no CO2 emission in the whole process.

3.3 Analysis of investment and operation cost of heating system with different coupling modes

The coupled system investment of hydrogen household CHP fuel cell + household heating system is mainly affected by the price of CHP fuel cell, and the heating load of the system is small and the sensitivity fluctuates greatly.

The coupling system of hydrogen fuel cell power station and ground energy heat pump central heating system is used to analyze the different coupling modes. The fuel cell system efficiency is 0.8, the power generation efficiency is 0.5, and the heating water thermal efficiency is 0.3. The investment of fuel power generation system is calculated according to the cost of 10,000 yuan /kW, and after industrialization, 5,000 yuan /kW and 0.1 yuan /kW respectively.

Operating cost 1 – Hydrogen energy sells for 44 yuan/kg.

Operating cost 2 – Hydrogen energy sells for 10 yuan/kg.

To sum up, the analysis of different coupling systems shows that when the price of hydrogen energy is 44 yuan/kg, the heating cost of 30%(hydrogen energy + shal-

Analysis table of initial investment and running cost of different coupling modes

Heating System	Energy Conversion Mode	Electric Power (kW)	Itemized Heating Load (kW)	Total Heating Load (kW)	Heating System Efficiency	Efficiency after energy transmission loss	Heating Area (m^2)	Energy consumption in one season	Energy Unit Price	Operating Costs (Yuan/kW)	Operating Costs (Yuan/m^2)	Investment (Yuan/kW) Fuel generation system 10,000 Yuan/kW	Investment (Yuan/kW) Fuel generation system 5000 Yuan/kW	Investment (Yuan/kW) Fuel generation system 1000 Yuan/kW	Proportion of heating load borne by hydrogen energy + shallow geothermal energy coupling system (%)
Electric Heating System	Electricity delivered through centralized grid to each household and converted into heat	100	100	100	1	0.37	2000	210,000 kWh of electricity	Electricity price of 0.52 yuan/KWH	1092	54.6	2200	2200	2200	/
Geothermal Heat Pump System	Power generation centralized to transport electric energy to drive the heat pump	100	400	400	4	1.48	8000	210,000 kWh of electricity	Electricity price of 0.52 yuan/KWH	273	13.65	4000	4000	4000	0
Coupling of hydrogen fuel cell power station and ground energy heat pump central heating system	Local hydrogen power generation is used to drive the heat pump	100	400	460	2.3	2.3	9200	Equivalent to 420000m^3 of Hydrogen, measured in 38.18 tonnes	Hydrogen at 44 Yuan/kg	3652	182.6	5652.2	4652.2	3695.7	100
			60						Hydrogen at 10 Yuan/kg	830	41.5				100

Heating System	Energy Conversion Mode	Electric Power (kW)	Itemized Heating Load (kW)	Total Heating Load (kW)	Heating System Efficiency	Efficiency after energy transmission loss	Heating Area (m^2)	Energy consumption in one season	Energy Unit Price	Operating Costs (Yuan/kW)	Operating Costs (Yuan/m^2)	Investment (Yuan/kW) Fuel generation system 10,000 Yuan/kW	Investment (Yuan/kW) Fuel generation system 5000 Yuan/kW	Investment (Yuan/kW) Fuel generation system 1000 Yuan/kW	Proportion of heating load borne by hydrogen energy + shallow geothermal energy coupling system (%)
50% (hydrogen energy + shallow geothermal energy coupling) +50% geothermal energy coupling system	Local hydrogen power generation is used to drive the heat pump	50	200	470	3.15	1.89	9400	Equivalent to 215000m^3 of Hydrogen, measured in 19.5 tonnes	Hydrogen at 44 Yuan/kg	1961.6	98.1	4808.5	4276.6	3851.1	50
			30						Hydrogen at 10 Yuan/kg	551.0	27.5				50
	Ground energy heat pump system	60	240					12,3000 kWh of electricity	Electricity price of 0.52 yuan/KWH	/	/				50
30% (hydrogen energy + shallow geothermal energy coupling) +70% geothermal energy coupling system	Local hydrogen power generation is used to drive the heat pump	30	120	458	3.49	1.726	9200	Equivalent to 126000m^3 of Hydrogen, measured in 11.45 tonnes	Hydrogen at 44 Yuan/kg	1290.7	64.3	4497.8	4170.3	3908.3	30
			18						Hydrogen at 10 Yuan/kg	440.7	21.9				30
	Ground energy heat pump system	80	320					16,8000 kWh of electricity	Electricity price of 0.52 yuan/KWH	/	/				70

low geothermal energy coupling) +70% geothermal energy coupling system is 64.3 yuan/square meter, 15% higher than that of electric heating system, indicating a high heating cost. When the price of hydrogen energy is 10 yuan/kg, the heating cost of 50%(hydrogen energy + shallow geothermal energy coupling) +50% geothermal energy coupling system and 30% hydrogen energy +70% geothermal energy coupling system are 27.5 yuan/square meter and 21.9 yuan/square meter respectively,

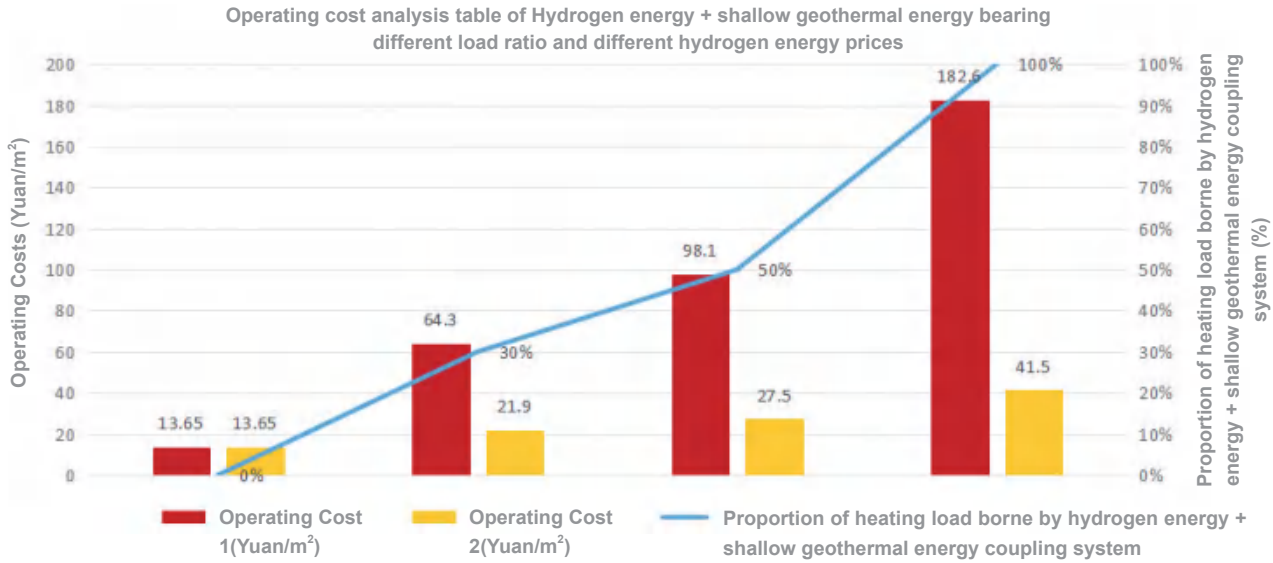

which is close to the urban heating cost standard and can be borne by users.

Initial investment 1 -- The cost of hydrogen fuel cell power generation system is 10,000 yuan /kW

Initial investment 2 -- The cost of hydrogen fuel cell power generation system is 5,000 yuan /kW

Initial investment 3 -- Hydrogen fuel cell power generation system investment at the cost of RMB 10,000 /kW

According to the investment of the ex-

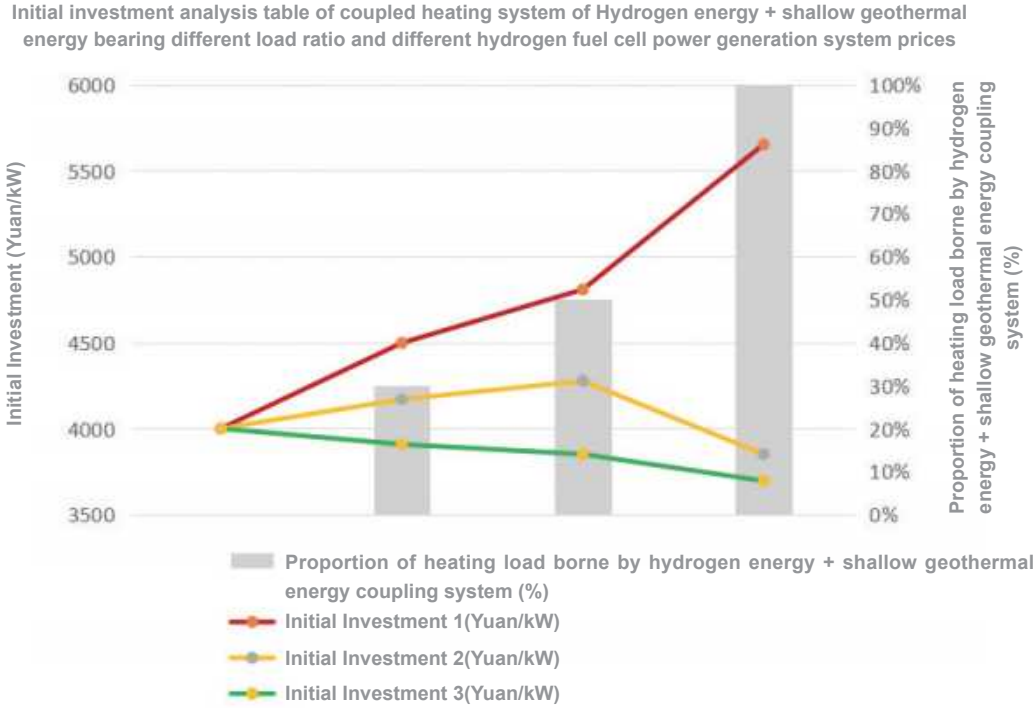

isting hydrogen fuel cell power generation system and the cost of 10,000 yuan /kW, the coupling investment of the hydrogen fuel cell power generation system and the ground energy heat pump central heating system is 5652.2 yuan /kW, the highest. The investment of 50%(hydrogen energy + shallow geothermal energy coupling) +50% geothermal energy coupling system and 30% hydrogen energy +70% geothermal energy coupling system are respectively 16.8% and 11% higher than that of geothermal energy heat pump system.The investment after industrialization of the existing fuel power generation system is calculated according to the cost of 101,000 yuan/kW, and the investment of the geothermal energy heat pump system is the highest at 4000 yuan /kW. The investment of 30% hydrogen energy +70% geothermal energy coupling system is RMB 3908.3 /kW > 50%(hydrogen energy + shallow geothermal energy coupling) +50% geothermal energy coupling system is RMB 3851.1 /kW > the coupling investment of hydrogen fuel cell power station and ground energy heat pump central heating system is RMB 3695.7 /kW.

3.4 Innovations of the coupling system

In order to ensure that the fuel cell works at the appropriate temperature, the cooling method must be used to eliminate the heat. The heat taken away by the cooling can be used as hot water heating and hot water supply. The water/water heat exchanger is suitable for the fuel cell system because of its high heat transfer coefficient, small heat exchanger area and efficient and stable heat transfer.

For the coupled heating system of hydrogen energy and shallow geothermal energy,

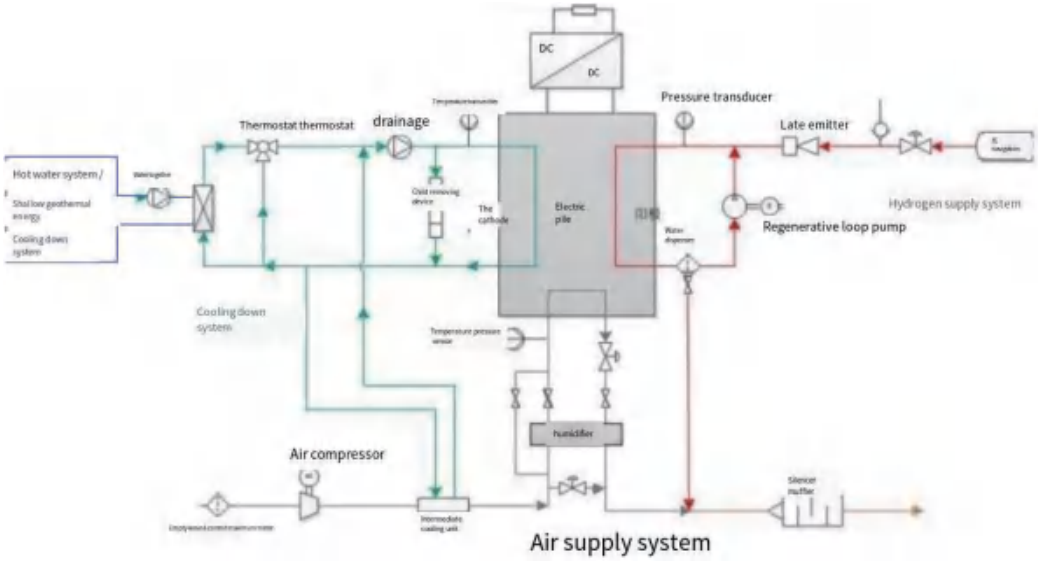

Diagram of hot water system/shallow geothermal cooling system for fuel cell stack

the heat generated by fuel cells in winter and transition season can be used as heat source for heating and domestic hot water. For the same system, the building itself needs to discharge a lot of heat to reduce the indoor ambient temperature in summer, and the heat generated by fuel cells will become excess heat. The shallow geothermal energy system can be used as a good low temperature cooling source for the battery stack system, including winter and summer conditions. The shallow geothermal energy cooling system can also be used as a low temperature cooling source for the fuel cell system. Through the rational design, configuration, and control of the coupling system, the shallow geothermal energy cooling system can improve the temperature of the shallow geothermal energy supply and the efficiency of the geothermal energy heat pump system in winter, which is an important measure to improve the comprehensive energy efficiency of the coupling system.

4. Conclusion

Hydrogen energy, the energy released by hydrogen (H) in the process of physical and chemical changes, is clean and efficient, can store energy, can be transported, and has various application scenarios. It can be made in a variety of ways with small resource constraints. Fuel cells can be used to convert hydrogen energy directly into electricity and water through electrochemical reaction without discharging pollutants. The power generation efficiency is more than 50%, making it a highly efficient energy with zero pollution.

As a green and environmentally friendly renewable resource, shallow geothermal energy has become the first choice to replace traditional heating energy because of its huge reserves, rapid regeneration, wide distribution, good stability and other advantages. Therefore, the development and utilization of shallow geothermal energy plays an important role in building a resource-saving and environment-friendly society in China, and also plays an important role in the reform of China's energy structure.

With the continuous expansion of large-scale application, the initial investment and operating cost are greatly reduced. Shallow geothermal energy is a clean and renewable energy, which has shown the characteristics of low operating cost, high efficiency and energy saving. Scientific coupling of hydrogen energy and shallow geothermal energy can provide a safe and reliable clean heating scheme with low initial investment, and low operating cost can be expected.

GLOBAL CONCENTRATIONS OF GREENHOUSE GASES HAVE HIT NEW HIGH

Author: Xu Xiaofeng

Incumbent President of China Meteorological Service Association and former Deputy Director of China Meteorological Administration

On Oct. 26, the World Meteorological Organization (WMO) released a unsettling update to its Greenhouse Gas Bulletin. According to the report, Carbon Dioxide, Methane and Nitrous Oxide, the three main greenhouse gases that contribute to climate change, are a major source of climate change in countries around the world, experienced heightened levels in the atmosphere which hit a record high in 2021, with 2015 to 2021 the seven hottest years on record.

The 2021 concentration of carbon dioxide was at 415.7 ppm, whereas for methane it was at 1908 ppb, and nitrous oxide at 334.5 ppb. These levels were 149%, 262%, and 124% above the average levels pre=industrialization, when human activity began to alter the natural balance of these gases in the atmosphere.

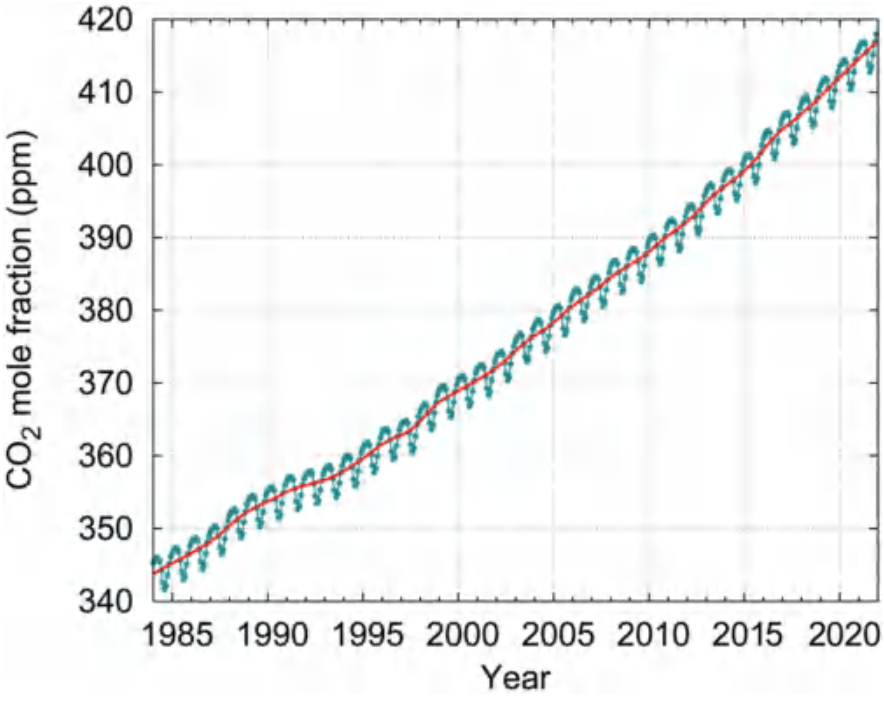

Changes in carbon dioxide growth over the Years (taken from WMO website)

Carbon dioxide levels, which are widely monitored, will increase further between 2020 and 2021 than the average annual increase over the past decade. Measurements from the WMO Global Atmospheric Observatory website show that levels continue to rise through 2022. The amount of greenhouse gases warming the climate through radiative forcing has increased by nearly 50 percent between 1990 and 2021, with carbon dioxide accounting for about 80 percent of the increase.

In 2021, the year saw the largest year-over-year increase in methane concentrations since systematic measurements began 40 years ago. The reasons for this abnormal growth remain to be analyzed, but it is thought to be caused by a combination of biological processes and human activities.

Changes in Methane growth over the Years (taken from WMO website)

Professor Petteri Taalas, Secretary General of WMO, cited: “WMO’s Greenhouse Gas Bulletin once again highlights the enormous challenge and the vital importance of taking urgent action to reduce greenhouse gas emissions in order to prevent further increases in global temperatures. The continued rise in concentrations of major greenhouse gases, including a record acceleration in methane levels, shows that we are still moving in the wrong direction.”

Year-on-year changes in nitrous oxide (taken from WMO website)

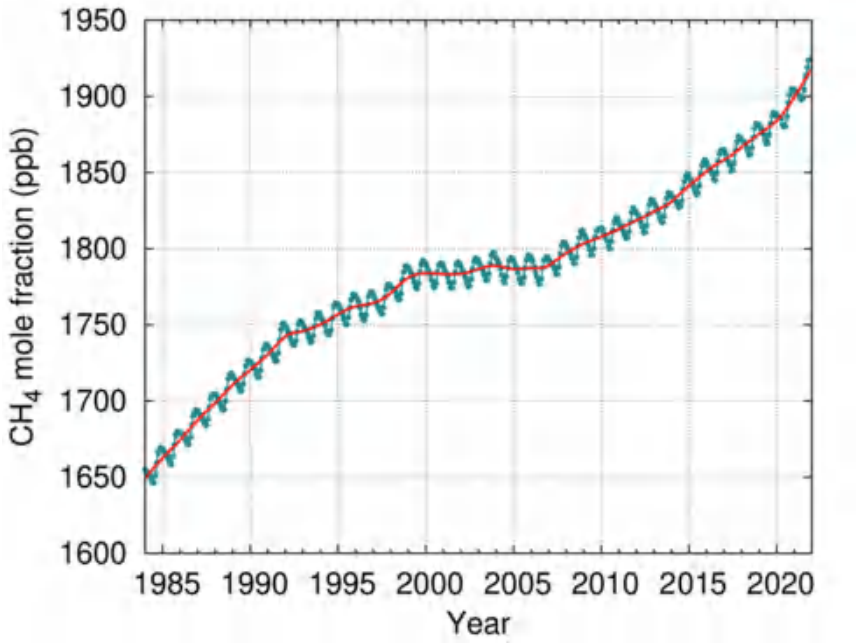

"We need to change the way we consume energy in our industry, our energy and transport systems, and our entire ways of living, especially by reducing emissions from fossil fuels," Taalas stressed. The changes that have been made are economically and technically feasible to achieve a cost-benefit balance, and we should adopt them without delay. "The climate effects of relatively short-lived methane are reversible, and the first and most urgent action should be to cut carbon dioxide emissions, which are a major contributor to warming and associated extreme weather events, causing polar ice loss and sea level rise, with climate effects that will be felt for thousands of years."

The WMO report, released on the eve of the 27th United Nations Climate Change Conference (COP27) in Sharm el-Sheikh, Egypt, from November 7 to 18, aims to promote COP27 negotiators as decision-makers for effective action to achieve the goals set out in the Paris Agreement, to limit the increase in global warming to 2 degrees Celsius over the pre-industrial average, and to 1.5 degrees Celsius if possible. The global average temperature is now more than 1.1°C above the pre-industrial average of 1850-1900.

According to the information provided by the WMO report, it is important to build consensus and establish rules and targets. Nevertheless, without feasible concrete measures and supervision mechanisms, countries may not be effective in taking actions together and form synergy, and the road to reducing emissions and addressing climate change will be difficult and tortuous.

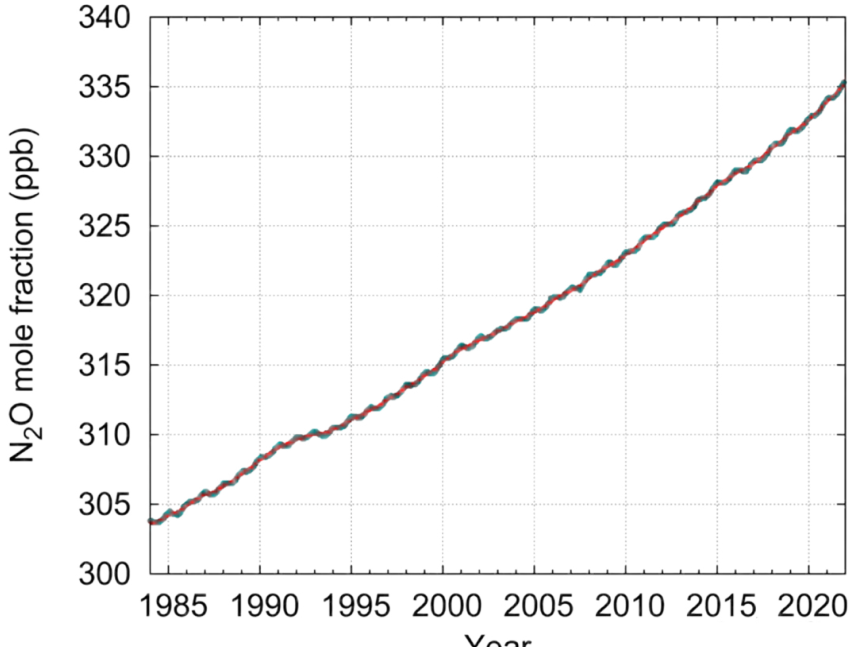

REVISITING THE TEN KEY GEOSCIENTIFIC PROBLEMS IN THE QINGHAI-TIBET PLATEAU

—— 《ACTA GEOLOGICA SINICA》100th Anniversary

Xu Zhiqin [1,2], Li Guangwei [1], Zhang Zeming [2], Li Haibing [2], Wang Yuejun [3], Peng Miao [4], Hu Xiumian [1], Yi Zhiyu [3], Zheng Bihai [1]

1) State Key Laboratory of Metallogenetic Mechanism of Endophytic Metal Deposits, School of Earth Sciences and Engineering, Institute of Continental Dynamics, Nanjing University, Nanjing 210043, China;

2) Institute of Geology, Chinese Academy of Geological Sciences, Beijing 100037, China;

3) Sun Yat-sen University, Zhuhai 510275, China; 4) China University of Geosciences, Beijing 100083, China

Abstract

This paper reexamines the key scientific issues of the Qinghai-Tibet Plateau, providing new clues for solving the "landing" problem of plate tectonics theory, and providing new ideas for understanding the evolution of continental lithosphere and its energy resources, geological hazards and global environmental effects at the plate convergence boundary. In this paper, ten key geological problems of the Tibetan Plateau are discussed as follows: ① The Indian continental Northward drift model; ② Initial collision time between India and Asia; ③ Paleo Tethys orogeny in the Tibetan Plateau; ④ Crustal shortening in the Paleogene Himalayan orogenic belt; ⑤ the deep melting mechanism of the high Himalaya; ⑥ The time limit and difference of the uplift of the Qinghai-Tibet Plateau; ⑦ Structure-denudation-climate interaction and South Asian monsoon; ⑧ Distribution and origin of key mineral resources on the Qinghai-Tibet Plateau; Active fault zone and seismogenic mechanism of the Qinghai-Tibet Plateau; What is the course of the Indian Plate after the collision? Deep dynamic processes. These problems can be regarded as the focus of the current research on the continental dynamic evolution of the Qinghai-Tibet Plateau.

Keywords：Qinghai-Tibet Plateau; Plate tectonics; Dynamics of continents

As the highest, largest, thickest and newest plateau in the world, the Qinghai-Tibet Plateau is the optimal laboratory for developing solid earth science theories. The study of the Qinghai-Tibet Plateau has a history of more than 200 years since the beginning of the Himalayas. Re-examining and exploring the key scientific issues of the Qinghai-Tibet Plateau can provide important new information for the study of the evolution of the continental lithosphere and its energy resources, geological hazards and global environmental effects at the plate convergence boundary, and make contributions to solving the “landing” problem of the plate tectonic theory.

The Indo-Asian collision is the most spectacular geological event since the Cenozoic era, resulting in the rise of the Himalayas, the uplift of the Tibetan Plateau, the formation of the extremely thick crust, the mass escape of the Tibetan Plateau to the east, southeast and southwest, the dispersion and deformation of the inner Asian continent within 2000km, the basin system and oil and gas resources around the Tibetan Plateau, the South Asian monsoon and Asia Inland drought, etc. The author puts forward the following key geological questions for the study of the Qinghai-Tibet Plateau: (1)The Indian continent North drift model; (2) Initial collision time between India and Asia; (3) Paleo Tethys orogeny in the Tibetan Plateau; (4) Crustal shortening in the Paleogene Himalayan orogenic belt; (5) the deep melting mechanism of the high Himalaya; (6) The time limit and difference of the uplift of the Qinghai-Tibet Plateau; (7) Structure-denudation-climate interaction and South Asian monsoon; (8) Distribution and origin of key mineral resources on the Qinghai-Tibet Plateau; (9)Active fault zone and seismogenic mechanism of the Qinghai-Tibet Plateau; The fate of the Indian subduction Plate after the collision -- Deep dynamic processes. This essay commemorates the 100th anniversary of the Geological Journal.

1.Model of the northern drift of the Indian continent

Traversing through the tunnels of time and space to the Mesozoic era, India and Eurasia was still a vast ocean, called the New Tethys Ocean. Studies suggest that the Triassic Indian plate began to disintegrate from the supercontinent Gondwana, followed by a Cretaceous opening, where at the beginning of the northward drift, it collided with Eurasia at about 60 Ma(Zhuetal.,2011;Metcalfe,2013,2017,2021;-MaXuxuanetal.,2018,2021c) . Therefore, the rise of the Himalayas, the uplifting of the Qinghai-Tibet Plateau and the escape of a large number of materials to both sides, and the dispersion and deformation of the inner Asian continent within the range of 2000km formed the thickest crust on Earth (70 ~ 80km) in the Himalayan orogenic belt and South Tibet (Zhao Wenjin et al., 1993; Yin An, 2000; Schulte-Pelkum et al., 2005; Zhang Zhongjieet al., 2011) . During the northward drift of the Indian continent since the Early Cretaceous, a counterclockwise rotation of 90° occurred, which caused the paleo-latitude changes of the Indian plate(Besse et a., 2002; Zhang et al.2017).

There are two different structural reconstruction models for the northern drift of the Indian continent: the Great India Northern drift (which is the view of most scholars) and the “Great India Basin” northern drift (van Hinsbergen et al., 2012) (Fig.1).

The former suggests that with the subduction and closure of the Neo-Tethys Ocean basin, the north-drifting Great Indian

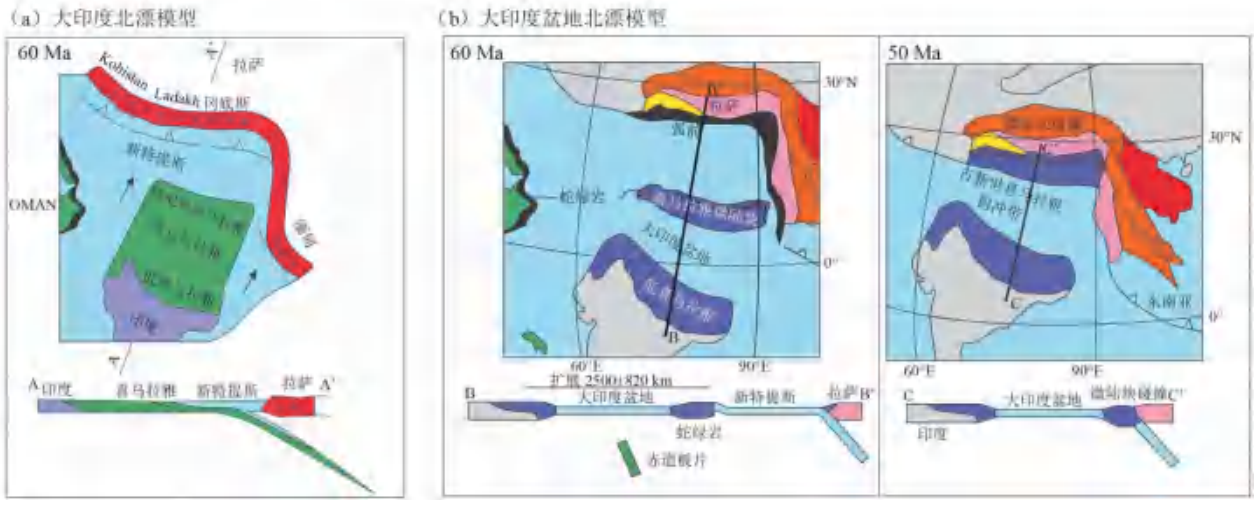

Fig.1 Comparison of models for the restoration and northwards drift of the Indian Plate

（a）-The model shows the single Indian contiguous plate with a wide continental margin incorporating Lesser.Greater and Tethyan Himalaya as one plate.and the India.Asia collision at 50 Ma;

（b）-the model after van Hinsbergen et al.2012).shows a separated Tibetan Himalaya microplate Tethys Himalayan Sequence+Greater Himalayan Sequence)with an intervening ooean.the socalled Greater Himalayan Basin'separating this from the main Indian Plate.This model involves Soft collision'at 50 Ma and a hard collision'at 25~20 Ma

plate collided with Eurasia. The latter proposed that the northern drift of the Great India plate occurred before the Cretaceous, and the Himalayan microlandmasses (including the Tethyan Himalaya and the High Himalaya) separated from the main continent of India in the Late Cretaceous, separating the Great India Basin in the middle, and then both landmasses and the Great India Basin drifted northward at the same time. During the period of 50 Ma, the Himalayan microlandmass firstly had a soft collision with Eurasia, and during the period of 25 ~ 20 Ma, the closure of the Great India Basin resulted in a hard collision between the main continent of India and Eurasia (van Hinsbergen et al., 2012) .

Based on the Northward drift model of the Great India Basin, some new two-stage collision models have been developed in recent years (Yang Tianshui et al., 2015, 2019; Yuan Jie et al. 2021; Jadoon et al. 2021) .Yuan Jie et al.(2021) According to the paleomagnetic data of the northern Tethys Himalayan belt in Gynze and Sagar area, the northern boundary of the Great India Basin is defined. The continental crust of the Great India Basin does not exist, and a northern Indian Ocean of about 1000km is emphasized in the Late Cretaceous. It is the result of the separation of the Himalayan microlandmass from the main continent of India in the Late Cretaceous (about 75-61 Ma). The Himalayan microlandmass collided with the Lhasa terrane at about 61 Ma, and the Indian continent collided with the Tethyan Himalaya at 53 ~ 48 Ma. Jadoon et al. (2021) established a similar Indo-Asian multi-stage collision model based on paleomagnetic data from Late Cretaceous Marine red beds in Pakistan. In this regard, the author believes that the main debate over the northern drift of the Indian continent is the size of the Greater India plate. For paleomagnetic data, further provenance analysis is needed to define its affinity with India or Lhasa terrane, so as to make the judgment of its tectonic location convincing. In addition, how did the approximately 90° rotational northerly drift of the Indian continent during the Early Cretaceous-Late Cretaceous-make a difference in the Tethys Himalaya.

The latitudinal changes in the region and whether they caused “stretching” between the Indian continent and the Tethys Himalayan terrane are worthy of further study. Due to the existence of a main central thrust fault (MCT) between the Himalayan microlandmass and the lower Himalaya on the northern margin of the Indian main continent, no ophiolite or extensional basin representing oceanic crust fragments has ever been found, and the two-stage collision model is still questioned by field geologists. In addition, the complexity of the NeoTethian ocean-continental pattern should be considered in the discussion of the NeoTethian subduction process, including: (1) Was there a transition from intracontinental subduction to ocean-continental collision? When and

how to convert? (2) The variation of Indo-Asian convergence rate over time and space?

2. Indo-Asian initial collision time limit

The timing of the initial India-Asia collision has been debated.The key depends on how one defines “initial collision”,the initial collision times obtained by different scholars using different methods vary widely (from 70 Ma to 34 Ma)Powellet al.,1973 Patriat et al.1984 Le Fort,1987 Wang et al,2003 Ding Lin et al.2005 Aitchison et al.2007 Mok et al.,2007 Garzanti,2008 Huang et al.,2010 Najman et al.2010 van Hinsbergen et al.2012 DeCelles et al.2014 Wu Fuyuan et al.2014 Hu Xiumian et al.2015 2016a,2016b:Zhuang Guangsheng et al.2015,2017a:Zhu et al.,2017.Methods to constrain the fine timing of the initial collision include paleomagnetic evidence of the deceleration time of the Indian plate’s northward drift Molnar et al,1975 Treloar etal.1991 Klootwijk,1992 Ali et al.2005 Najman et al.2010 Copley et al.2010 van Hinsbergen et al.2012,where evidence for the last Marine sedimentary time at the Indo-Brahmaputra suture zone and along the northern margin of the Indian Plate Garzanti et al.’1987:Searle et al.1987 Hu Xiumian et al.2015 2016a,deposition time of the oldest continents along the suture zone Searle et al.,1987 St.Onge et al.,2010 DeCelles et al.2014,end of magmatism of the “I’type granitic base in the magmatic arcassociated with subduction on the southern margin of Asia(Chung Sun-Lin et al.1998a:St. Onge et al.2010 Ma et al.,2021a:Ma Xuxun et al.,2021b,20210as well as the duration of UHP metamorphism along the northern tip of the Indian plate Leech et al.,2005 and so on.

Recently, paleomagnetic studies have provided a new time limit for the initial Indo-Asian collision, and obtained clastic magnetite + biommagnetite through fold examination and magnetic mineral extraction from the Gamba Zonpu Formation (about 62 ~ 59 Ma) of the Tethys Himalayan terrae. It is proved that the paleomagnetic results are primary remanence, indicating the paleomagnetic latitude of 6.6°±3.5°N（Yi Zhiyu et al., 2011, 2021; Zhao Qian et al., 2021）.At the same time, according to the gravel studies, Ar-Ar chronology and petrography of the “Dianzhong Formation” in Linzhou Basin

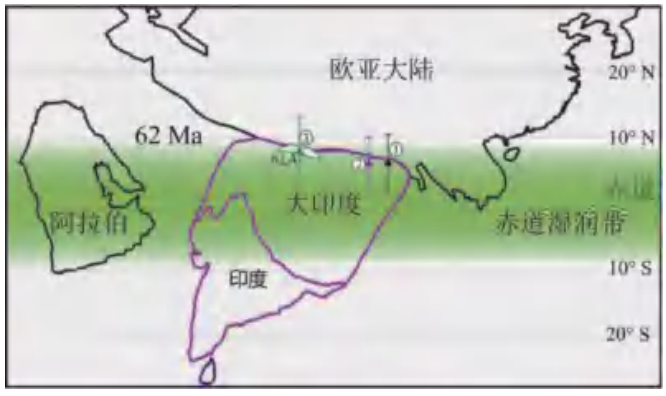

Fig . 2 Timing of the India Asia initial collision (modified from Yi Zhiyu et al ., 2021)

(data from 1 Yi Zhiyu et al 2021. 2 Yi Zhiyu et al ., 2011; 3 Martin et al ., 2020: KLA Kohistan. Ladakh arc)

of Lhasa terrae reveals the paleomagnetic results (64 ~ 60 Ma) are the primary records, indicating the paleo-latitude of 6.7°±4.4°N. According to the comparison of the latest paleomagnetic (primary remanence) data of the Tethys Himalayan and Lhasa terrains, the initial collision time of Indo-Asia is no later than 62±2Ma , and the initial collision location is within the equatorial humid zone (6.7°±4.4°N) (Yi Zhiyu et al., 2021) (Fig.2)

In addition, according to the three common definitions of the initial continental collision time: ① The initial time of collision is the "collisional basin" where the oceanic crust disappears and the subducted continental crust enters the overlying active continental margin trench; ② Take the time of ocean disappearance between the two continents as the initial collision time; ③ The time of intense tectonic deformation between continents is taken as the initial collision time, and only ① represents the actual initial collision time. Recent studies on the co-collision basin provide new evidence for the Indo-Asian initial collision. The upper part of the Sandulin Section (Sandulin Formation) in the Saga area of Tibet has been found to be the product of the initial collision event of the trench basin in the co-collision period. The initial collision was precisely limited to 59±1 Ma (Hu Xiumian et al., 2015) (Fig.3). It should be noted that the evidence for the new initial collision date is mainly from the mid-section of the Gangdise-Himalayan arc. In particular, the East-west tectonic junction has not yet found the evidence of the initial collision event in the trench basin

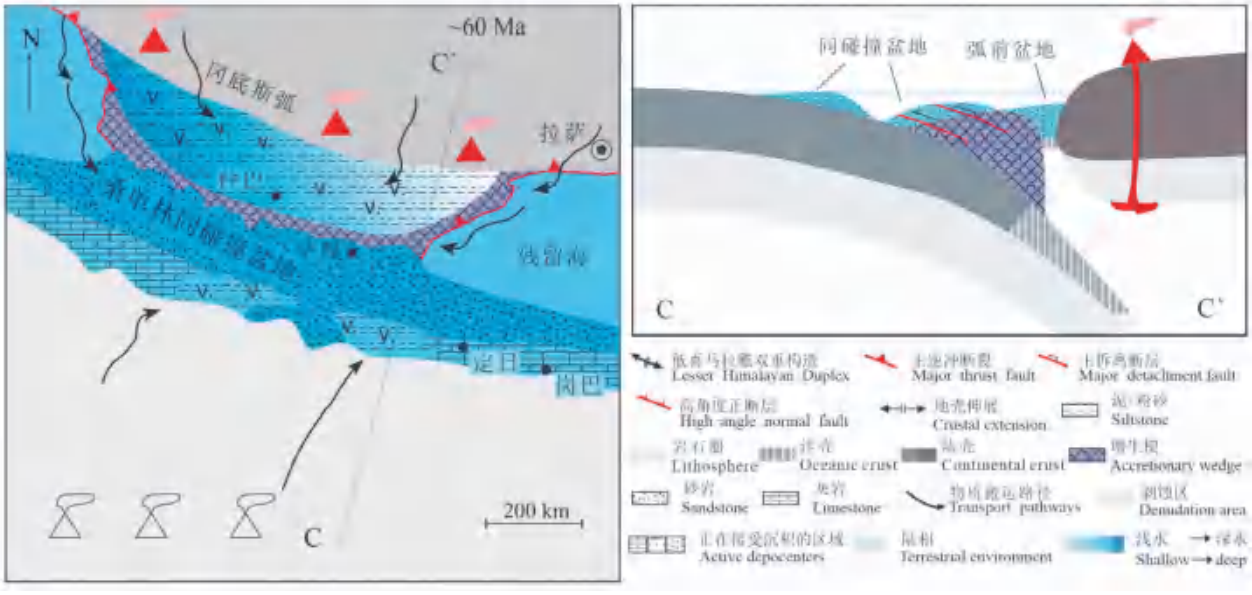

Fig .3 Geological map and cross section of syn–collisional oceanic trench basin of the Saga area,South Tibet (after Hu Xiumian et al ., 2015)

Initial collision at 59 ±1 Ma evidenced by provenance transition between Indian and Asian sources in the Sangdanlin sequences

of the typical collision period, that is, the evidence of the initial collision event. Only the end time of the last sea basin and the formation time of the ultra-high pressure metamorphic belt cannot determine the time limit of the initial collision.

3.Paleo-tethys orogeny in the Tibetan Plateau

Tethys was a huge ocean located between the northern and southern Gondwana supercontinents during the Phanerozoic eon. It underwent a series of oceanic subduction, terrane collision and accretion-collision orogeny, and finally closed in Cenozoic, resulting in the present nearly east-west spread of the giant Tethys orogenic belt. Tracing the evolutionary history of the Tethys Ocean is an important basis for reconstructing the formation process of the Qinghai-Tibet Plateau. Sengör (1979) emphasized that the Paleo Tethys Ocean developed between the Lloyd supercontinent and Gondwana supercontinent in the Late Paleozoic, and expanded north of Gondwana to form the New Tethys Ocean due to the subdivision and shrinkage of the ocean in the early Mesozoic. Sengör (1979,1987,1989) argued that there were two oceans (the Ancient Tethys and the Neo-Tethys) between the northern and southern continents and a Cimmerian continent sandwiched-between them, The Chimuri continent consists of the Iran-Turkey-North Pamir-Songpanganzi and Indochinese terranes between the Balkan and Malaysian peninsulas. It is a continental patchwork that split from the Gondwana supercontinent in

Fig.4 First.order palaeogeographical/palaeotectonic elements taking part in the architecture of the Tethysides,and their place in the present structure of our planet (modified after Sengor et al.,1987)

1-Laurasiancontinent;2-Gandwana continent;3-Cimmerian continent:4-exotic area:5-Paleo-Tethyan suturei 6-Neo Tethyan suture

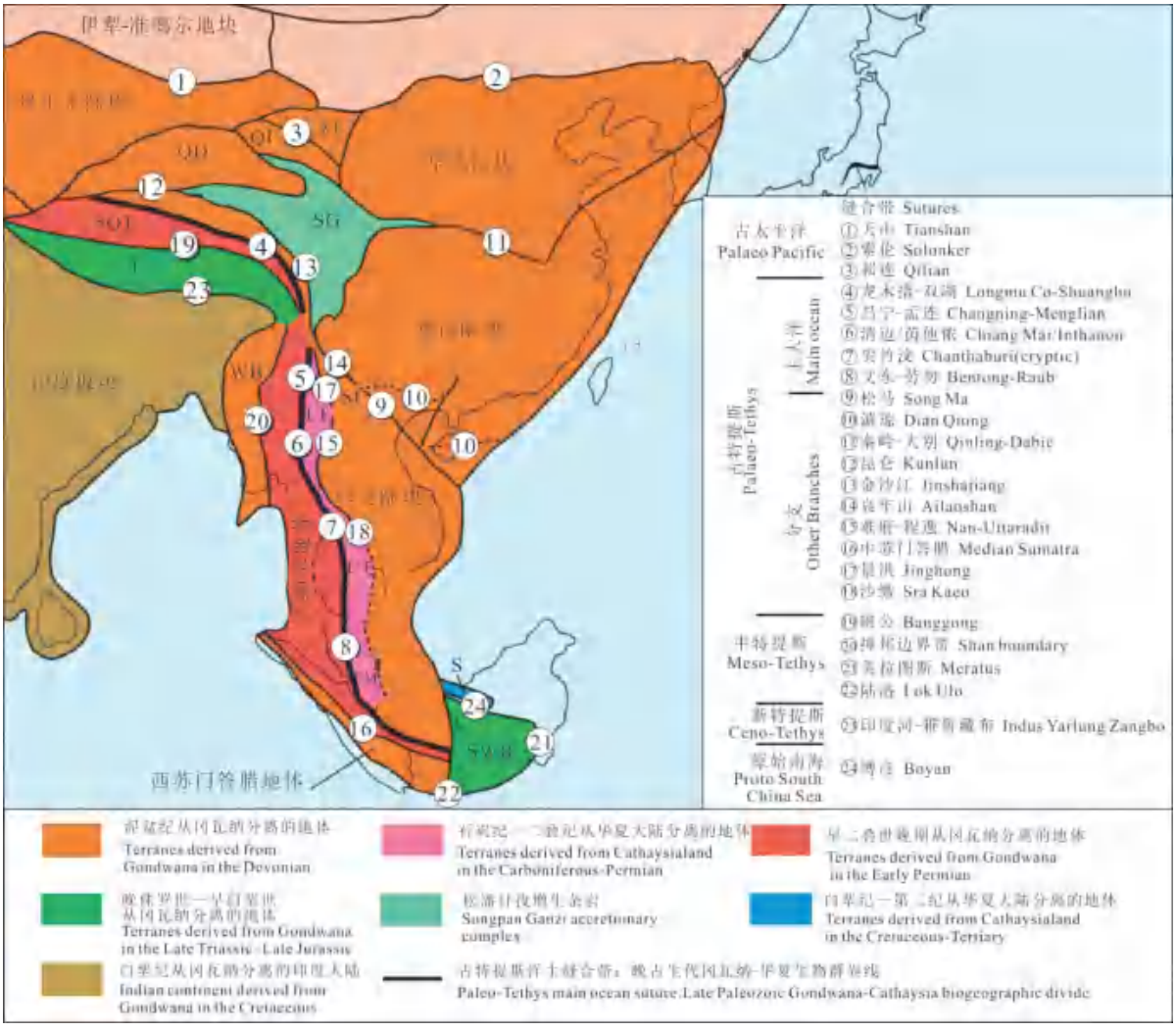

Fig.5 Distribution of principal continental terranes and sutures of East and Southeast Asia (modified after Metclfe,2013)

WB-West Buma terrane:SWB-Southwest Borneo terrane:S-Semitau terrane;L-Lhasa terrane;NQT-North Qiargtang terrane:QT-Sourth Qiangtang terrane:QS-Qamd.Smao terrane SI-Simao terranei SG-Songpan Ganzi accretionary complexi QD-Qaidam terrane;AL-Ala Shan terrane;KT-Kurosegawa terrane;LT-Lincang arc terrane:CT-Chanthaburi arc terrane; EM-East Malaya:QI-Qilian terrane

the Triassic and collided with the Laurian continent in the north during the Late Trians-Middle Jurassic to form the Chimuri orogenic belt composed of the super orogenic complex (Sengör, 1979, 1987; Boulin, 1981; Audley—Charles, 1984; Golonka, 2006; Li Haibin et al., 2009) (Fig.4).

However, according to the distribution of cold water and warm water fauna, more and more researchers have taken the Longmuscuo-Shuanghu-Changning-Menglian rift zone in the middle of the Qinghai-Tibet Plateau as the boundary between the cold water fauna and the warm water fauna of the Chinese

land mass, and disintegrated the original Chimaurian continent into north and south parts. On the south side is the Chimauri continent composed of the Western Chimauri, South Qiangtang and Sibumasu terrane collage, while on the north side is the southern part of the Cathaysian landmass formed by the North Qiangtang, Songpan Ganzi and Simao-Indosinian terrane collage (Fig5) (Metcalfe, 2006, 2013; Xu Zhiqin et al.,2012; Wang Qing et al.,2021).

French scholar Fromaget (1927,1952) once put forward the concept of Indosinian orogeny when studying the geology of Vietnam, and called the Late Permian-Middle Triassic orogeny as the Indosinian movement. Later, many scholars emphasized the importance of the Vietnam-Western Yunnan Indosinian movement in the tectonic evolution of Mainland China (Meng, 1937; Huang, 1945; Ren, 1984). New progress has been made in the study of Paleotethys in Southeast Asia in the last 20 years. In particular, the opening and closing of the ancient Tethys Ocean basin and its collisional orogenic processes reflected in the east and west suture zones of the Southeast Asian landmasses have gained new insights (Sone et al., 2008; Metcalfe, 2013; Wang Yujun et al., 2018; Tran et al., 2020).

The suture zone on the east side of the Southeast Asian landmass, namely the Jinshajiang-Ailaoshan-Songma suture zone, is the boundary between the Simao-Indosinian terrestrie and the South China landmass, reflecting the closure of the branch ocean basin (or back-arc basin) of the ancient Tethys. the collision time of the two landmasses is about 247 Ma. The co-collision and post-collision orogenic events are limited to 247 ~ 237 Ma and 237 ~ 200 Ma respectively (Wang Yujun et al., 2018).

The western suture zone is the Changning-Menglian suture zone, which is the

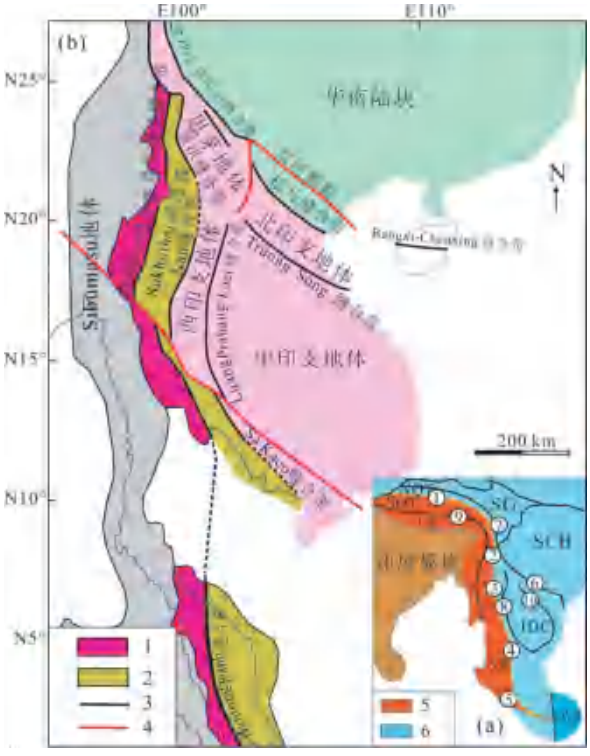

Fig.6 Tectoric backgrourd (a) and major continental blocks urits (b)of Southeast Asia (modified after Wang Yuejun et al.,2018)

1-LongmuCo-Shuanghu suture:2-Changring-Mengliang suturei-Inthanon suture:-Jinghong-Nan-Sa Kaeo suturei⑤-Bentong-Raub suture zone;@-Song Ma suture; ⑦-Jinshajiang. Ailaoshan suture;-Luang Prabang.Loei suturei-Bangong-Nujiang suture:-T ruong Son suture:NQT-North Qiangtang terranei SQT-South Qiangtang terrane;LS-Lhasa terrane;SB-Sibumasuterranei SG-Songpan-Ganziterrane:SCB-South China block;IDC-Indochina block;SWB-Southwest Borneo terrane:1-main Paleo.Tethyan suture;2-main Paleo.Tethyan arc:3-other Paleo.Tethyan suture:4-Cenozoic active fault;5-high latitude cold climate Gondwena typefaunasdflrs6ltitude wamm cimate Cathaysian type faunas and floras

closed boundary of the ancient Tethys main ocean basin between the Yunnan-Thai block and the Simao-Indosinian terrane. The collision of these two bodies occurred at about 237 Ma, and the orogenic events of co-collision and post-collision occurred at 237 ~ 230 Ma and 230 ~ 200 Ma, respectively (Fig.6) (Wang Yujun et al., 2018). Therefore, the Kumurian orogeny not only involved the Kumurian landmass and the Indosinian terrane, but also overlaid the early Indosinian orogenic belt between the Indosinian terrane and the South China landmass. So Tranetal. (2020) proposed that the IndoChinese movement proposed by Fromaget (1952) on the basis of geological phenomena in Vietnam was not suitable for the post-collision orogenic event of late Triassic to Jurassic between Yunnan-Burman-Thai and Simao-Indochinese terrane. It is suggested that the Indochinese movement of Late Permian-Middle Late Triassic should be renamed "Trans-Meigongheorogen" according to the region.

The above results show that the time limit of collision orogeny between Yunnan-Burmese terrane and Cathaysian landmass in Southeast Asia coincides with the time of the event, while the orogeny between Indosinian terrane and Cathaysian landmass in Southeast Asia started from the Indosinian movement and ended at the same time as the event. Therefore, the author believes that the Chimaurian orogenic events reflected between the Southeast Asia Chimaurian continent and the Indosinian and South China landmasses are extensive and powerful. However, it is worth discussing whether there are regional and temporal differences in the Indosinian orogeny in Southeast Asia, which represents the ancient Tethys orogeny, what relationship it has with the Chimaurian orogeny event, and whether it represents the precursor of the Chimaurian orogeny also needs to be further identified. As part of the Cathaysia continent, the Songpan-Ganzi terrane is bounded by the East Kunlun Qaidam terrane in the north, the South China landmass in the southeast, and the North Qiangtang terrane in the south. It is

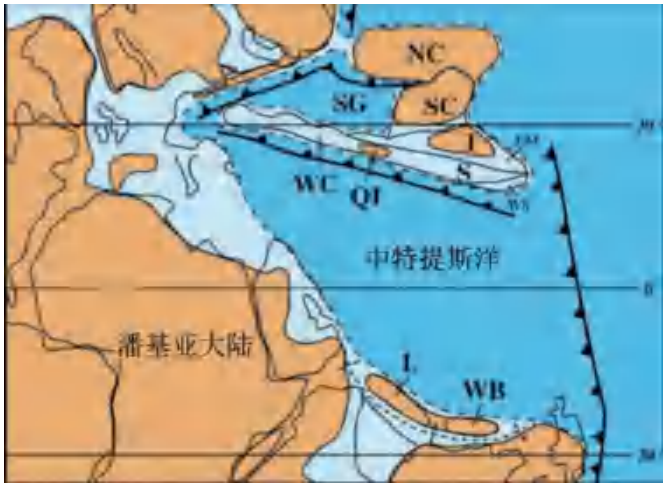

Fig.7 The paleo-geographical location of the Songpan-Ganziterrane in the Late Triassic according to Metcalfe,2006)

NC-North China block:SC-South China block; I-Indosintianblock:EM-East Malay terrane:WS-West sumatra terrane;S-Dunyan Burma Thai terrane:SG-Songpan-Ganzi terrane:WB-West Burma terrane:QIQiangtang terrane:L-Lhasa terrane: WC-West Cimmerian continent

a triangular-accretive complex termites defined by the East Kunlun - Anemaking suture zone in the north and the Jinshajiang Paleotethyan suture zone in the south, and composed of the Triassic super-thick (5 ~ 15km) deep-sea turbidite (Xu Zhiqin et al., 1992). Predecessors have proposed different models for the tectonic properties of Songpan-Ganzi deep-sea basin, such as back-arc basin (Klimetz, 1983; Sengör, 1987; Watson et al., 1987; Gu Xuexiang, 1994) foreland deep sea/residual ocean basin (Nie Shangyou et al., 1994; Zhou Da et al., 1996; Weislogel et al., 2006) intercontinental rifted valley basin (McElhinny et al., 1981; Chang Edmend, 2000; Meng Qingren et al., 2000) etc.

Many scholars have classified the Songpan-Ganzi terrane into the Indosinian orogenic belt（Ren Jishun, 1984; Xu Zhiqin et al., 1992, 2012; Harrowfield et al., 2005). Based on the closure of the Middle to Late Triassic PaleoTethys Ocean basin, the Songpan-Ganzi Late Triassic accretive orogenic wedge is characterized by strong crustal shortening and thickening, massive granite empositioning of 228 ~ 180 Ma, accompanied by supernormal enrichment of lithium metal elements (Zhang Hongfei et al., 2006, 2007; Yuan Chao et al., 2010; Xu Zhiqin et al., 2020). Different from the hard collision orogeny between other rigid terranes (or landmasses), the "soft collision" orogeny between the Songpan-Ganzi terranes and the surrounding rigid landmasses (Fig.7), which is composed of Triassic strata, occurred in the late Triassic to Early Middle Jurassic, later than the Indosinian Movement, and similar to the period of the Kumurian orogeny.

Studies show that the East Kunlun - Anemaquin suture zone is connected with the Mianluo suture zone of Qinling terrane to the east (Li Chunyu et al., 1978, 1982; Zhang Guowei et al., 1995), and the NE-SW trending "Ningshaan-Xianghe" left strike-slip shear zone is connected with the subduction front of the East Qinling-Dabie-Sulu terrane ultra-high pressure metamorphic zone (Xu Zhiqin et al., 2015a). The time of UHP metamorphism in Dabie-Sulu orogenic belt is 240 ~ 225 Ma, and the return time of UHP metamorphic rocks from high pressure eclogite facies to amphibolite facies is 225 ~ 200 Ma (Edie et al., 1994; Ayers et al., 2022; Li Shuguang et al., 1993，2003; Liu Fulai et al., 2011; Xu Zhiqin et al., 2006; Liu Fulai and Liou，2011; Zheng Yongfei, 2008). Therefore, the continental collision time of the South China and North China landmasses should be earlier than 240 Ma. The initial time limit of the collision orogeny is similar to that of the Indosinian movement, and the end time is similar to that of the Kimurian orogeny. Hence, some authors have speculated that the northern Paleo-Tethian ocean basin (i.e., the East Kunlun - Anemaking-Mianlui-Qinling/Dabie/Sulu suture zone) had a shear type of ocean basin closure form, which resulted in the collision orogeny of the whole central orogenic belt

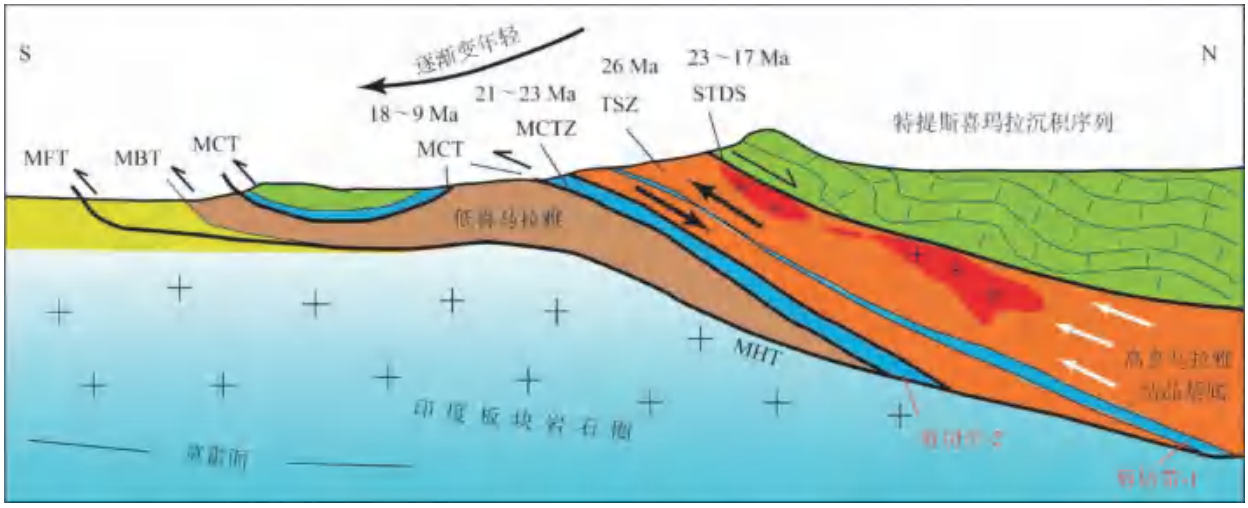

Fig.8 Himalayan structural (section from Carosi etal.,2010)

STDS-South Tibet Detachment systemi MCT-Main Central Thrust;MBT-Main Boundary Thrust;MFT-Main Frontal Thrust;TSZ-Tajem thrust shear zone MHT-main Himayan thrust

with the characteristics of early east and late west.

Because the Cenozoic orogeny was established on the ruins of the ancient Tethys orogenic movement, it is very difficult to reconstruct the complete and independent orogenic system of the ancient Tethys. The Qinghai-Tibet Plateau is composed of Eo-Tethys, Paleo-Tethys and Neo-Tethys. It is very important to re-examine the Paleo-Tethys orogeny, especially considering the regional and temporal differences of orogenesis to understand the formation and evolution of the Qinghai-Tibet Plateau. Just as the "Caledonian" and "Warisee" orogenic processes in Europe do not apply to the orogenic belt in mainland China, the impact of the Indosinian and Cymorian orogenic processes in mainland China needs to be examined by global comparisons.

4.Mechanism of crustal shortening in the Paleogene Himalayan orogenic belt

The Himalayan orogenic belt runs from north to south from Tethys Himalaya(THS), High Himalaya (GHS), Low Himalaya (LHS) and sub-Himalaya (SHS) are composed of four tectonic units, and the boundaries between each unit are successively the South Tibet Detachment System (STD), the main central thrust fault (MCT), the main boundary thrust fault (MBT) and the main forward thrust fault (MFT) (Fig.8). Vanney et al. (1996) systematically studied the tectonic deformation, petrology, metamorphism and chronology of the high Himalaya in the Kali Gandaki section, central Nepal, and divided the evolution of the Himalayan orogenic belt into three stages: In the early to middle

Eocene, the Tethian Himalayan sedimentary rocks developed a southern folding and thrust belt, which underwent low grade metamorphism. This thin-skin structure may have been controlled by the thrust nappe of the main detachment fault in the Paleozoic strata of Tethian Himalayas. Beginning the Himalayan period (Eohimalayan episode) high Himalayan buried subduction to tethys under the Himalayas, in middle Eocene to Oligocene kyanite phase into the characteristics of metamorphism and embedded depth of more than 35 km; New Himalayan period (Neohimalayanepisode) high Himalayan in the main central thrust fault and southern Tibet detachment system under the control of rapid exhumation, in Oligocene, Miocene annealing characteristics of metamorphism and new Himalayan peak metamorphism in 23 ~ 21 Ma.

The Himalayan Paleogene deformation records are often strongly superimposed or erased by metamorphism and deformation since the Miocene. According to the opposite kinematic direction and contemporanial tectonic activity of the main central thrust fault and the southern Tibet detachment system at 24 ~ 16 Ma, different high Himalayan extrusion models have been proposed, including: Wedge-shaped extrusion (Burchfiel and Royden, 1985), crustal tunnel flow (Nelson et al., 1996; Chemenda et al., 2000; Beaumontetal., 2001), Tectonic wedge (Yin, 2006; Webb et al., 2007) and dual structuring (He et al., 2016), etc.

The 40Ar / 39Ar age of illite or light granite growing along the bedding of Tethys Himalaya fold and thrust belt shows that the formation age of Tethys Himalaya fold and thrust belt is 56 ~ 45 Ma (Ratschbacher et al., 1994; Wiesmayer et al., 2002). Therefore, as the boundary between the Miocene Tethys Himalaya and the High Himalaya, the Eocene crustal shortening of the upper Tethys Himalaya cannot be explained in terms of time, kinematics and driving force. The above structural model based on the high Himalayan reentry in Miocene cannot be applied to the crustal shortening and deep melting in Eohimalaya.

Recent studies in the eastern Himalayan orogenic belt show that the crustal short-

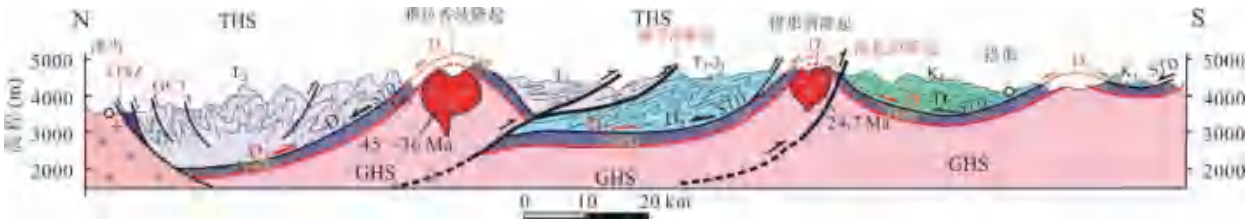

Fig.9 Structural profile in the eastem Himalayan orogen

GHS-Greater Himalaya Sequence;THD-Tethyan Himalayan decollemenent;STD-South Tibet Detachment:ITSZ-Indus-Yarlung suturezone;GCT-Great Counter Thrust;THS-Tethys Himalayan Sequence

ening during the Eo-Himalayan period was influenced by the slip fault at the bottom of the Tethys Himalaya (Tethys Himalaya slip zone, Tethyan) Himalayan Décollement, THD) (Fig.9). The Tethys Himalayan detachment zone is about 4km thick and developed in the Early Paleozoic metamorphic strata. It was formed between 50 and 17 Ma with advanced metamorphism and partial melting. It has a southward shear direction of the host-wall and controls crustal shortening and thickening in the Tethys Himalayan unit. On the top of the Tethys Himalayan detachment zone, the south-Tibet detachment system with the northward shear of the hanging wall is superimposed, indicating that the Tethys Himalayan detachment zone is the predecessor of the south-Tibet detachment fault and the tectonic boundary of the Tethys Himalaya and the High Himalaya during the Eocene-Oligocene. This is a new interpretation of the early tectonic framework of the Himalayan orogenic belt and has important significance for understanding the tectonic deformation of the plate boundary in the early Indo-Asian collision. The westward extension of the Tethys Himalayan detachment zone is a problem worthy of further study, which will help us to understand the structural differences along the strike of the Himalayan orogenic belt .

5.The genesis of the high Himalayan deep melting

As a product of deep crustal melting, pale granite is widely found in the upper Himalaya (Dietrich and Gansser, 1981; Le Fort et al., 1987; Burchfiel et al., 1992; Guillot et al., 1994; Hodges et al., 2000; Wu et al., 2015) and at the bottom of Tethys Himalaya (Xu Zhiqin et al., submitted). It was long believed that Himalayan pale granites were mainly formed from 23 ~ 22 Ma to 13 ~ 12 Ma, with the youngest outbursts (less than 4 Ma) occurring in the east and west tectonic junction. However, the discovery of pale granite earlier than 40 Ma in the nearly east-west spreading northern Himalayan gneiss dome in the Tethys Himalayan system has attracted much attention (Zeng Lingsen et al., 2011; Wu et al., 2015) .

How did the High Himalayan pale granites form? Le

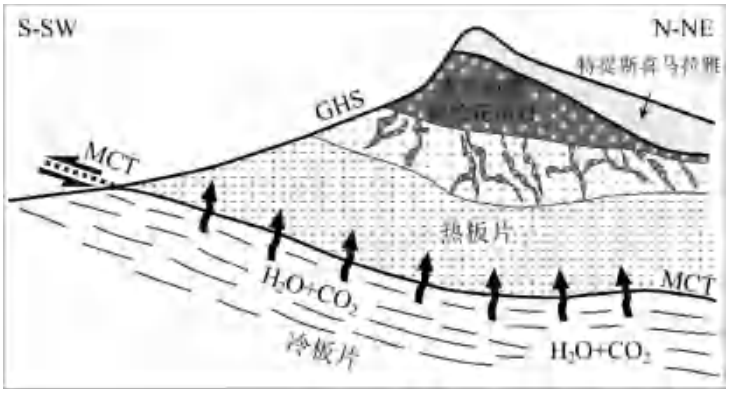

Fig.10 Classic view of anatexis triggered by the overthrust(Main Central Thrust,MCT)of the Greater Himalaya Sequence(GHS)and fluids released through metamorphism of the colder Lesser Himalaya Sequencee (after Le Fort et al.,1987)

Fort et al (1987) proposed a Flatiron model in 1987, which suggested that the thrust of the main central thrust fault at the bottom of the high Himalaya unit caused metamorphism in the lower cold lower Himalaya unit, releasing fluids and resulting in partial melting of the High Himalaya unit (Fig. 10). However, this model cannot explain why the pale granite is mainly produced in the upper part of the high Himalayan unit, nor can it explain the formation of the early pale granite.

Most studies believe that the Himalayan pale granite was formed by deep melting of metamorphic argillaceous rocks in the high Himalayan crystalline rock series (Le Fort et al., 1987; Guillot et al., 1995; Harris et al., 1995; Patiño-Douce et al., 1998; Aoya et al., 2005; Guo Zhengfu et al., 2012; Zeng Lingsen et al., 2012; Weinberg, 2016). A series of factor models of pale granite have been proposed. For example, high Sr/Y pale granite was formed by partial melting of Himalayan and thick lower crust (Zeng Lingsen et al., 2011) formation was completed along the high differentiation of parent magma of the detachment system in southern Tibet (Wu Fuyuan 2015), formation of asthenosphere mantle upwelling and contribution of partial melting of metamorphic rocks (Hou Zengqian et al., 2012).

Three different mechanisms of partial melting of the Earth's crust have been proposed: progressive metamorphism and heating melting during pressurization (Visonà et al., 2002; Groppo et al., 2013),Pressure drop melting in the return passageways (Harris et al., 1994; Patiño-Douce et al., 1998; Guo Zhengfu et al., 2012), as well as water injection melting (Knesel et al., 2002; Weinberg, 2016; Gao Li'e et al., 2017).

In addition to different melting mechanism, different protolith types, partial melting degree and melt mixing will lead to the change of chemical composition of Himalayan pale granite. The results show that the argillaceous, felsic and basic rocks of the Eastern Himalayan tectonic junction have undergone partial melting to varying degrees. According to geochemical composition, Himalayan pale granites with different initial isotope ratios of 87Sr / 86Sr originate from two different protoliths: Two-mica pale granites originate from metamorphic heteros and stone (87Sr / 86Sr) i < 0.752 and εNd < 15), and tourmaline pale granites originate from metamorphic argillite (87Sr / 86Sr) i > 0.752 and εNd > 15) (Guillot et al., 1995), and the Eocene high Sr/Y granites may be the product of partial melting of amphibolites in the thickened lower crust of the Himalayan orogenic belt (Zeng Lingsen et al., 2011; Hou Zengqian et al., 2012). Beyond this, Gou Zhengbin et al. (2016) claims that tourmaline-muscovite pale granite is formed by dehydration and melting of Muscovite, while Muscovite pale granite is the product of dehydration and melting of biotite during the metamorphic process of argillaceous and felsic granulite in the high Himalayan crystalline rock series. From the Late Oligocene to the Miocene, partial melt-

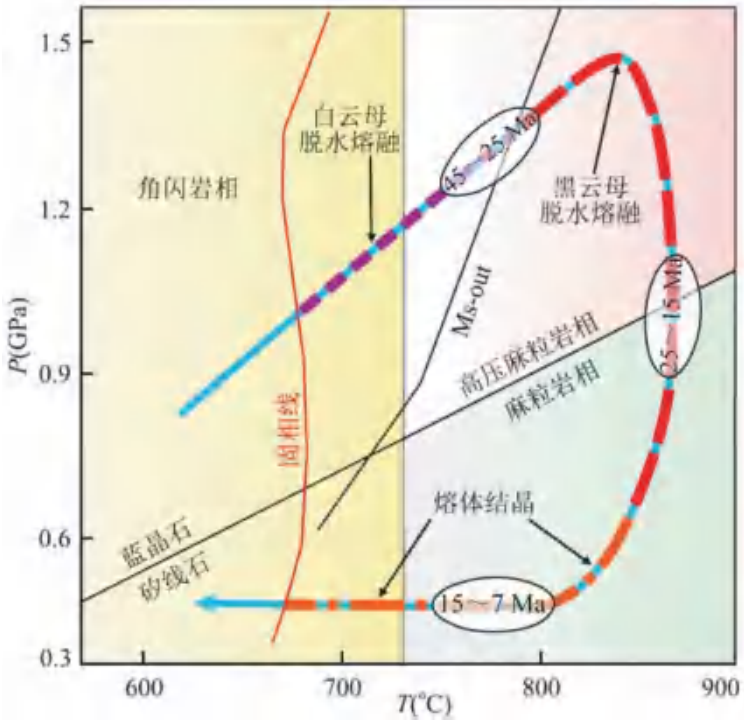

Fig.11 P.T paths of high temperature metamorphism,anataxis and melt crystallization of the Himalayan orogen(after Zhang Zeming et al.,2010)

ing occurred in the high Himalayan argillaceous rocks, heterogeneous sandstones and granitic gneisses. Due to the change of lithology dominated by the deep melting source area, the geochemical characteristics of the high Himalayan pale granites changed with time (Ji Min et al., 2021).

Studies on the relationship between metamorphism and partial melting show that the progressive metamorphism occurred at about 45 ~ 23 Ma under medium and high pressure granulite facies strips (Searle et al., 1992; Ding Lin et al., 1999; Hodges et al., 2006; Zhang Zeming et al., 2010). whereas demetamorphism occurred at 23 ~ 14 Ma under amphibolite facies (Searle et al., 1992; Walker et al., 1999; Hodges, 2000). Zhang Zeming et al. (2010) suggests that in the early stages of the Eo-Himalayan progressive metamorphism and Neo-Himalayan retro-metamorphism, the high Himalayan crystalline rock series experienced long-term and continuous high-temperature metamorphism and dehydration melting (including the dehydration melting of Muscovite and biotite in argillaceous granulites and the dehydration melting of amphibole in basic granulites). The complex S+I granite was formed by melt mixing, magmatic mixing and separation crystallization. Therefore, the high Himalayan deep melting is likely the result of long-term continental subduction, crustal thickening, continuous high-temperature metamorphism, and dehydrating melting (Fig.11).

6.Difference in Time limit and uplift of the Qinghai-Tibet Plateau

Due to the Cenozoic continental collision between India and Asia, the Qinghai-Tibet Plateau with an average elevation of nearly 5,000 m was formed, and the Himalayan mountain chain known as the "roof of the world" was created. The analysis of the uplifting and stripping history of the Tibetan Plateau is of great significance to reveal the kinematic process and dynam-

ic mechanism of the collision orogeny. At the same time, the uplifting and exfoliating process of the plateau has had a profound impact on global and regional climate, Marine chemistry and biological evolution (Burbank et al., 1993; An Zhisheng et al., 2001; Tapponnier et al., 2001; Molnar et al., 2010; Spicer, 2017; Deng Tao et al., 2019).For a long time, predecessors have carried out a lot of research on the uplift process and dynamic mechanism of the Qinghai-Tibet Plateau, and there are many controversies. Early stages of research are based on paleontological fossils (Gao,Shi, Li, 1964, 1979), potassic volcanite activity at different times (Turner et al., 1993), fault activity (Harris et al., 1995) and beyond, culminating in discovering that the uplift time of the faulted Tibetan Plateau was 13 ~ 3 Ma. Afterwards, Chung Sun-LinHarris et al., 1995.(1998b) suggested that the uplift of the Qinghai-Tibet Plateau is different from that of the east (about 40 Ma) to that of the west (about 20 Ma).Tapponnier et al. (2001) proposed that after the initial India-Asia collision, the Qinghai-Tibet Plateau gradually grew from south to north; Later, the results of oxygen isotope paleo elevation study provide evidence for this model (Rowley et al., 2006). Wang Chengshan et al.(2008), aaccording to the sedimentary records and the low temperature thermochronology data,argued it is proposed that the plateau is formed from the central part of the outward expansion,

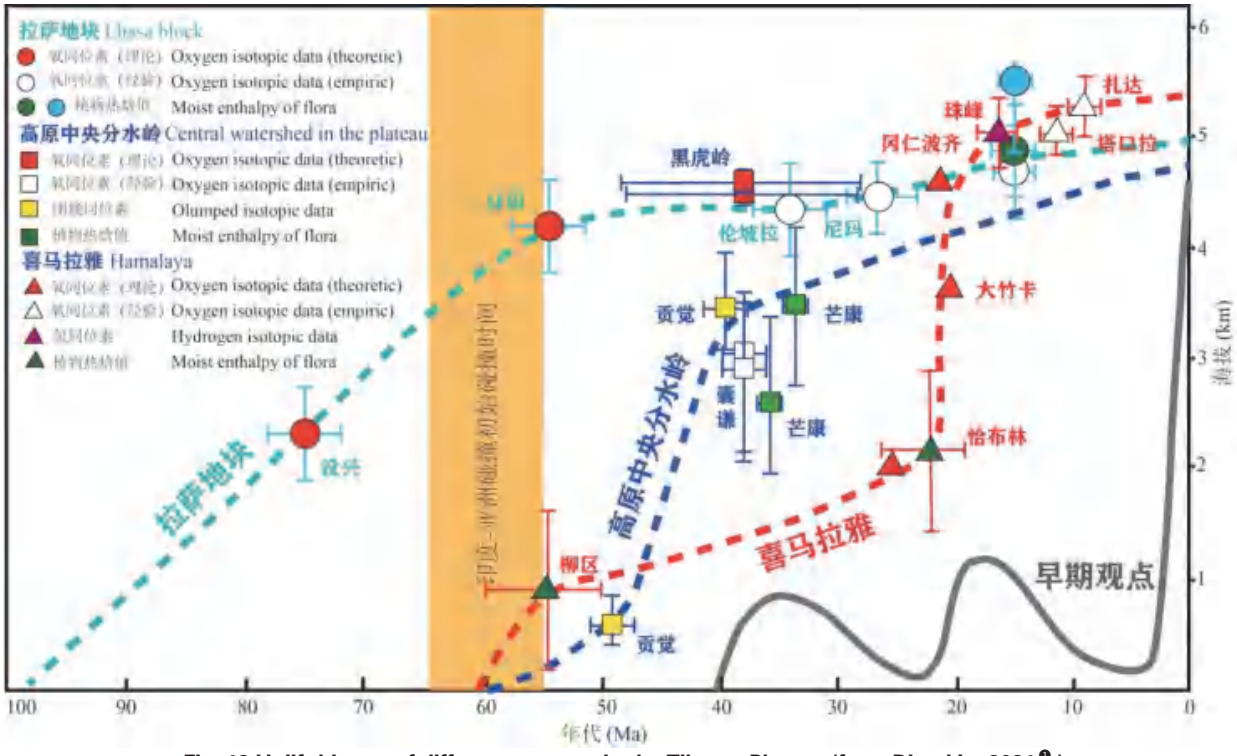

Fig. 12 Uplift history of different terranes in the Tibetan Plateau (from Ding Lin, 2021[9])

which has been recognized by many scholars (Rohrmann et al., 2012; Li Yalin et al., 2015; Li Guangwei et al., 2016). However, in recent years, ancient fish and other animal and plant fossils have been found in Nyima and Lumpola basins in the Bangong-Nujiang suture zone in the central Tibetan Plateau (Wu Feixiang et al., 2017; Deng Tao et al., 2019), iindicating that the central Tibetan Plateau remained at a relatively low altitude (at least < 2500 m) until about 26 Ma. Ding Lin et al.(2014) and Fang Xiaomin et al.(2020) proposed that the central Tibetan Plateau in the Eocene-Oligocene period presented a form of "two mountains sandwiched by a valley." Based on isotopes and plant fossils, Ding Lin has summarized the uplifting evolution history of the Tibetan Plateau and showed the uplift difference of various plateau areas (Fig.12).

To sum up, the current debates on the uplift process of the Qinghai-Tibet Plateau mainly focus on the following questions: ① Is the uplift of the Qinghai-Tibet Plateau uniform or differential, and what is the specific uplift process of each block? ② Was the Tibetan Plateau formed by the middle spreading north and south? Are there early (Cretaceous) plateaus in Ganzi and Kunlun? ③ Did the Himalayan uplift occur gradually in the Miocene or in the late Pliocene? The dif-

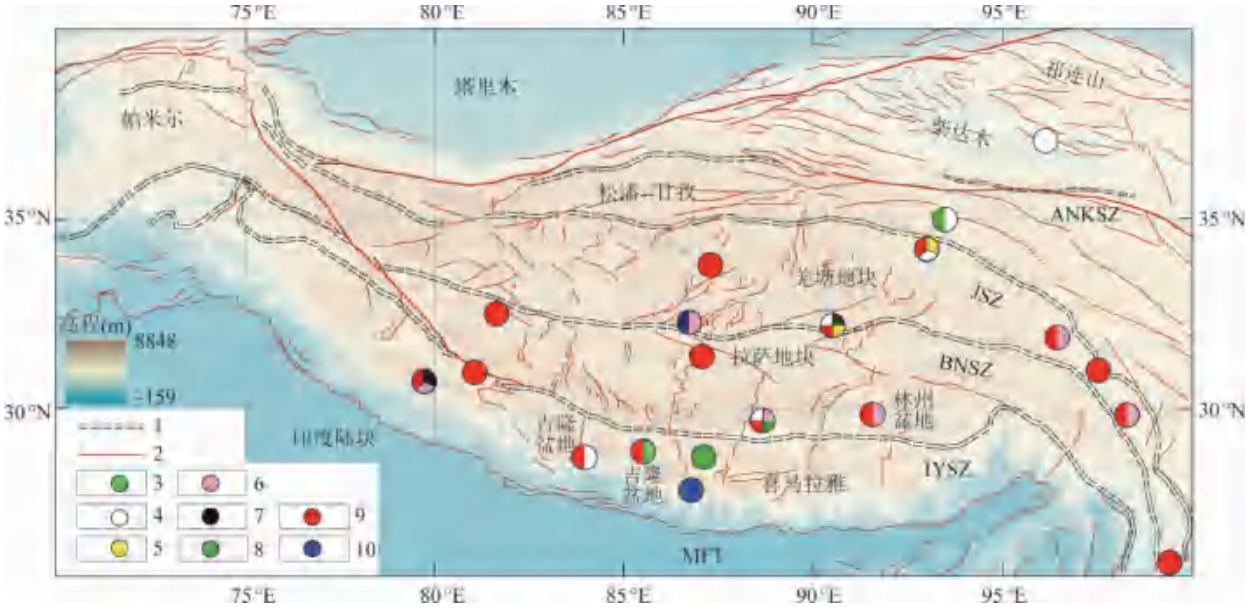

Fig 13 Distributionof basins for estimating paleo elevation in Tibetan Plateau and related methods (data from Li Lin et al.,2019:Chen Chichao et al.,2020 and references therein)

MFT-Main Frontal thrust;ANKSZ-Anemagen.Kunlun suture zone;JSZ-Jinsha suture zone;BNSZ-Bangong-Nujiang suture zone:IYSZ Indus-Yarlung suture zone;Data from Li Lin etal.(2019),Chen Chichao et al.(2020)and reference therein:1-sutrue zone 2-active fault:3- $\delta^{13}C$ of fossil teeth:4- δD of plant wax n.alkanes:5-pdllen assemblages 6-dumped isotope of carbonates; 7-mammatlian fossils:8-foliar physiogromy of fossil leaves:9- $\delta^{18}O$ of carbonates fossil teeth:10- δD of hydrothemmally altered hydrous minerals

ferences in the study area and the estimation methods of ancient elevation are the main reasons for the above-mentioned controversies. In the early stage, many scholars used tectonic or magmatic indicators to study the plateau uplift, but with the deepening of the research, due to the multiple solutions of the respective causes, its reliability remains to be discussed. For example, Harrison et al. (1995) Proposed that the Qinghai-Tibet Plateau occurred at the E - W extension at 9 ~ 7 Ma. At that time, the plateau was considered to have risen to its maximum height and become unstable due to gravity and it began to collapse. However, the north-south extrusion of India and Asia can also form an east-west extension in the Himalayan region, so it is insufficient to use the activity of extensional fault as an index of plateau uplift. In the same way, the potassic magmatism cannot be regarded as the paleo-elevation of the plateau due to its polysolvability is an indicator of dependence (Turner et al., 1993; Chung Sunlin et al., 1998b; Wang et al., 2009) Many scholars also utilized the piedmont basin in research (Najaman et al., 2010) in conjunction with submarine alluvial fan to carry out the study of plateau uplift (McNeill et al., 2017; Zhou Peng et al., 2020). Another example is studies surrounding methodologies in thermochronology of denudation rate (Thiede et al., 2013) which directly reflects the rate of rock temperature change. When applied to uplift, attention should also be paid to the limitation of conversion docking conditions and other observed data.

In recent years, many methods used to define ancient elevation have been developed, such as: Paleo-environment analysis (specific animal fossils or combinations, paleo-plant fossil combinations, stable isotope method), plant structure and morphology analysis (leaf edge analysis, CLAMP method), quantitative isotope analysis (hydrogen and oxygen isotopes, "cluster isotope" thermometer method), closed stoma morphology of volcanic lava, etc. However, due to the limitations of various methods and differences in sampling, there are often large differences in the elevation of the plateau estimated by different methods or different regions (or even the same method for the same region) (Fig.12 and 13) (Huntington et al., 2015; Ding Lin et al., 2017b; Li Lin et al., 2019; Chen Chichao et al., 2020; Spicer et al., 2020). Therefore, in order to more accurately characterize the uplift and denudation process of the Qinghai-Tibet Plateau, it is necessary to strengthen the detailed investigation in multiple areas and the development and improvement of new techniques and methods, and strengthen the combination and mutual verification of various methods to distinguish the local effect and the overall effect, so as to comprehensively explore the uplift history of the Qinghai-Tibet Plateau and provide a reliable basis for the discussion of the dynamic mechanism of the uplift of the Qinghai-Tibet Plateau.

(Reprinted from Acta Geologica Sinica, No.1, 2022, The rest of the next periodicals will be published in the upcoming volume)

SINGLE-WELL CIRCULATION GROUND SOURCE HEAT PUMP SYSTEM PROJECT AT BEIJING HAIDIAN FOREIGN LANGUAGE EXPERIMENTAL SCHOOL, BEIJING NORTH CAMPUS

A Case Study by the National Energy Conservation Center

Author: Ma Xiaofang (Special Correspondent) Li Yanchao (Specialized Chief Engineer)

In the selection of "the Third Typical Case of Key Energy-saving Technology Application" organized by the National Energy Conservation Center, a subsidiary unit of the National Development and Reform Commission, Hengyouyuan Science and Technology Development Group Co., Ltd. applied for "Single Well Circulating Ground Source Heat Pump System Project of Beijing Haidian Foreign Language Experimental School Jingbei Campus." After preliminary evaluation, on-site verification, among other aspects of screening, selection was finally successful. On the official website of the National Energy Conservation Center, it was announced nationwide that among the 16 key energy-saving technology application typical cases finalized, Hengyouyuan "Beijing Haidian Foreign Language Experimental School Jingbei Campus Single-well circulating Ground source heat pump System Project" proved to be exemplary: it not only utilized cutting-edge technology to achieve energy-saving, but also represents the future of energy saving application development.

Beijing Haidian Foreign Language Experimental School Jingbei Campus is located in Zhangjiakou, 80 kilometers away from Beijing, which also boasts the host city of the 2022 Winter Olympics. The new campus is a continuation from the 12-year-old international school, Haidian Foreign Language Experimental School. The new campus has been deemed the Beijing 2022 Olympic Education Demonstration School and the ice and snow sports base of the State General Administration of Sport to reserve talents for the Chinese National Youth Team for the Olympic Games. The campus covers an area of 660 acres, which can accommodate more than 5000 students and staff to live and study simultaneously. The total planned construction area of the campus is 300,000 square meters, and construction is divided into three phases. Up to now, 10 buildings totaling 140,000 square meters in the first

and second phases have been put into use, and the third phase is under construction.

At present, Beijing Haidian Foreign Language Experimental School Jingbei Campus has a total of 10 buildings. In order to adapt to the characteristics of large campus area, scattered buildings, large difference in surface elevation, different use time and frequency of each building, the system applies the constant active "single well circulation heat exchange geothermal energy acquisition technology". The Hengyouyuan single-well shallow geothermal energy distributed cooling and heat source system, which adopts centralized geothermal energy collection and independent energy supply from distributed cooling and heat source stations, has realized the clean energy supply for all the heating, cooling and domestic hot water of the project, saving 60% of energy compared with the traditional cooling and heat source system.

Upholding the spirit of the Winter Olympics, energy conservation and environmental protection to build a good school suitable for students to live and learn

Founded in 1999, Beijing Haidian Foreign Language Experimental School has developed into Haidian Foreign Language Education Group after more than 20 years, with many campuses at home and abroad.Beijing has established "two schools, one park and multiple sites", "two schools" refers to Beijing Haidian Foreign Language Experimental School and Beijing Haidian International School, "One Park" refers to the affiliated kindergarten of Beijing Haidian Foreign Language Experimental School (Haidian/Jingbei/Chaoyang Park), and "multiple sites" refers to the two campuses of Haidian and Jingbei: The Haidian campus is located in the Haidian District of Beijing, while the Jingbei Campus is located in the Ecological New Area in the north of the capital, located in Huailai and Yanqing of Hebei Province, which are also very close to the Winter Olympics venues.

The first phase of Jingbei Campus of Haidian Foreign Language School is located in Yuanxiang, Beixinbao Town, Huailai County, Zhangjiakou City. There are 6 buildings in the campus, including 1 primary school, 2 middle school, 3 overseas theater, 4 comprehensive sports center, 5 snow and ice center, ski hall, etc. The total heating and cold construction area is 59,292.93 ㎡ .Since September 2019, it has been put into use. The building design of Jingbei Campus is very humanized. Students' dormitories, classrooms, canteen, indoor basketball court, swimming pool and other places are interlinked with each other, which can well avoid the situation that children sweat in different temperature differences between indoor and outdoor after sports. Not only that, the school also for each dormitory is equipped with central air conditioning and fresh air system, warm in winter and cool in summer. Jingbei Campus is equipped with all kinds of facilities, including the zoo, swimming pool and large indoor sports venues, as well as the ice and snow sports center, ski practice, tennis, badminton, fencing, large theater

and other venues. In addition to the architectural design, there is another essential factor to ensure the indoor environment of Jingbei campus constant throughout the seasons: constant active single well circulation heat exchange ground energy acquisition technology. As early as 2000, the constant source energy heat pump environmental system with the core of "single well circulation heat exchange geothermal energy acquisition technology" has become the heating and cooling system of Beijing Haidian Foreign Language Experimental School, and has achieved good results. The school is located in Huailai County, Zhangjiakou City, with fresh air and superior natural environment, but the heating period is long and the temperature is low in winter. In order to ensure the normal heating of the project, reduce the carbon emissions of the heating system, and achieve clean and green heating, the project continues to use the Hengyouyuan energy heat pump environmental system as the project heating system, so as to realize the low carbon and low-cost heating cold operation of the project. To contribute to the green development of the Winter Olympic City.

Employing on-demand shallow geothermal energy to provide 24-hour hot water for heating in winter and cooling in summer

The main campus of Haidian Foreign Language School has been using Hengyouyuan shallow geothermal energy technology for nearly 20 years. The data and application process make teachers and students fully feel the huge advantages brought by Hengyouyuan single well circulation heat exchange geothermal energy collection technology: heating in winter and cooling in summer, low carbon and environmental protection, 24 hours of hot water. As a leading enterprise in the shallow geothermal energy industry, Hengyouyuan Group adheres to the concept of "Everything for the children" when building Beijing Haidian Foreign Language Jingbei Campus, focusing on the joint efforts of the company, using the shallow geothermal energy to escort children in every spring, summer, autumn and winter. The first phase of Beijing Haidian Foreign Language Jingbei Campus Project includes primary school, middle school, overseas theater, comprehensive sports center, ski hall and comprehensive sports center. The second phase includes international Department of junior high School, International Department of senior high school, kindergarten and logistics office building with a total of about 140,000 square meters. The third phase is under construction. The buildings of the project span more than 1000 meters from east to west, more than 800 meters from north to south, and the elevation difference of the terrain is more than 60 meters. The location of the collection Wells around the buildings is tight.The scheme adopts the constant active distributed shallow geothermal energy cooling and heat source system as the project's cooling and heat source scheme.The constant

active distributed shallow geothermal energy cooling and heat source system consists of a single well circulating heat exchange geothermal energy collection well, a shallow geothermal energy centralized heat exchange station, a distributed cold and heat source station and a building heating cold end.

The project uses multiple sets of single-well circulating geothermal energy collection Wells to collect shallow geothermal energy. The primary collection pipe network is used to transport shallow geothermal energy to the shallow geothermal energy central heat exchange station, and the secondary heat exchange pipe network distributes the shallow geothermal energy to the distributed cold and heat source station. The distributed cold and heat source station is equipped with three times of energy enhancement pipe network to reach the temperature grade of heating and cooling demand. It is transported to the heating and cooling terminal system in the building by four pipe networks to complete the heating and cooling process.

According to the requirements of the phased construction of the project, a set of constant active distributed shallow geothermal energy cooling and heat source system is set in the first phase and the second phase of the project, among which 22 sets of geothermal energy collection Wells, 1 centralized heat exchange station, and 4 distributed cooling and heat source stations are set in the first phase. In the second phase, 28 sets of geothermal energy collection Wells, 1 centralized heat exchange station and 3 distributed cooling and heat source stations are set.

Advantages of constant active distributed shallow geothermal energy cooling and heat source system applied to the project:

1.Centralized collection of shallow geothermal energy to achieve on-demand energy supply

The energy consumption and frequency of the project buildings are different. The method of centralized collection of shallow geothermal energy is adopted, and the circulation flow is adjusted by setting the temperature of the circulating water back water in the collection well, so as to realize on-demand energy collection, how much is used, how much is taken, how much is taken, and how much is taken, so as to save the power consumption of the collection pump.

2.Secondary network closed cycle transmission of shallow geothermal energy; reduction in transmission energy consumption

The distribution height difference of the project buildings is up to 60 meters. If the conventional constant source energy heat pump environment system is adopted, the circulating water from the collection well needs to be directly transported to each hot and cold source station. Each collection pump needs to overcome the 60m hydrostatic pressure difference caused by the elevation difference of the terrain, and the total electric power of the collection pump needs to be 1250kw.After the scheme adopts the centralized heat exchange station, the circulating water of each collection

well only needs to be transported to the centralized heat exchange station, and the centralized heat exchange station is set near the ground energy collection well, which greatly reduces the collection well needs to overcome the hydrostatic pressure difference, and the total electric power of the collection pump only needs to be 750kw.Due to the centralized heat exchange station, it is necessary to increase the secondary pipe network to transport the circulating pump. The total power of the circulating pump is 200kw. After deducting the increased power of the circulating pump conveyed by the secondary pipe network, the total electric power of the acquisition system is also reduced by 24% compared with the conventional system. At the same time, the secondary pipe network transmission circulating pump adopts frequency conversion control, which can further reduce the energy consumption during operation.

3. Secondary pipe network transmits low temperature geothermal energy to reduce heat loss

When the conventional constant source energy heat pump environment system is used, the water supply temperature of the circulating water of the ground energy collection well is 15°C. After the central heat exchange station is set, the secondary water supply temperature of the central heat exchange station transported to each cold and hot source station is reduced to 13°C. According to the calculation of the soil temperature of the buried depth of the pipeline in winter is 0°C, the heat loss can be reduced by 13%.

4. Distributed heat and cold source stations are set according to demand, which is highly suitable for cooling and heating demands of buildings

According to the cold and heat load of each building, the installed capacity of the heat pump unit in the distributed cold and heat source station is reasonably set, and the operation of part of the load is considered. The installation of multiple units and multiple heads of each unit can realize the high fit of the building energy supply and the building demand, avoid the situation of the big horse and car at the same time, further reduce the energy consumption of the current system operation.

Remarkable results have been achieved in saving electricity every year

Energy saving and environmental protection are the great advantages of Hengyouyuan single well cycle heat exchange ground energy acquisition technology. The data of Beijing Haidian Foreign Language Experimental School since its operation in Beijing North Campus just shows this point. The total energy consumption of the project in the 2021-2022 heating season is 2,593,300 kWh of electricity, equivalent to 318 tons of standard coal. Compared with electric boiler heating, it can save about 800 tons of standard coal, reduce CO2 emission by 1,976 tons, SO2 emission by 16 tons, and dust emission by 8 tons.

The total electricity consumption of annual summer cooling is 508,900 KWH, which saves

about 171,100 KWH of electricity compared with the traditional central air conditioning system. Because no cooling tower is used, there is no evaporation loss of water, saving 396 tons of water every year.

Operation analysis and calculation shows the average power consumption of the project is 38.2kW·h/ ㎡ for heating and hot water in winter (including domestic hot water for 1400 people), 8.6kW ·h/ ㎡ in summer (free hot water and auxiliary cooling for waste heat recovery in summer), and the total power consumption for heating, cooling and domestic hot water supply is 46.8kW·h/ ㎡ in the whole year. According to the residential electricity price 0.52 yuan/kW·h calculation, the annual operating cost is 24.4 yuan/ ㎡ (146 days of heating, 200 days of hot water, 365 days of pool heating, 90 days of cooling).

The project utilizes the single-well circulating heat exchange geothermal energy collection technology to collect the low temperature heat energy below 25°C contained in the soil, sand and groundwater within 100 meters below the surface, which is combined with the mature heat pump technology to provide heating, cooling and domestic hot water for buildings. There is no water consumption in the process of using the technology, no pollution to groundwater, no potential geological disasters, is a kind of soil source heat pump.

The heat generated by the system refrigeration can be directly recycled through the heat pump unit for the preparation of domestic hot water or for the heating of the pool water, so as to realize the recycling of the system energy. At the same time, the project has realized the complete marketization of the original technology. By referring to the actual operation situation of previous similar projects and combining with the characteristics of this project, the low-cost operation of the project can be realized without obtaining any project-related subsidies. The annual operating cost is 24.4 yuan/ ㎡ , which is 44.7% less than the non-resident (school) heat supply price of 44.1 yuan/ ㎡ (building square meter) issued and implemented by Zhangjiakou in 2018.

Multifaceted advantages of shallow geothermal energy promote environmental protection

The distributed cooling and heat source system of constant active shallow geothermal energy consists of a single well circulating heat exchange geothermal energy collection well, a shallow geothermal energy centralized heat exchange station, a distributed cooling and heat source station and a terminal system inside the building. The project sets multiple single-well circulating geothermal energy collection Wells to collect shallow geothermal energy in a centralized manner. The primary collection pipe network is used to transport the shallow geothermal energy to the central heat exchange station, and the secondary heat exchange pipe network distributes the shallow geothermal energy to the distributed cold and heat source station. The distributed cold

and heat source station is equipped with three times of energy enhancement pipe network to improve the temperature grade of heating and cooling demand. It is transported to the end system of the indoor heating and cooling building by four pipe networks to complete the heating and cooling process.

Advantages of constant active shallow geothermal energy distributed cooling and heating source system include:

1. Centralized collection of shallow geothermal energy is conducive to system overhaul and maintenance

2. Secondary pipe network delivers low-temperature geothermal energy to reduce heat loss

3. Distributed cold and heat source station is set according to the energy demand of the building, the frequency of use and other characteristics, to ensure flexible operation, to achieve on-demand energy, how much to use, how much to take, how much to save energy

The core technology of the project is single-well circulating heat exchange geothermal energy collection technology, which is an original and advanced shallow geothermal energy collection technology applicable to a variety of geological conditions. It uses circulating water as the medium to collect the heat energy of the shallow underground temperature below 25°C, which can realize the recharge of all groundwater in the same layer. According to the different geological conditions applicable, it can be divided into no heat transfer particle collection Wells for strong pervious geology and heat transfer particle collection wells for weak pervious geology. The collection well is composed of pressurized backwater area, sealed area and pumping area. With water as the medium, the heat collected from the pumping area will enter the heat exchanger, and the medium after heat exchange will be circulated through the pressurized backwater area to the pumping area, and the closed circulation heat exchange can achieve the purpose of heat consumption without water, and the shallow geothermal energy can be collected safely and efficiently, saving land and provides a much more economic option. It also provides favorable technical support for the large-scale safe development and utilization of clean renewable energy for building heating and cooling. The technology is suitable for the heating and cooling of the new, renovated and expanded various public buildings, civil buildings, farmers and other buildings. It can further promote the energy-saving and low-carbon operation of the building and realize higher economic and environmental benefits.

Single well circulation heat exchange ground can be safe and efficient

The single well circulating geothermal energy acquisition technology is a safe, efficient, land saving and economical application technology to collect shallow geothermal energy. It has been successfully applied as early as 2000. After more than 20 years of technological development and updates, it has

become an advanced shallow geothermal energy acquisition technology applicable to various geological conditions. The single-well circulating heat exchange geothermal energy collection well uses the pressure difference to get the temperature difference, and the circulating heat exchange collects the geothermal energy in the rock and soil mass. The whole process of geothermal energy collection and utilization does not consume or pollute groundwater, which is safe for groundwater and avoids potential geological disasters.

According to the structure of single well circulating heat exchange geothermal energy collection well can be divided into two forms: geothermal energy collection well with heat exchange particle and geothermal energy collection well without heat exchange particle. The geothermal energy collection well with heat transfer particles is suitable for weak permeable strata, the well depth is 40-100 meters, and the geothermal energy collection capacity of a single well is 100-300kW; the geothermal energy collection well without heat transfer particles is suitable for strong permeable strata, the well depth is 60-100 meters, and the geothermal energy collection capacity of a single well is 15-500kW. The single well circulating heat exchange geothermal energy collection well is an original independent intellectual property rights technology in China. It has been recognized as an original technology by the Literature and Information Center of the Chinese Academy of Sciences both at home and abroad. It has a number of international invention patents and the international advanced level of provincial and ministerial identification. In December 2012, the Beijing local standard “Technical Specification for Single-well Circulating Heat Exchange Geothermal Energy Acquisition Well Engineering” (DB11/T935-2013), which was compiled by Hengyouyuan Science and Technology Development Group Co., LTD., was approved and issued by Beijing Municipal Bureau of Quality and Technical Supervision. After years of promotion and implementation, it has been applied to the heating and cooling of more than 21 million square meters of buildings, becoming an important technical measure to reduce the carbon emission of building operation, and contributing to the early realization of the double carbon goal. Hence, it is seen as an important low-carbon path to solve building heating cooling.

There are many technical advantages of constant active single-well circulation heat exchange ground acquisition:

1.High efficiency

Single-well circulating heat exchange geothermal energy collection well is based on groundwater as the medium, and adopts the small temperature difference method of direct heat exchange with underground soil sand and stone to collect shallow geothermal energy, which greatly reduces the heat transfer temperature difference, improves the water supply temperature of heat exchange well, thus improving the energy efficiency of the whole heating (cooling) system.

2.Safety and environmental protection

The whole process of geothermal energy collection and utilization does not consume or pollute groundwater, which is safe for groundwater and avoids potential geological disasters.

3.Land saving

Its heat transfer efficiency is 20-100 times of the traditional soil source, and the ground only accounts for one maintenance well cover area after the completion of a single well, covering an area of 1/ (20-100) of the traditional way, which provides technical support for the application of shallow geothermal energy in the urban center where the land is tight and the buildings are dense;

4.Wide applicability

Ground energy collection Wells are divided into energy collection Wells with and without energy storage particles, which can be applied to different geological conditions with strong designability and wide application range.

5.Short construction period

The number of collection Wells is set according to the cold and heat requirements of the project. The construction cycle of a single well is 3-7 days, which can realize the simultaneous construction of multiple Wells and greatly shorten the construction period.

Shallow geothermal energy is widely distributed, abundant and operates at a constant temperature. Combined with the advanced single-well circulating heat exchange geothermal energy acquisition technology, it has been used for many years for building heating and cooling. A plethora of examples support that it can be used as an alternative energy for heating and cooling. Constant source energy heat pump environment system has strong designability, which can be specially designed according to the scale of the project, the characteristics of building distribution and the rules of use. This project is a typical case. The Hengyouyuan shallow geothermal energy cooling and heat source system realizes the clean energy supply for all the heating, cooling and domestic hot water of the project, saving 60% energy compared with the traditional cooling and heat source system. Constant source energy heat pump environment system saves significant energy in the operation process, greatly reduces the carbon emissions of the system, and promotes the realization of harmonious coexistence between human and environment.

Throughout the current various forms of heating, shallow geothermal energy has the unique characteristics of energy saving, high efficiency, and zero-pollution, and has become an advantageous option in helping the heating industry achieve the “double carbon goals.” Therefore, it is imperative to continuously increase the scientific and technological research and development efforts of shallow geothermal energy industry, strive to improve the share of clean heating of shallow geothermal energy, supported by facts and data to promote shallow geothermal energy to become the prime option amongst alternative heating energy, actively promoting the transformation of heating energy in the new era.

敬告读者

TO INFORM THE READER

《中国地热能》是由中国地热能出版社主办，北矿大（南京）新能源环保技术研究院、首都科技发展战略研究院、北京工业对外经贸促进会、北京节能环保促进会浅层地（热）能开发利用专业委员会、中国地热与温泉产业技术创新战略联盟、中国热冷一体化能源研究院协办的科技期刊，双语半年刊。我们的办刊宗旨是为政府制定能源政策提供参考建议；为地能开发企业提供宣传平台；为设计者、大众提供交流空间；推广浅层地热能利用经验，展示应用实例。

我们始终不忘读者的期待，用心用力办好期刊。毫无疑问，优化空气、节能减排、治理雾霾是当前摆在全体中国人民面前一个重大课题，我们期望《中国地热能》这本小小的期刊能够为攻克这一难题贡献微薄之力。

立足长远，着眼当前，在继承中创新，在变革中发展。自创刊以来，期刊一直得到了业内专家学者和广大读者的热情支持，在此致以我们的衷心感谢。大家的关注是我们的追求，大家的支持是我们的动力。让我们携手共进，共同打造《中国地热能》的美好明天。

《中国地热能》编辑部

投稿及广告联系人：彭芳
电话：010-62599774
邮箱：journal@chyy.com.hk

中國地熱能
CHINA GEOTHERMAL ENERGY


中國地熱能
CHINA GEOTHERMAL ENERGY
六年风雨兼程
六载始终如一
勇于开拓奋进
促地热能腾飞


中國地能
1
中國地能


中國地能


中國地能


5,6
中國地能


7
中國地能


8
中國地能


9
中國地能


10
中國地能


11/12
中國地能


13
中國地能


14
中國地能


15
中國地能


16/17
中國地能


18
中國地能


19
中國地能


20
中國地能


21
中國地能


22
中國地熱能


23
中國地熱能


24
中國地熱能


25
中國地熱能


26
中國地熱能


27
中國地熱能


28
中國地熱能


29
中國地熱能


30
中國地熱能


31
中國地熱能


32
中國地熱能


33
中國地熱能


34
中國地熱能


35
中國地熱能


36
中國地熱能

地能热宝

取代传统供热方式，更节能，更安全！

“地能热宝”系统是以浅层地热能作为供暖替代能源，可分间配热宝设备和分间计量，是高效电替煤自采暖系统。宏源地能热宝技术有限公司专注于农村建筑户式地能热冷机产品的开发、制造、系统集成和销售，旨在实现乡村清洁取暖，提高百姓生活品质。

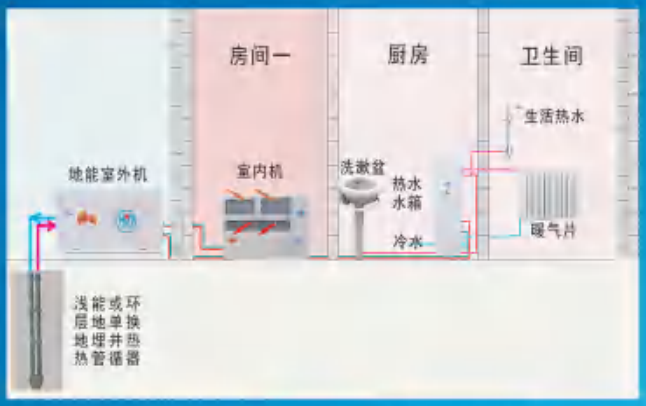

一间房暖冷及生活热水一体化地能热宝系统

两间房暖冷一体化地能热宝系统

三间房暖冷一体化地能热宝系统

八间房暖冷一体化地能热宝系统

特点：

低碳环保：无燃烧零排放，安全、干净、省心、省事；

操作简单：分间恒温控制，遥控器简单操作；

行为节能：能实现人在哪屋开哪儿设备，系统设计符合和继承了中国“省着用”的节俭传统；

初投资低：交钥匙工程300-350元/平米；

运行费用低：北京用户单位面积采暖费用约10元；

无需电增容：三间房暖冷一体化地能热宝系统配电仅为2.1kW（220V），相当于家用空调设备的配电量；

供暖有保证：浅层地热能温度相对恒定，不受室外恶劣天气影响。

宏源地能热宝技术有限公司

地址：四川省绵阳市涪城区金家林下街 29 号

联系电话：010-62592341 400-666-6168

传真：010-62593653

电邮：dnrb@hyy.com.cn

诚招各地区代理商

期待您的加盟

扫描二维码

获取更多地能知识